ADDIS ABABA UNIVERSITY

SCHOOL OF EARTH SCIENCES

Title: Geochemical Studies of Volcanic Rocks for the implication of their petrogenesis in between southern Lake Hayk and western part of Lake Hardibo, South Wollo, Amhara Regional State, Ethiopia

By: Getie Berlie

Advisor: Professor Dereje Ayalew

The thesis work is submitted to the school of graduate studies of Addis Ababa University, school of earth science for the partial fulfillment of masters of sciences in geological sciences (geochemistry).

September, 2021

Addis Abeba Ethiopia

ADDIS ABEBA UNIVERSITY

SCHOOL OF GRADUATE STUDIES

SCHOOL OF EARTH SCIENCES

Geochemical Studies of Volcanic Rocks for the implication of their petrogenesis in between southern Lake Hayk and western part of Lake Hardibo, South Wollo, Amhara Regional State, Ethiopia

By: Getie Berlie

Advisor: Professor Dereje Ayalew

The thesis work is submitted to the school of graduate studies of Addis Ababa University, school of earth science for the partial fulfillment of masters of sciences in geological sciences (geochemistry).

September, 2021

Addis Ababa, Ethiopia

ADDIS ABEBA UNIVERSITY

SCHOOL OF GRADUATE STUDIES

SCHOOL OF EARTH SCIENCES

Geochemical Studies of Volcanic Rocks for the implication of their petrogenesis in between southern Lake Hayk and western part of Lake Hardibo, South Wollo, Amhara Regional State, Ethiopia

BY; Getie Berlie Tesfaye

Professor Dereje Ayalew _____ ___/____/____

Advisor Signature Date

Dr.Balemwal Atnafu _____ ____/___/____

Chairman School of Earth Science Signature Date

Prof. Gezahign Yirgu _____ ___/____/__

Examiner Signature Date

Prof. Bekele Abebe _____ ___/___/___

Examiner Signature Date

September, 2021

Addis Ababa, Ethiopia

Declaration for Originality

I hereby declare that the thesis entitled "*Geochemical Studies of Volcanic Rocks for the implication of their petrogenesis in between southern Lake Hayk and western part of Lake Hardibo, South Wollo, Amhara Regional State, Ethiopia*" is my original work prepared for the partial fulfillment of Master Degree of Geological Science in Geochemistry, School of Earth Sciences, Addis Ababa University during the year of 2021 under the supervision of Professor Dereje Ayalew. I declare that this work is not presented and published anywhere else, and all the used sources are well referenced and acknowledged.

Getie Berlie Tesfaye _____ _____

MSc candidate Signature Date

This is to certify that the above declaration made by the candidate is correct to the best of my knowledge.

Prof. Dereje Ayalew _____ _____

Advisor Signature Date

Abstract

The study area is located around Lake Hayk northeastern central part of Ethiopian. In this study petrographic, and geochemical (trace and major elements) data of mafic to felsic rock are presented, integrated, and interpreted to characterize the geochemistry of cogenetic suite and petrogenetic processes involved in the evolution of these flood basalts to differentiated rhyolite rock units. Fieldwork for sampling and mapping, petrographic investigations, and major and trace element geochemical analysis using ICP-AES and ICP-MS procedures are all completed to meet this objective. The area constitutes of bimodal composition of flood basaltic to rhyolitic rock with scarce intermediate composition. The rock units that make up the research area are basalt, basaltic andesite, trachydacite, and rhyolite, based on total alkalis versus silica (TAS) classification. The basaltic rock (La/Yb) N ratio = (5.34-10.97), basaltic andesite to rhyolite (La/Yb) N ratio = (6.19-11.74), basalt is less to moderately fractionated than moderately fractionated basaltic andesite to rhyolite. The basalt, basaltic andesite to rhyolite samples have ratios of Ce/Pb >19.65-33.2 and 6.13-15.6 respectively and basalt sample has ratios of Nb/U = 39.55-45.81 and basaltic andesite to rhyolite have Nb/U= 21.59-33.68 and basalt and basaltic andesite to rhyolite has ratios of Nb/Th=9.7-12.3, 5.08-8.63 respectively. Basalt have low Rb/Nb = 0.5-0.58, La/Nb = 0.88-1.06 and high TiO_2 = 2.08-3.04,basaltic andecite have higher Rb/Nb =2.7, La/Nb = 1.81 and low TiO_2 1.96 and rhyolite Rb/Nb = 0.97-1.69, La/Nb = 0.51-1.08 and lower TiO_2 = 0.41- 0.71.MgO against incompatible trace elements such as Th, La, and U has a negative correlation this testifies that there is insignificant continental crust involvement and Ce/Pb displays a positive correlation with MgO suggest that there is minimal crustal contamination. The positive and negative anomalies of Ba and K respectively, testify related to amphibole mantle source. The basaltic rock unit characterized by low CaO/Al_2O_3 ratios (0.71–0.99) and relatively no fractionation and flat HREE patterns with (TbN/YbN = 1.75-2.33) chondritic values this suggest a mantle source mostly containing spinel rather than garnet and the gentle slope in HREE show the source for mafic rock is garnet free. Rhyolite is characterized by a steep negative correlation in bivariate major oxides such as MgO,Fe_2O_3,TiO, and CaO against SiO_2 and positive anomaly of Ta with slight Nb trough which implicate that Rhyolites formed by fractional crystallization rather than significant crustal contribution, partial melting and assimilation. Detail isotope geochemistry and mineral chemistry studies are much recommended around Lake Hayk.

***Key words**: crustal contamination, fractional crystallization, Lake Hayk, major and trace element mantle source, OIB, petrogenetic processes*

Acknowledgment

Firstly, I would like to extend my grateful thanks to Samara University Geology Department for giving me a chance to study my master's degree. I am also thankful to Addis Ababa University, School of Earth Science for its complete support from the beginning to the end of this research work. My gratitude also goes to vice president for research and technology transfer (VPRTT) for funding the research fully. Foremost, I would like to express my sincere gratitude and respect to my enthusiastic advisor Prof. Dereje Ayalew for his constructive comment, valuable suggestion, encouragement, providing sponsor and remarkable support of my thesis work.

Besides, special mention to the instructors and mentors in Addis Ababa University School of Earth Sciences for their endless academic support during my classes, they nurtured my enthusiasm for Geological Sciences.

My gratitude also goes to professor Mohammed Hassen geography department head for his endless support by facilitating field work and my friend Mr. Kiflom Mulu and my colleague Mr.Jemal Ahimed, for their technical support during this work.

At the Last but not the least, Lake Hayk communities are greatly acknowledged for their kind help during field work.

Table of Contents

List of Figure

List of Table

List of Acronym

a.s.l	above mean sea level
CFB	Continental flood basalt
CFV	Continental flood volcanism
CIPW	Cross, Iddings, Pirrson and Washington
Cpx	clinopyroxene
GCD Kit	Geochemical data kit tool
GPS	Global Positioning System
HFSE	High field strength elements
HREEs	Heavy rare earth elements
HT1	High-Ti1
HT2	High-Ti2
ICP-AES	Inductively Coupled Plasma Atomic Emission Spectrometry
ICP-MS	Inductively Coupled Plasma Mass spectrometry 81
LOI	Loss on Ignition
LREE	Light rare earth elements
LT	Low-Ti
MORB	Mid-oceanic ridge basalt
OIB	Oceanic island basalt

PPL	Plane Polarized Light
ppm	parts per million
TAS	Total alkali silica
UTM	Universal Transvers Mercator
XPL	Cross polarized light

CHAPTER ONE

INTRODUCTION

1.1. Background

Continental flood volcanism (CFV) is often associated with rapturing of the earth's lithosphere. As continental breakup advances towards matured rifting, the geochemical characteristic of the lavas commonly evolves toward that of oceanic lavas (ocean island basalts, OIBs; and mid-oceanic ridge basalts, MORBs), suggesting the progressive involvement of the upper mantle materials (Pik et al., 1999). Although continental flood basalt (CFB) provinces are usually linked to deep origin hot mantle plumes the involvement of the upper mantle and crustal sources contribute a lot to their genesis (Richards et al., 1989). In addition, Dereje Ayalew et al. (2006) have noted that the initiation of continental flood basalt magmatism is spatially and temporally related to continental break-up, which results in the formation of oceanic crust, at least within the past 200 Ma. Nevertheless, the dating of relationships between rifting leading to ocean-floor formation and continental flood basalt (CFB) formation are complex and can vary in space and time (Courtillot et al., 1999; Hawkesworth et al., 1999).

Several petrogenetic models have been presented to explain the formation of silicic volcanic rocks in mafic LIPs. Rhyolites and associated silicic volcanic rocks (60 - 81 wt% SiO_2) are typically metaluminous to peraluminous, and they are generated by a combination of processes. (i) Assimilation and fractional crystallization (AFC) of mafic magma with significant crustal contribution or melting of continental crust (Ayalew et al., 2002; Dereje Ayalew and Gezahegne Yirgu, 2003, Haldera et al.,2020), and (ii) Parental mafic magma fractional crystallization with minimal crustal contamination (Dereje Ayalew et al.,2002; Haldera et al.,2020). According to Haldera et al.(2020), A minor to non-existent Nb-Ta anomaly, the presence of clinopyroxene phenocrysts, and steeply negative slopes in bivariate major oxides plots against SiO_2 describe rhyolites formed by considerable fractional crystallization. Rhyolites developed with large crustal inputs, on the other hand, are distinguished by the absence of clinopyroxene phenocrysts and significantly negative Nb-Ta anomalies. According to Garland et al. (1995), the rhyolites follow a similar pattern, with low- TiO_2 (LT) rhyolites occurring in association with low- TiO_2

(LT) basalts and high- TiO_2 rhyolites with high- TiO_2 basalts.in addition, Dereje Ayalew et al. (2002) have further documented that the plateau rhyolites are geographically correlated with the basalts, low- TiO_2 and high- TiO_2 rhyolites occurring in association with low- TiO_2 and high- TiO_2 flood basalts. This coincidence of basalt and rhyolite provinciality suggests that the rhyolites are related to the basalts either by extensive fractional crystallization of the exposed basalt magma types and varying amounts of crustal contamination (Chazot & Bertrand 1995; Baker et al. 2000) or by partial melting of underplated basic igneous rocks in the continental crust (Cleverly et al. 1984; Lightfoot et al. 1987).

Because continental crust is enriched in incompatible elements and so has different radiogenic isotope signatures, even tiny amounts of crust assimilation by primary/parental mafic magmas will result in large-scale compositional variability of the final eruptive products. The study of rhyolite and related silicic volcanic rocks in a LIP setting will contribute to a better understanding of the difficult petrogenetic aspects of mafic magma differentiation and the role of continental crust in silicic rock generation in continental mafic LIPs (Halder et al., 2020). Although the area is largely basaltic, the Oligocene volcanic products of the northern Ethiopian plateau show a significantly bimodal distribution of basalts and rhyolites (Dereje Ayalew and Gezahegne Yirgu, 2003). As noted for other continental flood basalt provinces, the coincidence of basalt and rhyolite provinciality suggests that the rhyolites were derived either by fractional crystallization of the associated basalt magma types or by partial melting of underplated basic igneous rocks (Dereje Ayalew et al. 2002). Moreover, Dereje Ayalew et al. (2002) have described the petrological and geochemical characteristics of the plateau ignimbrites and shown that these volcanic rocks are consistent with their derivation by fractional crystallization of basaltic magmas similar in composition to the exposed flood basalts.

The goal of the study is to investigate the petrogenetic evolution of volcanic rock around Lake Hayk area, which is located in the North central Ethiopian plateau based on their geological and geochemical (major and trace element) characteristics. The deposition of pyroclastic eruption and lava flow of volcanic rock units constitute the study area. The rock units are dominated by aphyric, porphyritic, and vesicular basalt, and a wide variety of silicic rocks are found in these areas that include dominantly rhyolite (strongly welded), ignimbrite, obsidian, less welded rhyolitic, and volcanic ash deposits. These lithological units are mafic and felsic in composition,

however, the mafic composition of rock units covers the majority of the area. The major lithological units located in the study area are exposed due to different activities like stream cut, fault scarps, road cut, hill side, and query site are the most common exposure site of rock outcrops. The research area is characterized by a variety of landforms, ranging from flat areas (plains) to steep slopes (chain of hills).

1.2 General Description of the study area

1.2.1 Locations and Accessibility

Lake Hayk area is located in the western margin of the Afar, South Wollo, Amhara Regional State, Ethiopia. Geographically it is bounded between the UTM coordinates of 0572000-0580000E and 1240000-1252000N. The area is accessed through Addis Ababa – Dessie - Lake Hayk (461km) and also can be accessed from Addis Abeba - Bahir Dar – Lake Hayk. It is about 31km on the way from Dessie town to Lake Hayk.

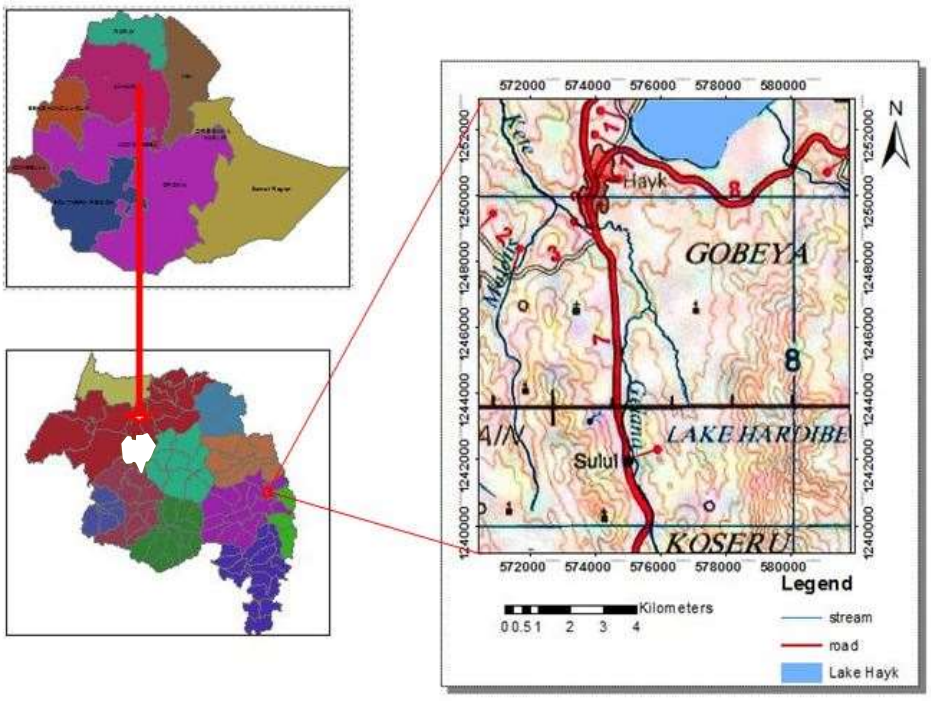

Fig 1. 1 Location map of Lake Hayk

1.2.2. Drainage pattern

The study area is dominantly characterized by a dendritic type of drainage pattern (Fig.1.2). The drainage pattern found in the study area is seasonal. During summer streams get a lot of water from different small seasonal tributary streams and form deep valleys around it. Most of the Stream Rivers are located in the western part of the study area but the biggest stream is called Gelan/Bishanako River, which flows throughout the year from the south to north direction of the study area.

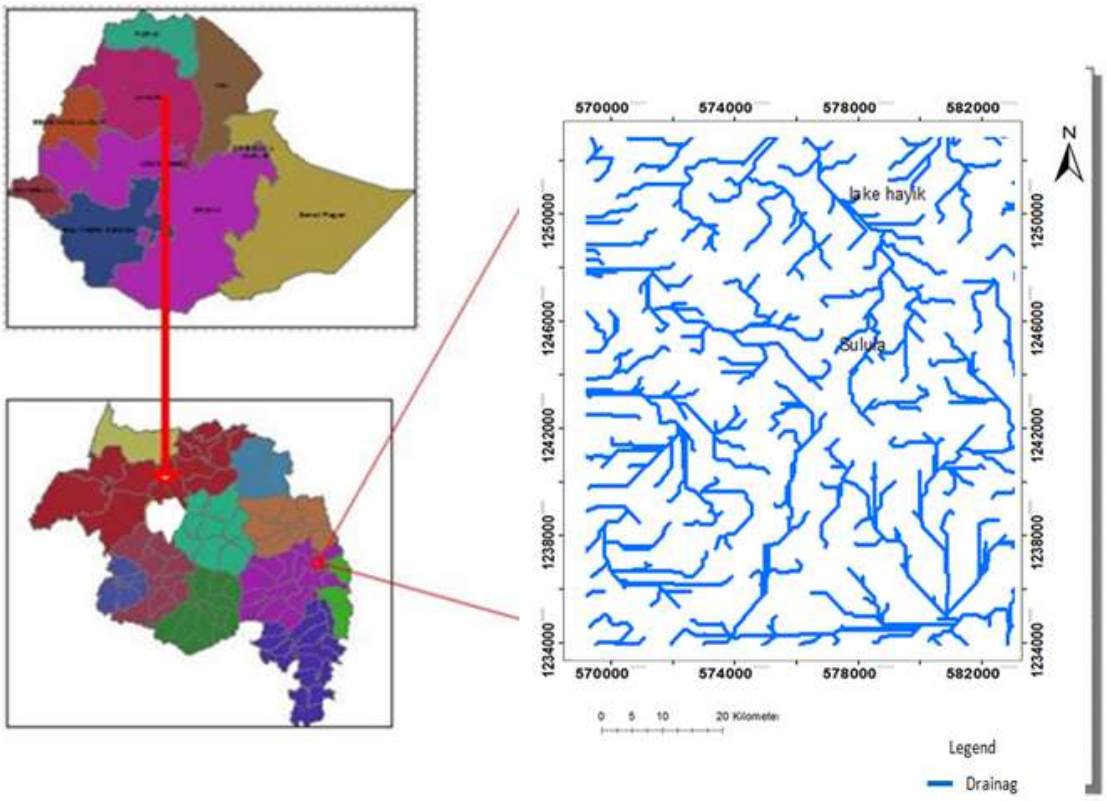

Fig 1. 2 Drainage pattern of the study area.

1.2.3 Physiography

The North-central Ethiopia plateau that formed by enormous volcano-tectonic events and subsequent denudation processes that took place after the Mesozoic time (Mohr, 1983). Lake Hayk is one of the extensional basins formed along the western escarpment of the Afar Depression. Study area Characterized by a deeply dissected gorge, plateau, and high altitude continuous chain of ridge. The research area's elevation ranges from 1700 meters near Hayk

town to 2850 meters on the top of a hill in the western section of the study region above mean sea level (m.a.m.s.l.) with a mean elevation of 2275 meters above sea level.

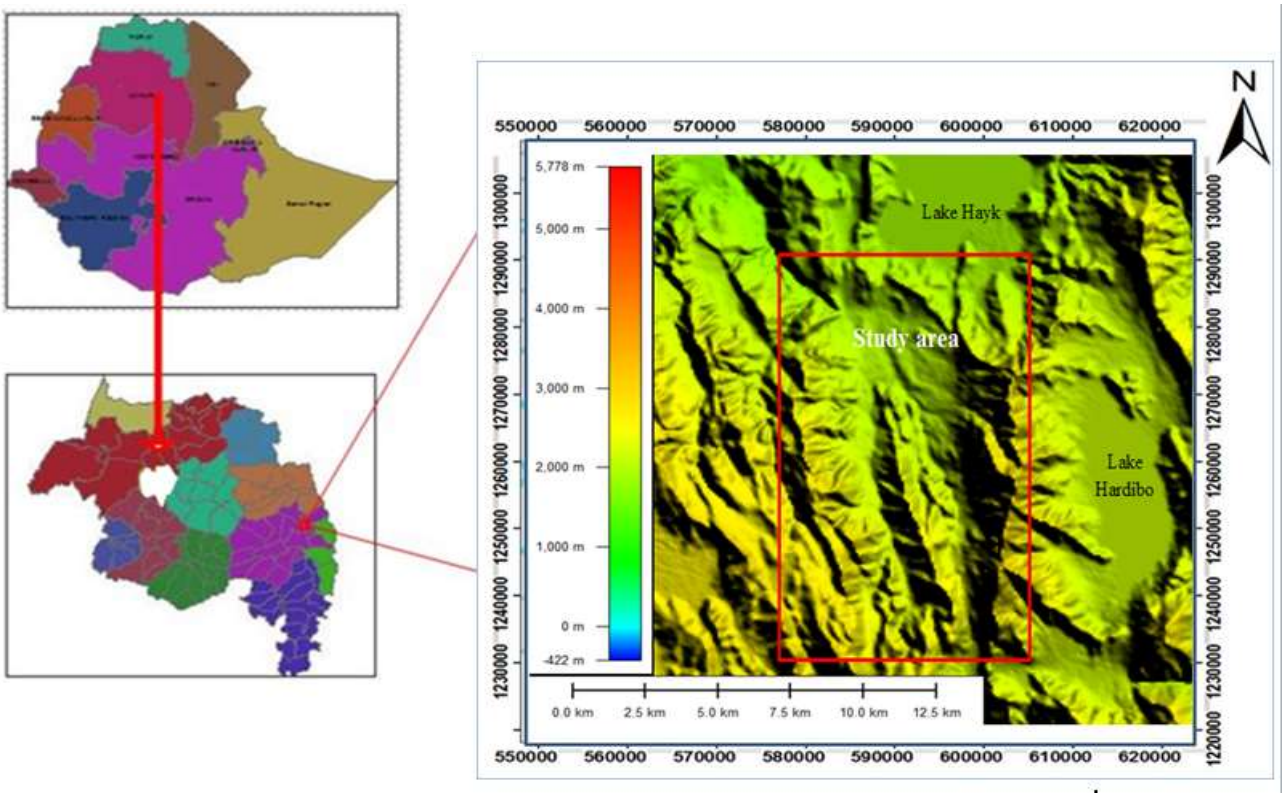

Fig 1. 3: Physiographic map of the study area.

1.2.4 Climate

According to the meteorology agency of Ethiopia (2019 and 2020) data the study area has different climatic conditions within a year. The maximum monthly average temperature is recorded during May -June –July 26.9-28.6 ^{0}C -, 30.3-29.2 ^{0}C, 28.7- 27.3^{0}C, with year of 2019 - 2020 respectively and minimum January (1.0, 5.4 ^{0}C) and the other are moderate condition. The average temperature of the year in the study area is 26.1, 25.6 ^{0}C max and min 8.7, 9.93 ^{0}C May and June is the warmest month and January is the coolest month. The driest months are November and December (0 mm) and the wettest month was July (207.3, 283.4) the annual

precipitation of the area is 1321.6, 1172.1mm, and August (364.7- 325.2mm); and the average precipitation is 110.2-97.7mm.

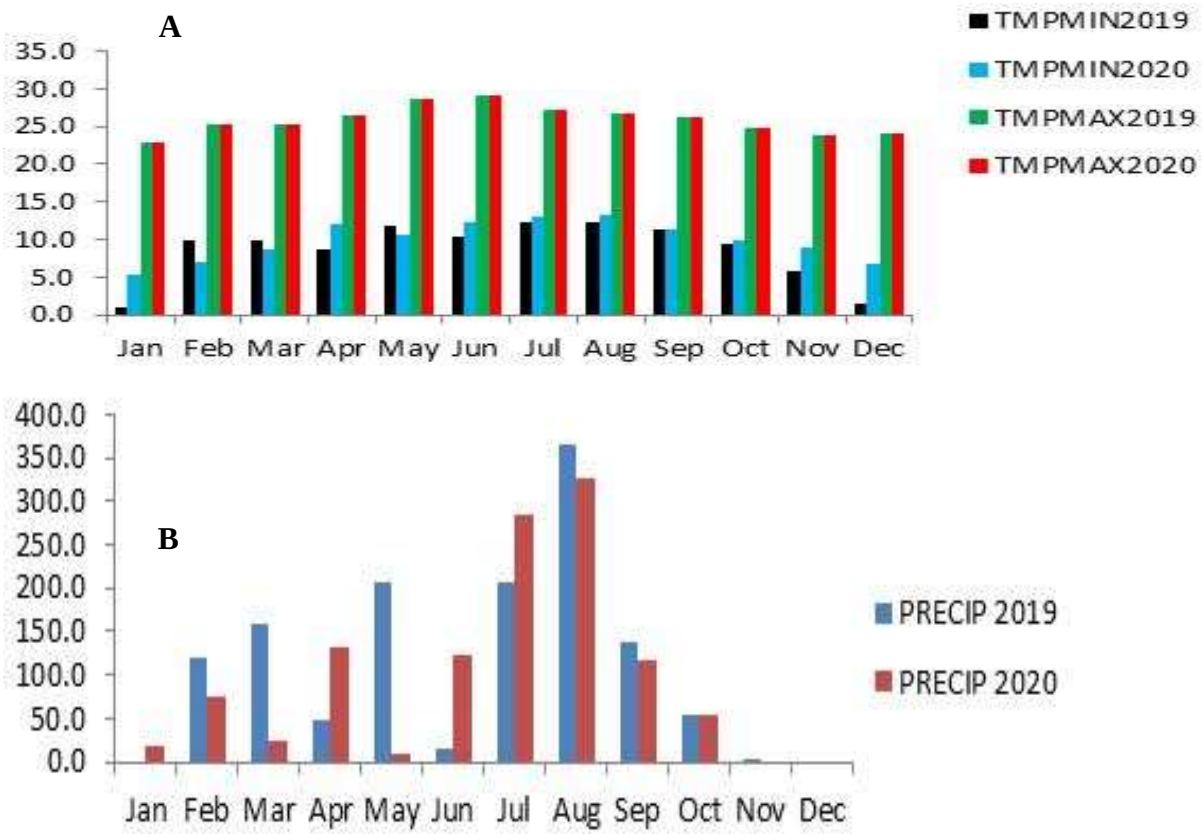

Fig 1. 4 climate data graph of Lake Hayk area which includes (A), temperature and (B), rainfall of the area according to Ethiopian meteorological data (2019-2020).TMPMAX2019- maximum temperature at 2019, TMPMIN2019-minimum temperature at 2019, TMPMAX2020- maximum temperature at 2020, and TMPMIN2020-minimum temperature at 2020.

1.2.5. Vegetation

The vegetation covering in the study region ranges from sparse to dense. The study area eastern and western parts have more vegetation covering than the remainder of the study area. The vegetation types found in the study area are mainly, shrubs, and bushes. The ridge (horst) and hills are densely covered by bushes, shrubs, and juniper trees, and the flat area is sparsely covered by Eucalyptus and chat.

1.3 Statement of Problem

This research is one part of thematic research. From this team, research geochemistry is one component to involve in the geochemical characterization of volcanic rock which is not studied in detail but different researches were done by different researcher in this area such as Blanford's, (1870) original classification of northern Ethiopia volcanic; great progress has been made in the study of the volcanic rocks in Ethiopia. According to Tefera et al. (1996), surrounding Dessie area lies in the central part of northeastern Ethiopia which is underlain by pre-and syn-to post-rift volcanic successions outpoured during Tertiary and Quaternary time and regionally the lithologies were mapped. Additionally, Merla et al. (1979), documented that the dominant bedrock in the Hayk Basin is the Miocene to Pliocene Termaber Basalt, which formed during the last stage of the Ethiopian plateau shield volcanism and The age of flood basalts and associated rhyolites erupted between 31 and 29 Ma (Hofmann, et al. 1997; Dereje Ayalew et al., 2002).

Further, the sedimentary succession at Lake Hayk has been studied recently using a combination of geomorphological, stratigraphic, and stable-isotope data (Lamb et al. 2007; Ghinassi et al., 2012). Furthermore, Ghinassi et al. (2012) studded the Lake Hayk lake sediments were also tephra-recorded in detail and identifying both visible volcanic ash (tephra) layers and fine-grained crypto-tephra layers.

Different scholars recommended detail geological and geochemical work is needed for Ethiopian igneous provinces. The majority of research on the Ethiopian plateau and rift magmatism has been done on a regional scale, with only a few comprehensive investigations on isolated plateau parts (Pik et al., 1999, Kieffer et al., 2004).

Moreover, Kurkura K, (2010), documented that the scarcity of a detailed geological map of any particular section of the Ethiopian flood basalt province makes it difficult to correlate much of the existing high-quality geochemical data from various parts of the Ethiopian flood basalt province.

So, to solve those problems, detail petrographic and geochemical understanding of volcanic rock for the implication of their petrogenesis and source rock characterization and also detail geological map preparation are necessary for this area.

1.3. Objective

1.3.1 General Objective

The general objective of this study is to investigate the geochemical characteristics of suite cogenetic rock to determine petrogenetic evolution of volcanic rocks.

1.3.2 Specific Objective

In addition to the principal purpose of this research, it has specific objectives that help to well complete the main objective of the research.

- To evaluate the process involved in the petrogenesis of the primary magma spectrum of basaltic rock.
- To evaluate the process involved in the differentiation of primary magma spectrum for the formation of rhyolitic rock unit and
- To estabilish and characterize the stratigraphic section, identify the type and distribution of rocks, petrographic characteristic, and produce geological map of the study area based on field observation.

1.4. Methodology

To reach the objectives of the research mentioned above, several steps were carried out.

1.4.1 Field Work

The field investigations were comprised;

- ✓ A proper lithological description was conducted.
- ✓ Representative fresh samples based on a stratigraphic section from all lithology were collected.
- ✓ Systematic rock sampling of the surrounding volcanic igneous rocks. Rocks were described at the outcrops and take Photographs at a representative outcrop with scale. During traverses, select complete sections having compositional variation were done.

1.4.3 Petrographic Analysis

In this research 15 samples were prepared for Petrographic analysis. The thin sections were described using a polarized petrographic microscope. A detailed petrographic study /thin section descriptions/ including mineral identification, modal proportion, textural descriptions, and rock

naming performed at Addis Abeba University petrographic laboratory. Representative mineral assemblage and textures taken photograph under the petrographic microscope.

1.4.4 Geochemical Analysis

In this research 10 samples were prepared for geochemical analysis. The sample preparation for geochemical analysis includes making a rock powder after removing the weathered part of the rock is done under ALS-Addis Ababa, Ethiopia. To accomplish this, three steps were taken: first, the weathered part of the rock sample was removed and broken into desired sizes, then the broken fresh sample was crushed in a jaw crusher, and finally, the crushed sample was milled down to micron size particles in an agate ball automatic milling machine. After crushing and milling each rock sample, the Jaw crusher and ball mills are blown out and washed to remove any possible pollutants, then dried before going on to the next sample to avoid cross-contamination. The sealed and packed powdered samples were submitted to Ireland through Australian Laboratory Science (ALS), to determine the concentration of major and trace elements. Different analytical instruments were used to geochemically analyze the powder samples for major, trace, and rare earth elements. Inductively Coupled Plasma Atomic Emission Spectrometry (ICP-AES) was used to examine major elements, whereas Inductively Coupled Plasma Mass Spectrometry was used to examine trace elements (ICP-MS). Besides, multi-element four acid digestions 81(ME-4ACD81) were used for base metal determinations such as Cr, Co, Ni, and V. In addition, loss on ignition (LOI) at 1000 ^{0}C is determined by an instrument WST-SEQ. For trace element analysis, ICP-MS is the most widely used method (Rollinson, 1993). To utilize the analyzed geochemical data(trace and major elements, base metals, and also loss on ignition) for this research work, the data have been integrated and exercised through different software packages such as geochemical data kit (GCDK it version 3.2.0) and Microsoft excel 2007. In particular GCDkit software has been used to construct classification diagrams (TAS), REE spider plot, and multi-element variation diagram along with various major and trace element variation diagrams. Further, Microsoft excel 2007 and petrograph was used to compute the values of some selected trace element ratios.

Analytical methods	Australian laboratory (ALS) services code	Data	Descriptions
ICP-AES	ME-ICP06	Major elements	Whole rock package
WST-SEQ	OA-GRA05	Total volatiles	Loss on ignition at 1000^0C
ICP-MS	ME-MS81 Using	Trace elements	lithium borate fusion ICP-MS
ICP-AES	ME-4ACD81	Base metals	Using 4 acid digestions
ICP-AES	TOT-ICP06	Major elements	The total calculation for ICP06

Table 1. 1 Summary for the geochemical analytical method.

1.5. Litterateur Review

A number of geochemical studies have been conducted on Ethiopian volcanic rocks, particularly on the middle to late Cenozoic basaltic volcanism in Ethiopian plateau, Afar, and MER(Furman 2007; Dereje Ayalew et al., 2016; Feyissa et al., 2017). It has been noted that oceanic basalts have geochemical and isotopic compositions that differ substantially from those of continental flood basalts (CFB). Such difference in compositional is attributed to differences in contamination of crustal materials and/or to mantle sources in CFBs (Fodor, 1987; Ellam and Cox, 1991;Arndt et al., 1998).

Dereje Ayalew et al. (2019), combined field observations, age, chemistry (major and trace elements), and isotope (Sr-Nd-Pb) data for felsic volcanic rocks from Central Afar to show rhyolite differential fractionation during Crustal Extension in the surrounding western Afar (Ethiopian Rift). In this study, the dates of felsic volcanic rock range from 30 Ma (prerift stage), 20 Ma (early synrift), 8–4 Ma (primary thinning event), and 2.5–0.1 Ma (late synrift/continental breakup), indicating the full volcanic-tectonic events that happened in sequence. With gabbroic cumulate fractionation, major element changes are expected. Assimilation appears to have diminished in recent times, with Quaternary rhyolites emplaced near active magmatic segments in Afar, which contain isotopic compositions that are closest to original mantle signatures. (Dereje Ayalew et al., 2019).

In traditional system of classification of the Ethiopian continental flood basalt province, which encompasses the Ashangi, Aiba, and Alaji formations was explained by (Berhe et al., 1987; Mohr, 1983). According to Coulie et al. (2003), the Ashangi and Aiba formations are characterized by tholeiitic-transitional basalts commonly found with interbedded felsic/rhyolite and pyroclastic products towards its top. However, this classification was not supported by any geochemical analysis and it was traditional then; Pik et al. (1998, 1999), introduced a geochemical classification for the northwestern Ethiopian flood basalts. These northwestern flood basalts have been classified into three major groups, the low-Ti (LT) and two high-Ti groups (HT1 and HT2) (Pik et al., 1998).additionally the flood basalts are defined on the basis of incompatible trace element and TiO_2 concentrations (Rogers, 2006). The HT (HT1 and HT2) basalts with elevated incompatible trace element contents and more fractionated REE patterns are found to the south, southeast and east of the volcanic province (Pik et al., 1998). The Low-Ti tholeiitic flood basalts have relatively low concentrations of highly-incompatible trace elements, variable depletions at Rb, Th, U, Nb and Ta, exhibit the lowest rare earth element (REE) contents and nearly flat patterns whereas the High-Ti flood basalts are enriched in strongly-incompatible trace elements and have depletions at Rb, K and Sr (Pik et al.,1999). Although the mineralogical and chemical composition of the flood basalts is relatively uniform (Kieffer et al. 2004).

Kieffer et al., (2004) compared the petrology, geochemistry, and isotopic compositions of shield volcanoes to flood volcanics, as well as differences in magma flux and eruption style of lavas with ages ranging from 30 to 10 Ma, or from the peak of flood volcanism to the start of major rifting in the northern part of the volcanic plateau.

Dercq et al. (2001) investigated the petrologic and geochemical characteristics of volcanic plugs on the North Ethiopian volcanic plateau, comparing them to those of volcanic rocks to determine their interrelationship.

CHAPTER TWO

REGIONAL GEOLOGY

2.1 Introduction

Because it links the Kenyan rift to the Red Sea and Gulf of Aden rift systems, the Main Ethiopian Rift (MER) is a significant part of the East African rift system. The extensional force and upwelling of molten materials create this fissure. It is critical to keep some in mind as the region's geodynamics evolve. Many experts have examined the tectonic and magmatic evolution of the Ethiopian rift. They each have their hypothesis for the rift Using and combining contemporary structural, petrological, and geological analytic tools, scientists from different countries have recently concentrated on the section magmatic evolution of the Ethiopian rift (WoldeGebrel et al., 1998) East Africa has at least 720,000 km^3 of Cenozoic magmatic activity, mostly basaltic lavas and secondary rhyolites/tuffs (Rooney,2017). Basaltic and felsic volcanic rock strata cover 600000 km^2 in Ethiopia's flood basalts (or traps). The thickness of this layer varies greatly, although it can reach 2 kilometers in some areas. According to (Mohr & Zanettin, 1988 and Mohr, 1983b, as cited in Kieffer et al., 2004), the total volume of volcanic and shallow intrusive rocks is approximately 350000 km^3. The relative volumes of flood and shield volcanoes in the northern section of the plateau can be approximated as follows; as Kieffer et al. (2004), calculated Flood basalts cover a total area of about 400km*600km = 240,000km^2 and The total volume of flood basalts is 400 * 600*0.75 = 180,000km^3 if the average thickness is 0.75km. Shields now cover around 20% of the plateau's surface, although they may have covered one-third before erosion.

Sub-region	Area of the polygon (km^2)	Sub-region Avr. lava thickness (m)	Total volume (km^3)
NE Ethiopian Plateau	274,395	1600	439,032
SE Ethiopian Plateau & Chew Bahir Basin	299,324	500	149,662
Turkana Basin	22,317	1000	22,317
Somali/Harrar Plateau	48,389	650	31,453
Yemen	77,108	1000	77,108

Total for the Province	721,533	-	719,572

Table 2. 1 Area and volume of African–Arabian Large Igneous Provinces.

According to Rooney ,(2017) area and volume revised and estimates by drawing polygons in Google Earth for African–Arabian Large Igneous Province. Discussions on Lava thickness estimates and geometry are discussed in the online supplement text.

The Ethiopian volcanic plateau, according to Kieffer et al. (2004), is not a thick, monotonous, rapidly erupted pile of undeformed, flat-lying tholeiitic basalts. Instead, it is composed of a variety of volcanic centers with varying magmatic characteristics and ages. The change in volcanic style is likely due to the tectonic setting and a decrease in magma flux, rather than a change in magma composition. At 30 Ma, tholeiitic and alkaline kinds of plateau volcanism erupted together, though following magmatism was primarily alkaline. Discrepancies in source composition and partial mantling are used to explain large differences in the contents of incompatible elements. The plateau's lavas developed from a broad region of mantle upwelling that was diverse in temperature and content, rather than metasomatized lithospheric mantle (Kieffer et al.,2004; Rooney, 2017). More than a million years ago, Ethiopia's largest basaltic eruption occurred about 30.2 Ma. A pulse of rhyolitic ignimbrite occurred 700 ka after the main event, followed by eruptions of mixed basaltic and silicic lavas till 25.3 Ma (Hofmann et al., 1997; Ukstins et al.,2002). The chemical and mineralogical composition of flood basalts is constant. Clinopyroxene and Plagioclase phenocrysts with or without olivine are found in the bulk of them, which are aphyric to sparsely phyric. The compositions of the majority of them range from tholeiitic to transitional (Mohr, 1983a; Mohr & Zanettin, 1988; Pik et al., 1998). Felsic lavas and pyroclastic rocks of rhyolitic or less typically, trachytic compositions interlayer with flood basalts, especially at high stratigraphic levels (Dereje Ayalew et al., 1999).

Location	Age(ma)	Rock type
Simien shield volcano	18.65 ±0.19	Alkali basalt
Guguftu shield volcano	23.3± 0.3	Plag-phyric basalt, trachyte
South of Lalibela	30.99 ±0.13	Hyaloclastite, alkaline picrite
Choke shield volcano	22.4 ±0.3	Plag-phyric basalt, trachyte
Bora	30.86 ±0.12	Plag from alkaline picrite

Guna shield volcano	10.76 ±0.05	Alkali basalt

Table 2. 2 Summary of Ar-Ar ages from the northern part of Ethiopian plateau (Kieffer et al., 2004)

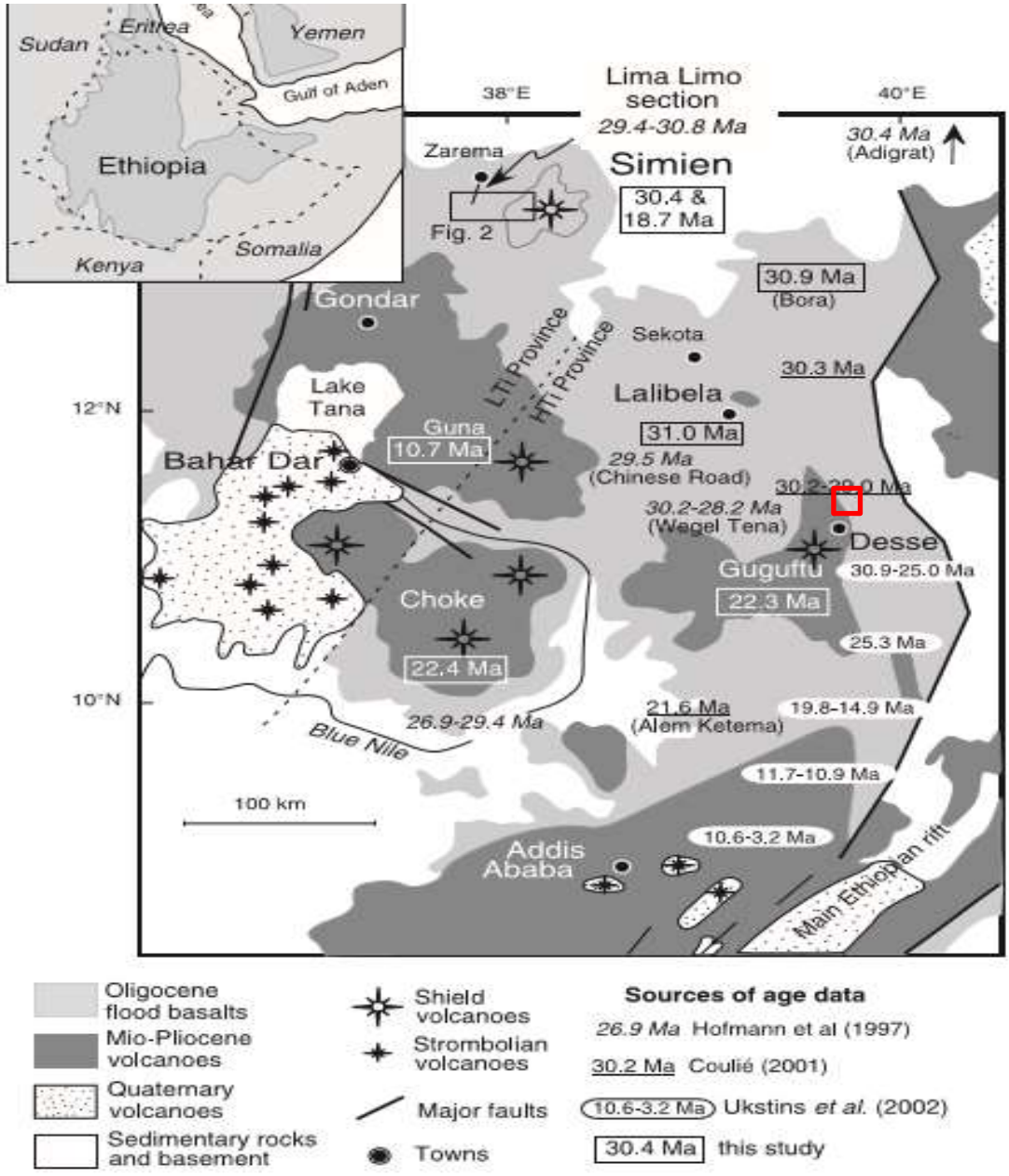

Study area

Fig 2. 1 Northern Ethiopian plateau flood volcanism Flood volcanism is depicted on a map of the northern Ethiopian plateau, as well as the dates and positions of the largest shield volcanoes

(modified from Pik et al., 1999; Zanettin, 1992), Using age data from this study as well as Hofmann et al. (1997), Coulie (2001), Ukstins et al., (2002), and Coulie et al., (2003). According to Pik et al,(1999)the dashed line denotes the border between the LT and HT provinces. The Ethiopian volcanic plateau (in grey) is located in the Horn of Africa (Kieffer et al., 2004).

Different studies categorized Ethiopian volcanic rock in various ways, including the following: According to conventional classification, Ethiopia's Tertiary flood basalts are split into four groups based on their ages and stratigraphic position from bottom/old to top/young which are known as the Ashange, Aiba, Alaje, and Termaber Formations, from bottom to top (Mohr, 1983). In addition to their age, flood basalts are geochemically separated into three different magma types: low Ti basalts (LT), high Ti1 basalts (HT1), and high Ti2 basalts (HT2) (Pik et al, 1998, 1999). In addition, Abbate and Sagri .(1980), categorize the volcanic rocks that cover the majority of Ethiopia into five primary provinces based on their lithological evolution, kind of activity, and frequency of eruption of volcanic centers, and age of effusion: (1) Northern plateau volcanites; (2) Southern plateau volcanites; (3) Somali plateau volcanites; (4) Afar volcanites; (5) Main Ethiopian Rift (MER) volcanites. The Ethiopian volcanites are mostly made up of the first three types (Merla et al. 1979). They're known as the "Traps series (Plateau Volcanics- Pre-Oligocene to Pliocene)" (Blanford 1870; Kazmin 1973), a broad name derived from an old Swedish word that means "steps." According to Dereje Ayalew, (2019), the ages of marginal rhyolites may be classified into four categories: Oligocene trap rhyolites (28.5–30.8 Ma, on average 30 Ma), early Miocene rhyolites (17.4–23.5 Ma, on average 20 Ma), Rhyolites from the late Miocene to Pliocene epochs (between 8 and 4 Ma), as well as Quaternary rhyolites.

2.2 Flood Volcanoes in Cenozoic Volcanic History

The Cenozoic Ethiopian continental flood basalt, which dates back to the opening of the Red Sea and Gulf of Aden in the Cenozoic, is one of the world's youngest flood basalts (Baker et al, 1996; George et al, 1998). These two oceanic rifts meet the east African rift at the Afar triple junction (Abbate et al., 2015). This triple intersection is situated in the central of a massive volcanic zone that spans Ethiopia, Eritrea, Yemen, and the Republic of Djibouti (Pik et al, 1998). The Ethiopian continental flood basalt (CFB) province, which dates back 30 million years, is one of the world's largest igneous provinces (Dereje Ayalew and Gezahegne Yirgu, 2003; Kieffer et al., 2004;Pik et al.,2003), This is linked to continent disintegration and the formation of ocean

basins (Dereje Ayalew et al., 1999;Baker et a., 1996). Furthermore, this flood basalt region is adjacent to the Afar triple junction (Dereje Ayalew et al., 2002;Mohr and Zanettin, 1988;Pik et.,1998;1999). The province's majority is in Ethiopia, with the remainder in Yemen on the Red Sea's eastern shore (Pik et al., 1998). The trap volcanics comprise at least 6* 105 km2 (western and eastern plateaus), with a total volume of at least 3.5* 105 km3 (Mohr, 1983; Mohr and Zanettin, 1988) and likely more than 1.2 *106 km3 (Mohr, 1983; Mohr and Zanettin, 1988).

2.2.1 The Northern Ethiopian Plateau Volcanites

Following Blanford's (1870) attempt to subdivide the northern plateau volcanites into a lower Ashangi Group unconformably overlain by a Magdala Group, Gregnanin and Piccirillo advocated a more comprehensive lithostratigraphic method in the 1970s. Zanettin and Justin Visentin (1974), as well as Zanettin and Justin Visentin Ala (1973), who distinguished the Ashangi and Aiba basalts, Alaji Rhyolites, and Termaber Basalts. The maps by Tefera et al. (1996) and Merla et al. (1979) included these units. The lateral heterogeneity of these volcanic rocks, the vertical recurrence of comparable lithology, and the various morphological responses of basalts with the same petrological or chemical features have all been noted by several writers (e.g., Kieffer et al. 2004)

2.2.1.1 Ashangi Formation

Transitional to tholeiitic olivine basalts, frequently extensively zeolitized, alternate with subordinate tuffs in the Ashangi Basalts (Mohr and Zanettin 1988). Because of their small thickness, restricted horizontal extent, and extensive weathering, the flows are hardly visible. The thickness of Ashenge basalts varies, according to Merla et al. (1979), from 600 to 800 meters along the escarpment and in the northern half of the plateau, to zero meters between Debre Markos and Addis Ababa.

2.2.1.2 Aiba Formation

The Aiba basalts, which unconformably overlay the Ashenge Formation in the northern Ethiopian plateau, are the second major pulse of fissural basalt volcanism (Mengesha Tefera et al., 1996; Merla et al., 1979). The Aiba Basalts are made up of massive transitional flood-basalt flows with well-developed columnar agglomerate layers in between. The flows are 15–50 m thick, reaching approximately 100 m in certain spots, and can be followed for a considerable

distance. They have a total thickness of 1,000 meters. The volcanic pile of the northern Ethiopia plateau is dominated by the above-mentioned fissural basalt blocks, which can reach a thickness of 2,000 meters in some places. Between 31 and 29 Ma, a massive outpouring occurred (Hofmann et al. 1997; Pik et al. 1998; Ukstins et al. 2002; Coulié et al. 2003). Although there is a noticeable change in geomorphology halfway through the sequence, from moderate relief to abrupt cliffs, this transition does not relate to any apparent petrological or chemical characteristic of the flows (Violle, 1999). For these reasons, Kieffer et al. (2004), like Pik et al. (1998), avoid referring to the upper and lower flood basalt strata as Ashangi and Aiba.

2.2.1.3 Alaje Formation

The Alaje Formation (Mohr & Zanettin, 1988) is mostly composed of aphyric flood basalts associated with rhyolites (ignimbrites) and subordinate trachytes, with an age range of 32-15 Ma (Mengesha Tefera et al., 1996). The Amba Alaji Rhyolites are a series of alkaline to transitional basalts and peralkaline rhyolites found exclusively on Ethiopia's northern plateau. Acidic words are mostly made up of whitish ignimbritic tuffaceous layers that can be followed over a long distance. Their maximum thickness is 500 meters, but it drops to zero about 100 kilometers west of the Afar margin. Outcrops of the Alaje formation range in age from the Late Oligocene in the north to the Early Miocene in the south (Zanettin et al. 1974).

2.2.1.4 Termaber Formation

On the northern and southeastern plateaus, the Termaber Formation, which dates from 30 to 13 million years ago (Mohr & Zanettin, 1988), displays Oligocene to Miocene basaltic shield volcanism (Mengesha Tefera et al., 1996). According to Mohr and Zanettin (1988), the mafic lavas of the Termaber Formation produce large, low-angle shields up to tens of kilometers in diameter, but smaller and steeper edifices also exist. The presence of shield volcanoes, with roughly 30 major sites, is a unique feature of the northern Ethiopian plateau. According to Mohr and Wood (1976), some of them have a diameter of up to 100 kilometers and rise 1,000–2,000 meters above the plateau (e.g., Semien, Guna, Choke, and Guguftu). They are listed together as Termaber Basalts in regional assessments and maps. They're made of lenticular, zeolitized alkali basalts with a number of tuffs, scoriaceous lava flows, peralkaline rhyolites and typical red paleosoils. Dike swarms and acidic extrusions are present.

2.2.2 The Southern Ethiopian Plateau Volcanites

The southern plateau volcanites feature a small number of basalts with ages ranging from 45 to 35 Ma (Davidson and Rex 1980; Ebinger et al. 1993; George et al. 1998). They are up to 15 Ma older than the traps found in northern Ethiopia (Rogers 2006). Researchers use the classifications proposed in for this volcanic succession, which rests immediately on the crystalline basement or, more rarely, over Eocene basalts and Mesozoic sandstones (Merla et al.,1979). A thick unit of rhyolites, acidic tuffs, and subordinate basalts that extends up to 1,000 meters follows a hundred meters of weakly alkaline basalts (Omo Basalts) (Jima Volcanites). Some dates, ranging from 30 to 50 million years ago, are extremely unusual (Merla et al. 1979; Davidson and Rex 1980). The Jima Volcanites, which reach a thickness of 1,000 meters in the Omo valley, the bulk of effusive is found in southwest Ethiopia, with a huge fringe in the southern half of the Somali plains, north of the Amaro Mountains and south of the west–east Bonga–Goba line (Abbate and Sagri 1980). Massive white, pinkish, and gray rhyolites, comendites, and pantellerites in thick flows alternate with tuffs and subordinate basalts in the Jima Volcanites. The Jima Volcanites in Omo village, near the top of the sequence, give a date of 27 Ma (Merla et al. 1979). This unit can be ascribed a general age range of 30 to 27Ma. The Wollega Basalts, which rest on the foundation and on the inclined Omo Basalts and Jima Volcanites, are made up of 200–400 m of prominent columnar alkaline basalt flows interbedded with acidic tuff and loose fluvial lacustrine deposits, especially in the top half. They are doubtfully attributed to the Pliocene based on their interactions with the neighboring volcanites (Merla et al. 1979).

2.2.3 The Somali Plateau's Volcanites

The Arussi and Bale Basalts of the Somali plateau are Miocene in age, with K/Ar ages ranging from 24 to 9 Ma and a thickness of around 3,000 m (Kunz et al. 1975; Morbidelli et al. 1975; Merla et al. 1979). (Juch ,1975). In the core of the Bale and Arussi Basalts, rhyolitic intercalations are particularly numerous and thick (Juch 1975).According to Juch. (1975), the Ghinir Unit has a thickness of several hundred meters based on the documentation provided. The large Plio-Quaternary volcanic complex of the Bale Mountain, with cones and plugs, reaches an elevation of 4,300 m and is potentially associated to the Bonga– Goba line (Merla et al., 1979), In the Somali plateau; it rests on the Bale and Arussi Basalts and is covered by bands of glacial deposits.

2.2.4 The Volcanoes of Afar

According to Barberi et al. (1975), the Afar volcanites belong to two periods of continental rifting, the first of which lasted around twenty million years and began around 25 Ma, and the second of which began around 4 Ma and saw the development of the oceanic bottom in the central section of Afar (Abate et al., 2014). Some of the first stage's oldest volcanites are the Mabla Rhyolites, Adolei Basalts, and Dalha Basalts. They're over 1000 meters thick and date from 26 to 6 million years ago, and they're related to mare alkaline and peralkaline granites that date from 25 to 22 million years ago, signifying early continental fracturing. The Plio-Pleistocene Afar Stratoid Series, which covers around two-thirds of the Afar depression, is the most extensive volcanic sequence linked with the second stage Afar depression. This consists of 1,500 m thick transitional basalts that lie unconformably atop the Dalha Basalts after a period of magmatic quiescence. Volcanics and marginal rhyolitic centers (e.g., Dubbi, Ado Ale) are intercalated in and above the Afar Stratoid Series (Barberi al. 1975). A morphological feature of the Afar depression is the axial volcanic mountains of Quaternary age, which rise sharply up to 1,500m.The northern range (Erta Ale) follows the Afar axis in a NNW direction, whereas the volcanic mountains to the south eventually shift to the WNW. These formations are made up of fissure eruptions and shield volcanoes with basaltic flows and alkaline to peralkaline silicic rocks. Many have previously been active, with the Erta Ale volcano producing a spectacular lava lake. The Afar region is a depressed terrain with a quasi-triangular form at the confluence of the Red Sea, the Gulf of Aden, and the Main Ethiopian Rift (MER). Volcanic rocks cover much of the Afar depression due to its 25-million-year history of rifting and incipient oceanization.

2.2.5 Ethiopia's Main Rift Volcanoes

According to WoldeGebrel et al.(1990), the Main Ethiopian Rift (MER) is a NNE–SSW to N–S trending trough 80 km wide in the centre and 1,000 km long. It connects the southern Ethiopian plateau to the Somali plateau, running west to east. Because it connects the Kenyan rift to the Red Sea and Gulf of Aden rift systems, the Main Ethiopian Rift (MER) is a significant part of the east African rift system. The extensional force and upwelling of molten elements create this fissure. It is critical to keep some in mind as the region's geodynamics evolve. Many experts have researched the tectonic and magmatic evolution of the Ethiopian rift, and they have their own theories about it. Using and combining contemporary structural, petrological, and geological

analytic tools, scientists from different countries have recently concentrated on the section magmatic evolution of the Ethiopian rift. In general, two basic kinematics evolution hypotheses for the Main Ethiopian Rift (MER) have been offered.

Some scholars argue that the evolution of the Main Ethiopian Rift (MER) has been dominated by practically pure extension (Mohr.,1983, Ebinger et al.,1993), while others argue that the rift valley has experienced an alert-lateral component of displacement during the quaternary (Abebe et al., 1998).

The Ethiopian volcanic plateau, according to Kieffer et al. (2004), is not a thick, monotonous, rapidly erupted pile of undeformed, flat-lying tholeiitic basalts. Instead, it is composed of a variety of volcanic centers with varying magmatic characteristics and ages.

CHAPTER THREE

GEOLOGY OF THE STUDY AREA

3. Introduction

The study area is around Lake Hayk which is part of western afar margin which constitutes of Oligocene volcanic rock (flood basalt 31 Ma to shield volcano 25Ma) (Hoffmann et al., 1997, Kieffer et al., 2004; Dereje Ayalew et al., 2019). The study area constitutes different volcanic rock units with different texture, mineral assemblages which shows their origin, evolution, and nature of magma generation. Volcanic rock in the study area are flood basalt (70-190m) In the form of sheet, low viscosity magma covering the bottom part or overline by rhyolitic lava(10 – 230 m) and shield volcanoes composed of successive layers of lava flows and pyroclasts and its thickness is (360 m). Flood volcano in the study area includes porphyritic basalt and aphyric basalt and welded rhyolite overlies flood basalt and at the top there is shield volcano constitutes intercalation of strongly welded rhyolite, less welded rhyolite, ignimbrite, amygdaloidal basalt, shied basalt, and glassy rhyolite. The flood volcano separated with shield volcano by reddish colored paleosol (near to 30 cm thickness). Farther volcanic rocks of the study area can be classified into mafic and felsic based on their color and visible mineralogical composition. The mappable rock units that are found in the study area are lower basalt, upper basalt, rhyolitic lava, rhyolitic tuff, and friable tuff. Furthermore, the study area is associated with geological structures such as joints and faults. The detailed field description for the lithological units, stratigraphic section, and their associated geological structure is discussed as follows.

3.1. Volcanic successions

From the combination of studies in the field description, geological mapping, and by using GPS elevation recording the surrounding Lake Hayk volcanic products from bottom to top are lower basalt, upper basalt, rhyolitic lava, rhyolitic ignimbrite, rhyolitic tuff, and intercalation of friable tuff with rhyolite and shield basalt. From those rock units representative fresh samples were collected and utilized for the analysis of petrographic and geochemical analysis. The surrounding Lake Hayk flood basalt, rhyolite, and shield volcanic products of sulula section from bottom to top are lower basalt, upper basalt, rhyolitic lava, rhyolitic ignimbrite, rhyolitic tuff, and intercalated friable tuff.

Amemo section from bottom to top are; lower basalt, friable tuff, rhyolite lava, rhyolitic ignimbrite, shield rhyolite, shied basalt and friable tuff. Gobeya section constitutes from bottom to top flood basalt, friable tuff, rhyolitic lava, friable tuff, shield rhyolite, shield basalt and friable tuff.

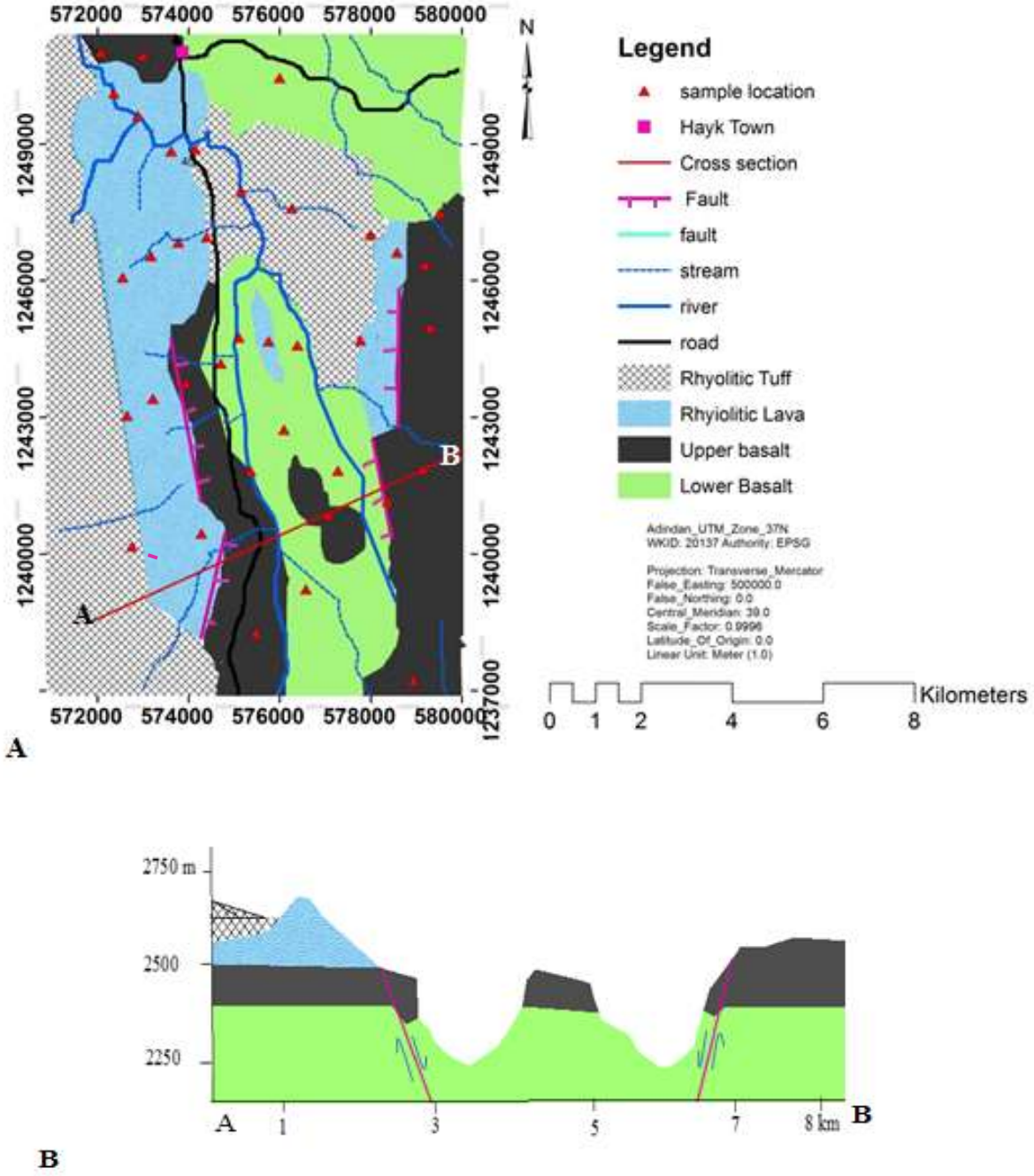

Fig 3. 1 (A), Geological map and (B), Geological cross (From A to B) section of Lake Hayk area

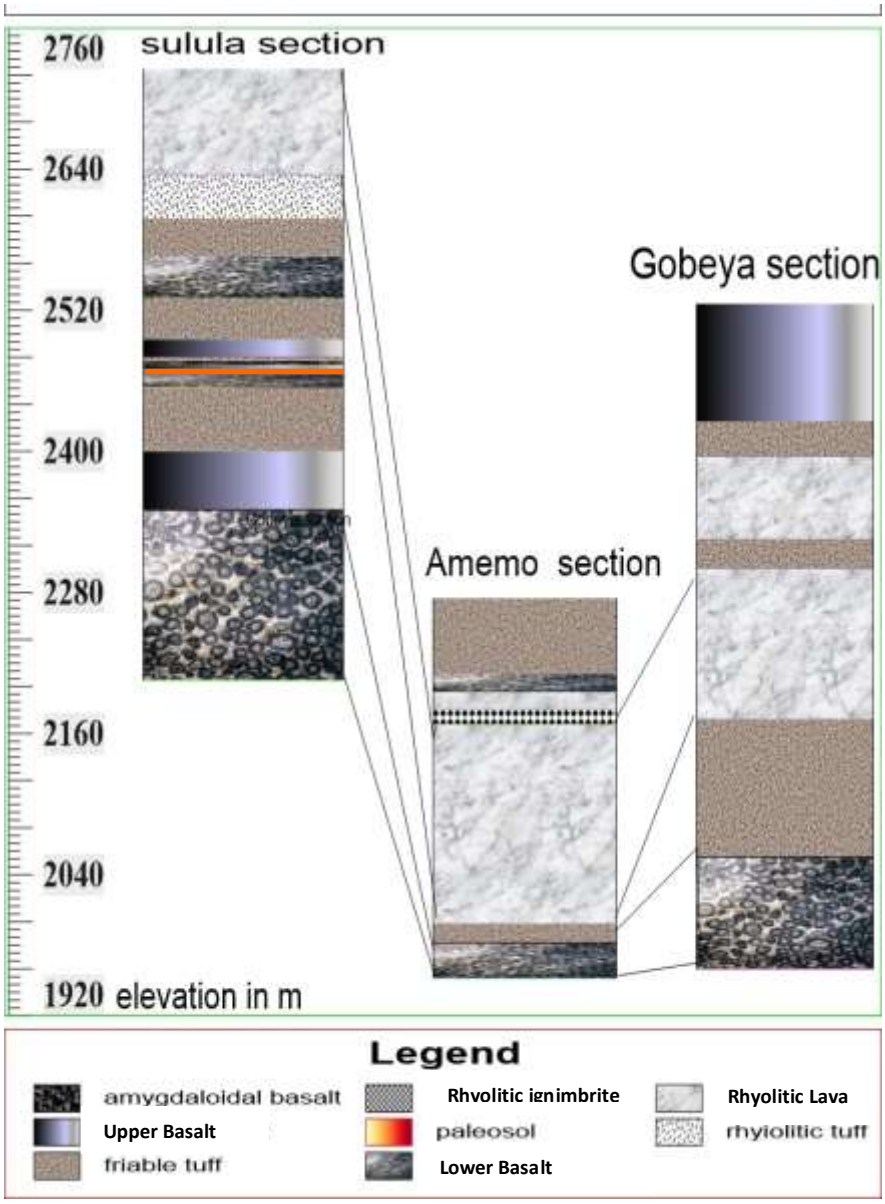

Fig 3. 2 Lithostratigraphic section of the study area

3.2 Petrographic Descriptions

3.2.1 Lower Basalt

This unit is found, in the study area mostly around Koseru,sulula, and the eastern part of Amemo. The lower basalt unit is stratigraphically overlian by upper basalt. it thick 70 -120 m whith black fresh and dark garay weatherd color. Furthermore, at the hand specimen level, this

unit is distinguished by its highly porphyritic texture with dominating olivine and plagioclase phenocrysts, which can be clearly identified without the need of a microscope. In addition, this unit is found generally as gentle forming topography which could be related to its forms lobes (basalt which is reach of oiliven and pyroxene phenocryst).

Fig 3. 3 field photograph of lower basalt A, lobe structure which is taken around korki town intercalated with lower flood basalt at the location of (0575284-1235046 -2468) B and C, lower basalt from the lower part of flood basalt. Note a pen scale for C and GPS for B at the location of (0575396: 1234356) D, Complex Columnar jointing observed at the top of rhyolitic lava sequence. Note hammer for scale.

3.2.2 Upper Basalt

This basaltic rock unit mostly covers eastern and southwestern part of the study area with commonly occurs as ridge forming unit and attains a maximum thickness of about 10(near sulula town) - 70m (around Gobeya ridge which is a border of lake Hayk and lake Hardibo). Moreover, the characteristic features of this rock unit are its black fresh color and light gray weathered (highly weathered on the most top of the ridge) color, aphyric texture, compact/massive and hard nature, cliff topography. In the eastern and western parts of the study area (around Amemo and Sulula) this rock unit is conformably underlain by porphyritic basalt rock unit and conformably overlain and intercalated by a friable tuff unit around sulula town.

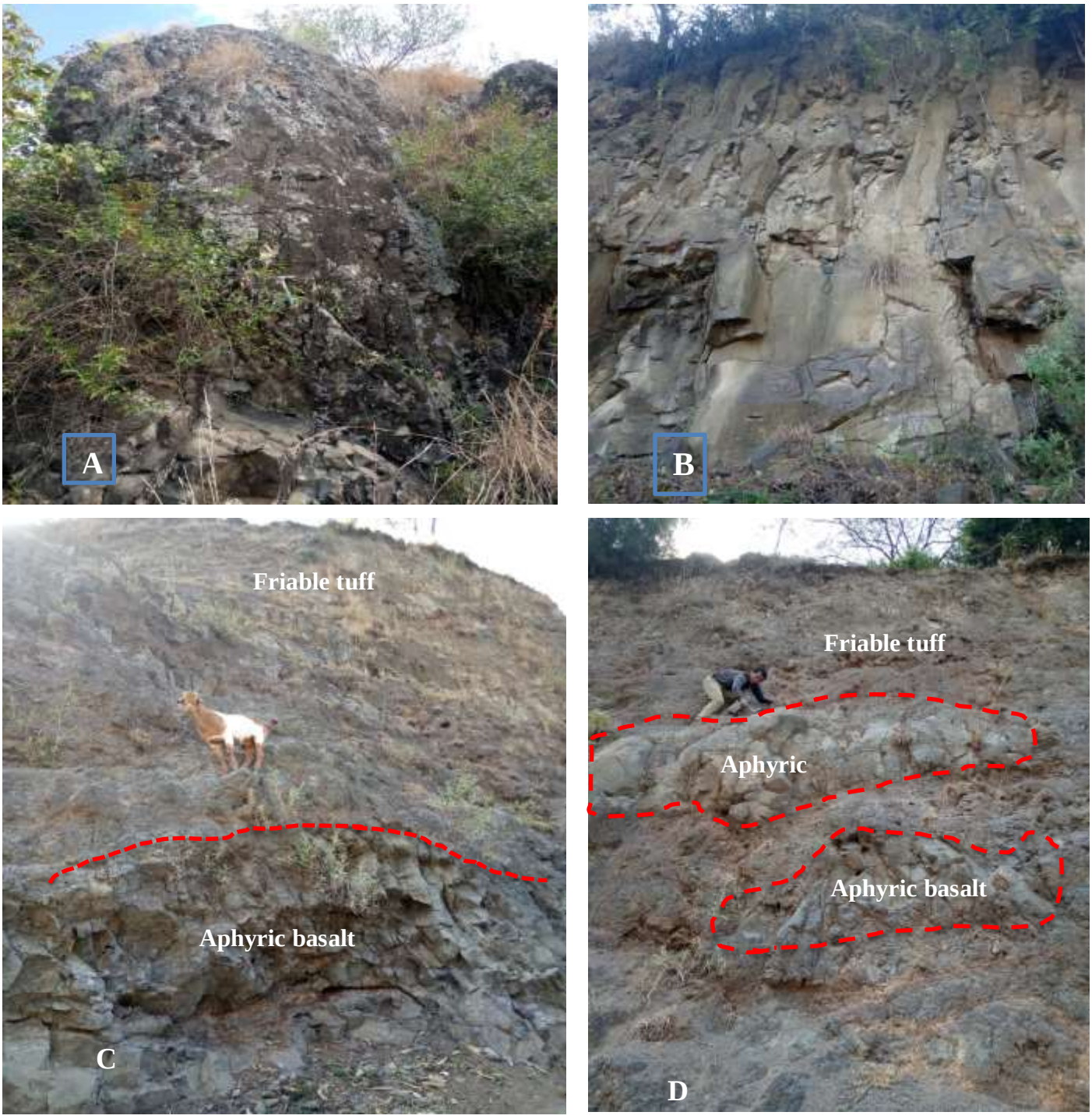

Fig 3. 4 field photograph of upper basalt A, upper basalt which is taken from at the top of Gobeya ridge northeastern part of the study area. (0575029 - 1241105) at an elevation of 2560 masl. B, upper basalt which from Mofa ridge western part of sulula town (0574149 -1241059) at

an elevation of 2300masl. C and D, field photograph shows upper basalt intercalated with friable tuff (0575029:1241105) at an elevation of 2202 masl.

3.2.3 Vesicular Basalt unit

This rock unit is exposed by river cut in the western and eastern part of Amemo and Sulula area. It is widely exposed along gentle topography. It is characterized by black fresh and gray weathered color, vesicular texture, and medium to coarse-grained. The basalt which is observed in the study area is porphyritic and vesicular in texture with the phenocrysts of olivine and plagioclase which is easily observed by naked at hand specimen.

Fig 3. 5 filed photograph of Vesicular basalt which has located (0575396E:1234356N)

3.2.4 Rhyolitic Lava

This rock unit is exposed almost in all parts of the study area but mostly southwestern and northwestern part of Hayk town and also its thickness vary from 10m (southwestern) to -230m (northwestern part). It is characterized by light grey to whitish fresh color and gray weathered color and there is also strongly welded and less welded rhyolite with glassy to the porphyritic

texture. This unites conformably (northwestern part of the study area) and unconformably overlies the flood basalts. The unconformable contact between the flood basalts and rhyolitic lava flows is marked by red clay (paleosol) and its thickness is varying between 10 cm to 30 cm. The unique or the typical property of rhyolite are clear stratification of flow layers or flow bandage especially in the northwestern part of the study area. It has vesicular (around gelan river at the top part of rhyolite unit it does have vesicles), porphyritic, and aphanite texture. It is exposed at the highest elevation compared to the other units. Sometimes it is associated with glassy rhyolite (obsidian) and pyroclastic materials, rhyolitic ignimbrite, and volcanic ash.

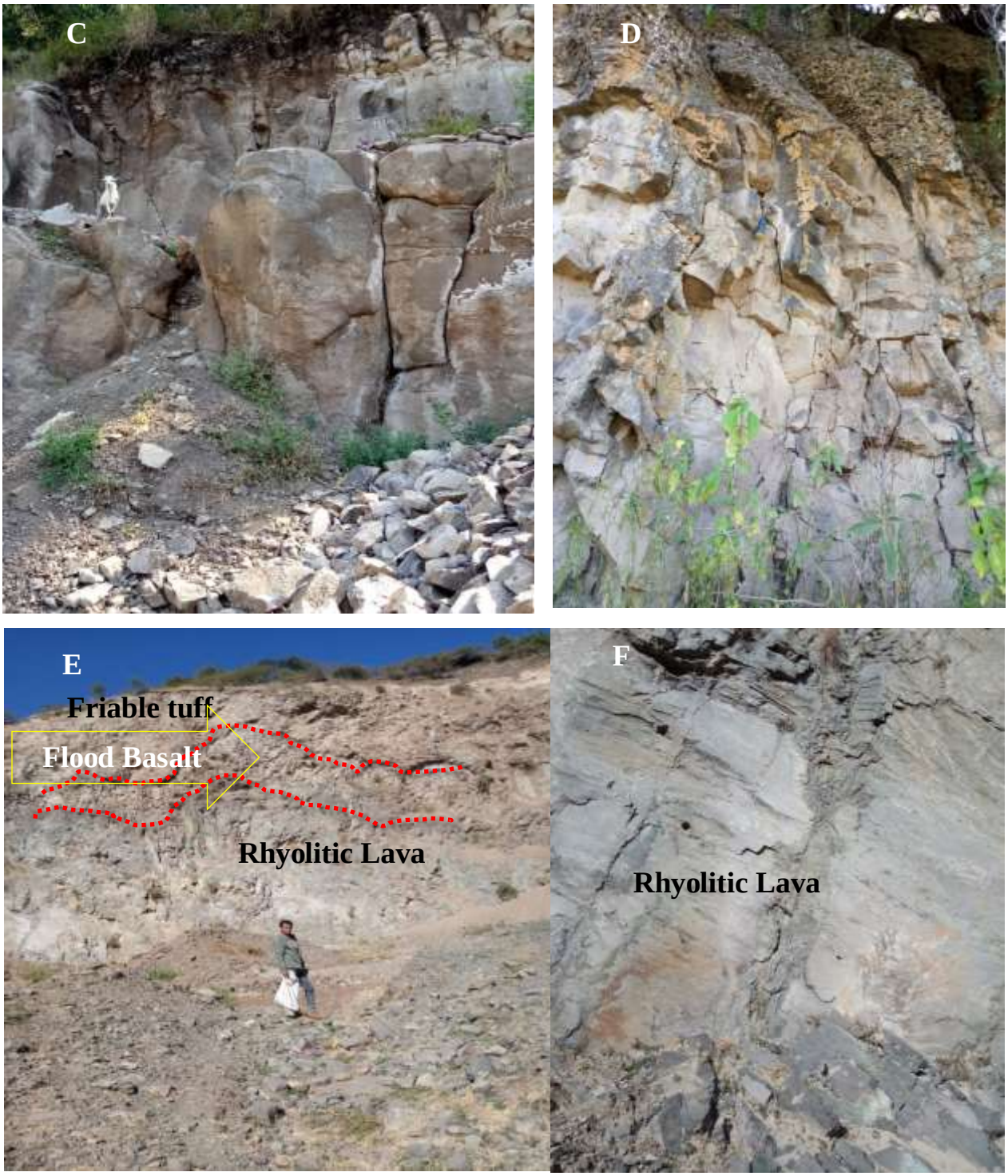

Fig 3. 6 field photograph of A,B and C are Rhyolite lava rock which shows strongly welded and underline by flood basalt A, location (0573183:1249769) B, location (0573362:1248648) C, location (0573049:1249577) D, rhyolitic lava there is vesicles at the top (0573195:1249180) E, which show intercalation of rhyolite(9 m) at the base, basalt at the middle (6 m), and friable tuff

at the top part (10 m) and F, rhyolitic lava which is the bottom from figure E and show a flow banding nature, location of both E and F (0572830:1248262)

3.2.5 Rhyolitic Tuff

Rhyolitic tuff and poorly welded rhyolite is exposed in all parts of the study area mostly the southwestern part of the study area and its outcrop is commonly exposed in a road cut and natural cliff. Which has horizontal alignment and intercalate with basalt and rhyolite rock unite. It has whitish, grey, and sometimes reddish weathered colors. It does have an easily friable nature and variable thickness from 1-10 m. This is characterized by its friable and unconsolidated nature, pyroclastic texture. In addition, this rock unit contains lithic fragments. In some parts of the study area less welded rhyolite unconformably underlain and overlain basalt and rhyolite and marked by paleosol.

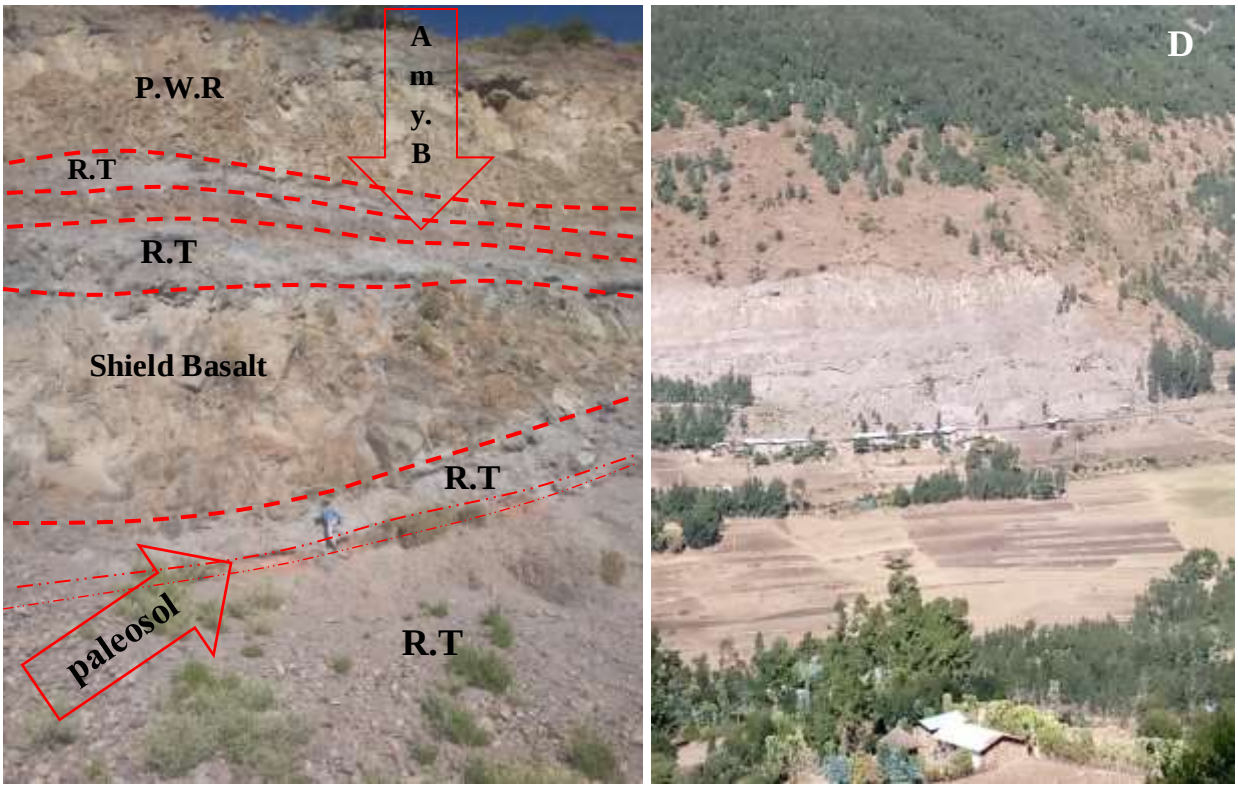

Fig 3. 7 field photograph of Friable tuff A, highly weathered reddish color friable tuff at the location of (057847:124666) B, friable tuff intercalated with aphyric basalt at the location of (0574334:1234996) exposed by road cut. C, it is the bottom part of the figure shown in D this section is near to sulula town exposed by a road cut, and part of shield volcano show intercalation of strongly welded rhyolite, P.W.R = poorly welded rhyolite, shield basalt, and amygdaloidal basalt. R.T = rhyolitic Tuff, Amy.B = amygdaloidal basalt

3.2.6 Rhyolitic Ignimbrite

These are moderate to strongly welded rhyolitic ignimbrites of pyroclastic deposits. It occurs as a distinct gentle to steep slope forming unit. The strongly welded Rhyolitic ignimbrite is exposed and sampled southwestern part of Hayk town around Gela River. It has a light grey color to dirty color (contain green, gray, black colored clasts). It is observed resting on a massive ash deposit that overlies the felsic rhyolitic rock. With detailed observation, it contains clasts and up to 20% lithic fragments. The size of the fragments is ranging from tiny sand size up to about 5-6 cm diameter. The rhyolitic ignimbrites generally underlay conformably on the rhyolite sequence.

Fig 3. 8 Field photograph of rhyolitic ignimbrite (0572830:1248262)

3.2.7 Pyroclastic breccia

The outcrop of this rock unit is on the floor of Gelan River and the western part of Amemo area is characterized by the abundance of large blocks (often exceeding 1m) and a more significant presence of the matrix. Pyroclastic breccias are from medium to coarse-grained, massive, and highly compacted by the fine-grained matrix material. Poorly sorted grain size features have been detected in the research area only locally, at particular levels, and on a few meter extensions. The breccia is mostly made up of angular volcaniclasts that range in size from a few centimeters to a meter in diameter. The volcaniclasts ranges from subangular to angular.

Fig 3. 9 field photograph of pyroclastic rock with large blocks both (0573049-1249577) at elevation of 1960

3.2.8 Volcanic Ash

This rock unit is exposed dominantly in the steep slope area of the eastern part of Sulula and western part of Amemo area and thickness varies between 4-5m. It has white fresh color and gray weathered color overlain by rhyolite and underline by aphyric basalt and associated with obsidian and pumice. It is a type of pyroclastic igneous rock formed from powder size to sand-size particles of igneous rock materials that have been blown into the air ejected from volcano and fall to the ground after the loss of the heat, its grain size is very fine to sand size.

Fig 3. 10 field photograph of volcanic ash (0574430:1241093)

3.2.9 Glassy Rhyolite

In the western part of the study area, the western part of Sulula and Amemo is obsidian associated with rhyolite, pumice and volcanic ash. It is found at a gentle to steep slope underlain by friable tuff and overlain by volcanic ash and also associated with rhyolite rock unit. It does have a black weathered and fresh color with conchodial texture.

Fig 3. 11 field photograph of Glassy rhyolite (0574483-1241128)

3.2.10 Pumice

This rock unit is found in the western part of the Amemo area. It is exposed in road cut site and topographically, located from steep slope underlain by fine volcanic ash and overlain by rhyolite. It is characterized by vesicular texture and grey to whitish fresh color and brownish weathered color. Within the pumice rock unit, there are different pyroclastic materials intercalated such as volcanic ash, unwelded tuff in some parts of the study area particularly, in the western part of Amemo area.

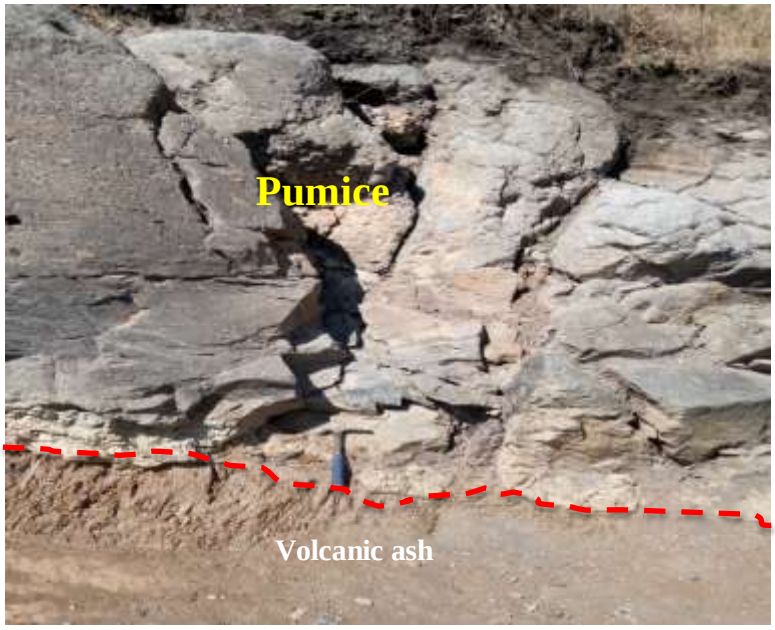

Fig 3. 12 field photograph of Pumice which has very light weight and underlain by volcanic ash at the location of (0573707: 1243329)

3.3 Geological structure

Geological structures are structures, which are formed due to geological processes. There are different geological structures found in the study area, most of these are formed during the marginal fault development and others as transverse structures. Some of the commonly observed structures in the study area are a fault and joints.

3.2.1 Beds Inclination

Lithological beds oriented $290^{o}/15^{o}$/NNE which is due to tectonic disturbance of the area which is part of western margin of afar depression.

3.2.2 Fault

Series of normal faults are found in study area and they are oriented $270^{o}/35^{o}$/NE located at 0573195 -1249180 and $315^{o}/45^{o}$/SW located 0575029 - 1241105 directions. These normal faults are dipping toward the graben and form the eastern and western escarpment of the graben. The type of fault found in the study area is normal fault.

3.2.3 Joint

This type of structure is observed in all part of the study area in all rock unit. The joint that recognized during the field were systematic to nonsystematic joint.

Fig 3.13 A , systematic joint in rhyolite rock unit which formed due to secondary geological process which is location of 0573195 - 1249180. B, columnar joint in basaltic rock which is formed due to primary geological process at location of 0573021 - 1249239

CHAPTER FOUR

PETROGRAPHIC STUDY

4.1 INTRODUCTION

For petrographic investigations 15 thin sections from representative rock samples have been prepared 8 from basalt, 6 from rhyolite, and 1 from ignimbrite rock unite. The analyzed samples were selected based on their stratigraphic location and lithologic unit variation. Mostly Porphyritic and seriate textures were found in the majority of the samples. The aphyric to severely porphyritic texture of the basalt observed in the study area is characterized by phenocrysts of clinopyroxene, plagioclase, and olivine with a groundmass of microcrystals of plagioclase, pyroxene, and opaque mineral (Fe-Ti oxide).

Rhyolite rock units, in addition to basalt rock samples, are characterized by an aphyric to porphyritic texture with phenocrysts of quartz and sanidine, and a groundmass of volcanic glass, as well as rock fragment and nepheline crystal in ignimbrite rock as a phenocryst. The petrographic analyses of the representative samples have been examined by using both plane-polarized light (PPL) and cross-polarized light (XPL). The petrographic description and analysis of the rock units are in detail described below and also in Appendix I.

4.2 Petrographic Descriptions

4.2.1 Olivine - Clinopyroxene Phyric Basalt

Petrographically, this rock unit is characterized by its highly porphyritic texture with phenocrysts of dominantly by olivine and secondly by clinopyroxene and embedded in groundmass very fine plagioclase and opaque mineral (Fe-Ti oxide).With a modal percentage of 70.51 – 76.8% phenocrysts of 36.88 - 41.5% olivine and 33.63 - 35.3% clinopyroxene and 15.3 – 23.2 % of groundmass of 8.6 - 9.5% microcrystalline plagioclase and 6.7 - 14.7% opaque mineral. The mineral grain shows a seriated texture because of the presence of a wide range of grain size variations from very fine plagioclase and clinopyroxene grain to coarse-grained olivine and clinopyroxene. Furthermore, olivine and clinopyroxene phenocrysts have a subhedral to euhedral shape, with irregular cracks and modest iddingsite alteration along the fissures in the olivine grain.

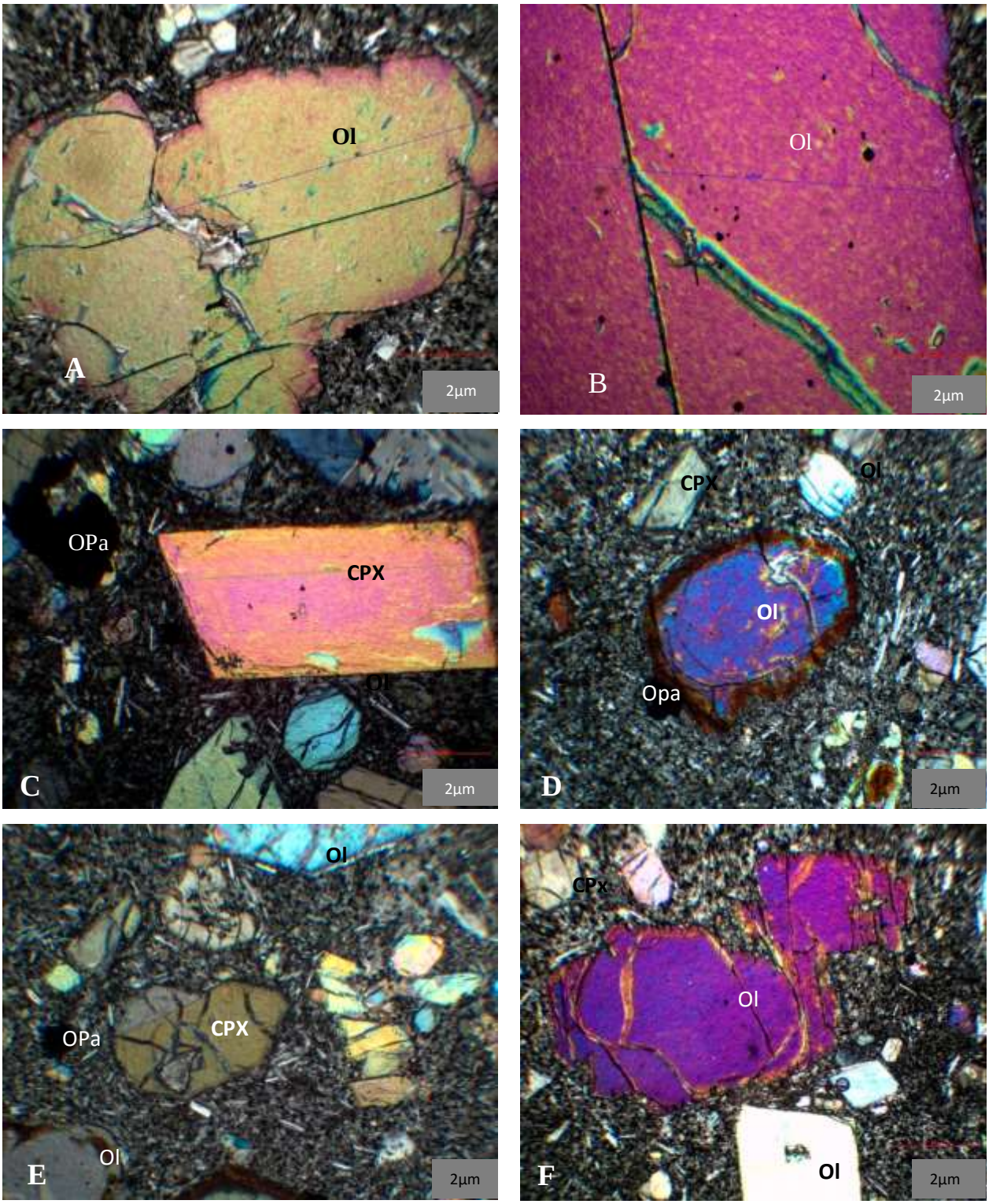

Fig.4. 1 microscopic photograph of Olivine-clinopyroxene phyric basalt of A, B, C and D, E, F are from sample T8S4 and T8S5 respectively A, Olivine (ol)-megacrystic texture embedded in the groundmass of fine-grained plagioclase and opaque (opa) mineral. Olivine grains are

subhedral and there is alteration within the fracture. B, a phenocryst of megacrystic of olivine with alteration following the fracture C, Euhedral to subhedral shaped phenocrysts of clinopyroxene with fine to coarse-grained laths and olivine embedded by fine-grained plagioclase groundmass.it shows a seriate texture. D, Subhedral to euhedral-shaped phenocrysts of megacryst olivine and embedded in a groundmass are dominantly fine-grained plagioclase laths and fine-grained clinopyroxene (CPX) with striate texture. E, Sub to euhedral-shaped clinopyroxene and olivine (show alteration at the border) are embedded in a groundmass of dominantly fine-grained plagioclase and the grain size show very fine plagioclase and opaque mineral to megacryst of clinopyroxene or it has a seriate texture. F, Subhedral to euhedral-shaped phenocrysts of megacryst olivine and embedded in a groundmass are dominantly fine-grained plagioclase laths and fine-grained clinopyroxene with striate texture

4.2.2 Aphyric Basalt

Basaltic rocks found in the study area which is aphyric in hand sample and petrographically microcrystalline in thin section when analyzed under petrographic microscope. These rocks have a dark gray color in hand samples, and crystals that are undetectable to the naked eye have a glassy appearance. In thin section, they contain few phenocrysts with some indistinguishable mineralogy in groundmass. The rock consists of <7% phenocrysts of euhedral to subhedral plagioclase and clinopyroxene. This unit is dominantly composed of microcrystal of plagioclase and with groundmass of pyroxenes and opaque mineral.

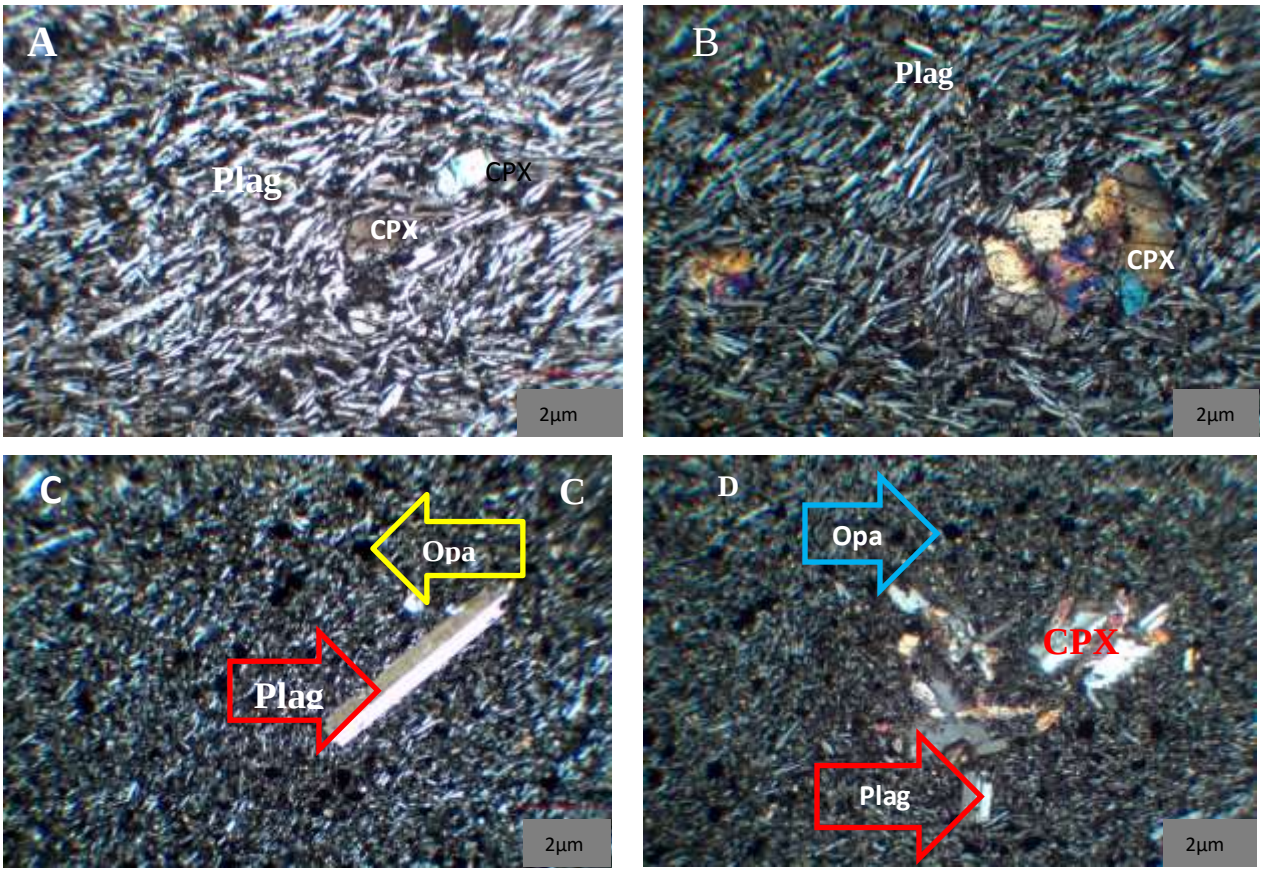

Fig4. 2 photograph of aphyric basalt under petrographic microscope of A and B from sample T5S2 and C and D from T6S4 A, intergranular texture (plagioclase and some pyroxene grain interlocked each other) or Aphyric–microcrystalline texture. The sample is from that overlying porphyritic flood basalt, (2247 masl). B, phenocryst of clinopyroxene surrounded in microcrystal of plagioclase and opaque minerals. C, Intersertal texture of aphyric basalt with elongated plagioclase embedded in microcrystals of plagioclase and opaque mineral. A sample is from on the upper flood basalt (2207 masl). D, Glomerophyric texture phenocryst of plagioclase and clinopyroxene embedded in microcrystal of pyroxene, plagioclase, and opaque minerals.

4.2.3 Plagioclase Phyric Basalt

Petrographically, this rock unit is characterized by its highly porphyritic texture with phenocrysts of plagioclase and embedded in the groundmass of microcrystals of plagioclase, clinopyroxene, and opaque mineral (Fe-Ti oxide). The modal composition of this rock unit is dominated by phenocrysts of plagioclases the mineralogical modal percentage is ~75.5% and ~24.3% groundmass, which are composed of 71.5 - 81.3% plagioclase phenocryst with a groundmass of

5 -18.7% clinopyroxene and 9.7 - 20% opaque mineral. Plagioclase, clinopyroxene, and opaque mineral microcrystalline textures account for the majority of the groundmass. In addition, plagioclase phenocrysts show subhedral to euhedral shape and occur as elongated penetrative twinning nature.

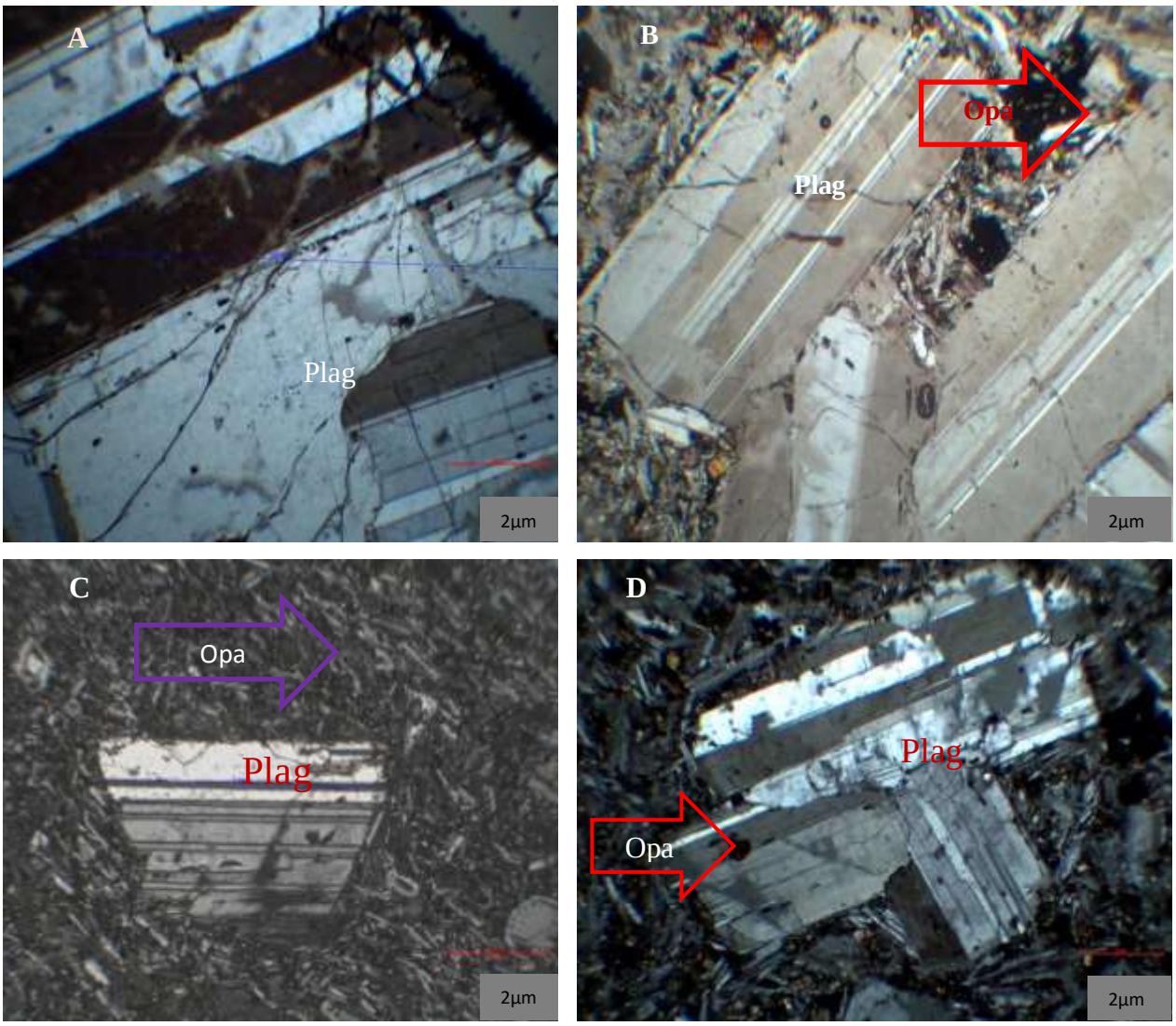

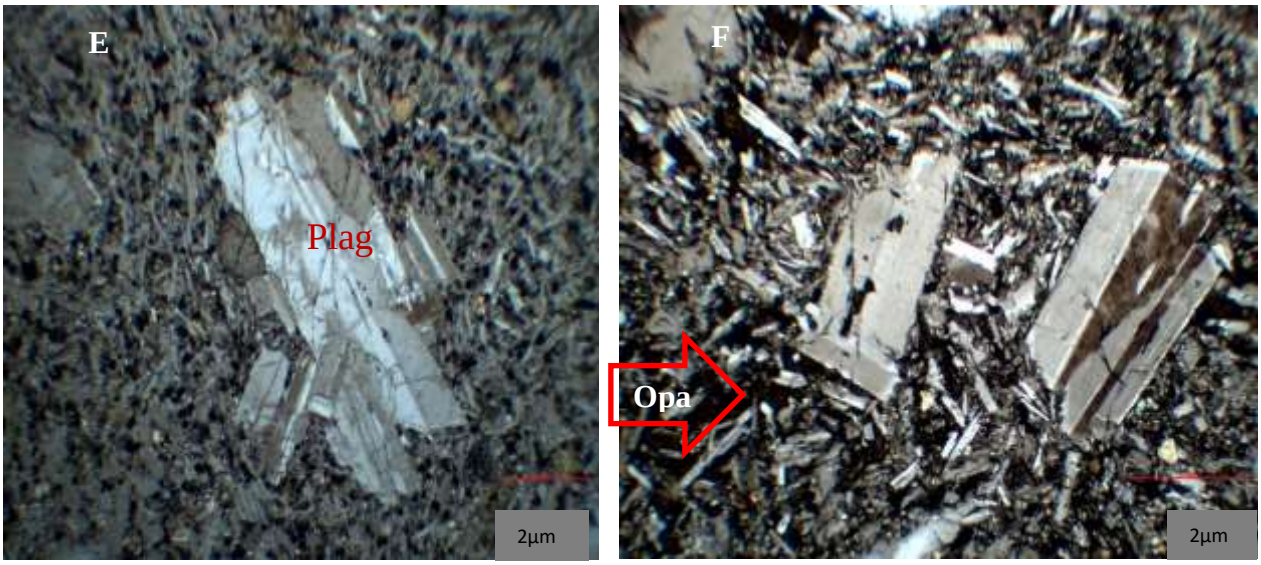

Fig 4. 3 photograph of plagioclase phyric basalt under petrographic microscope of A and C from sample T7S8, B, and D from T6S4, E from sample T9S4, and F from sample T1S5 A, Plag-megacrystic texture with oscillatory zoning subhedral shape. The sample is from the porphyritic flood basalt group. B, Phenocrysts of euhedral plagioclase crystals are embedded by an anhedral groundmass of clinopyroxene and opaque minerals of glomerophyric textured plagioclase. C, Plagioclase phenocryst with euhedral shape set in a groundmass of plagioclase microcrystals and opaque mineral. D, phenocryst of plagioclase embedded in opaque mineral (Fe-Ti oxides), clinopyroxene, and fine plagioclase groundmass, it has Glomerophyric texture, subhedral shape with oscillatory zoning. E, megacryst of plagioclase embedded in the fine grain of pyroxene, opaque mineral and plagioclase phenocryst of plagioclase show subhedral shape. F, plagioclase phenocryst with opaque mineral on the surface of plagioclase and embedded with opaque mineral and microcrystal of plagioclase. Note that the entire above microscopic photo pictures are under XPL and 4X magnifications and plagioclase phyric basalt.

4.2.4 Rhyolitic

Petrographically analyzed rhyolite rock samples such as T1S6, T4S5, T2S5, and T3S4. These rhyolitic rock samples show vitrophyric, Porphyritic, glassy, and banding texture flow. Phenocrysts are alkali feldspar (sanidine) and quartz minerals embedded in the groundmass of mainly volcanic glass and very few opaque minerals. Sample T3S4 shows that flow banding microstructure and felsic texture with phenocrysts (10%) and groundmass (90%). Sample T1S6,

T2S5, and T3S4 show similar petrographic characteristics. The rhyolite sample that petrographically analyzed shows porphyritic texture with 29.5-65.2% phenocrysts and 34.8-70.44% groundmass/volcanic glass. Compositionally, 18.5 - 27.5% sanidine, 3 - 35.7% quartz, 1% plagioclase, 4.2-8.9% opaque, and 30.8-62.3% a groundmass of microlithic sanidine, quartz, volcanic glass, and opaque. Once more, sample a similar petrographic characteristic.

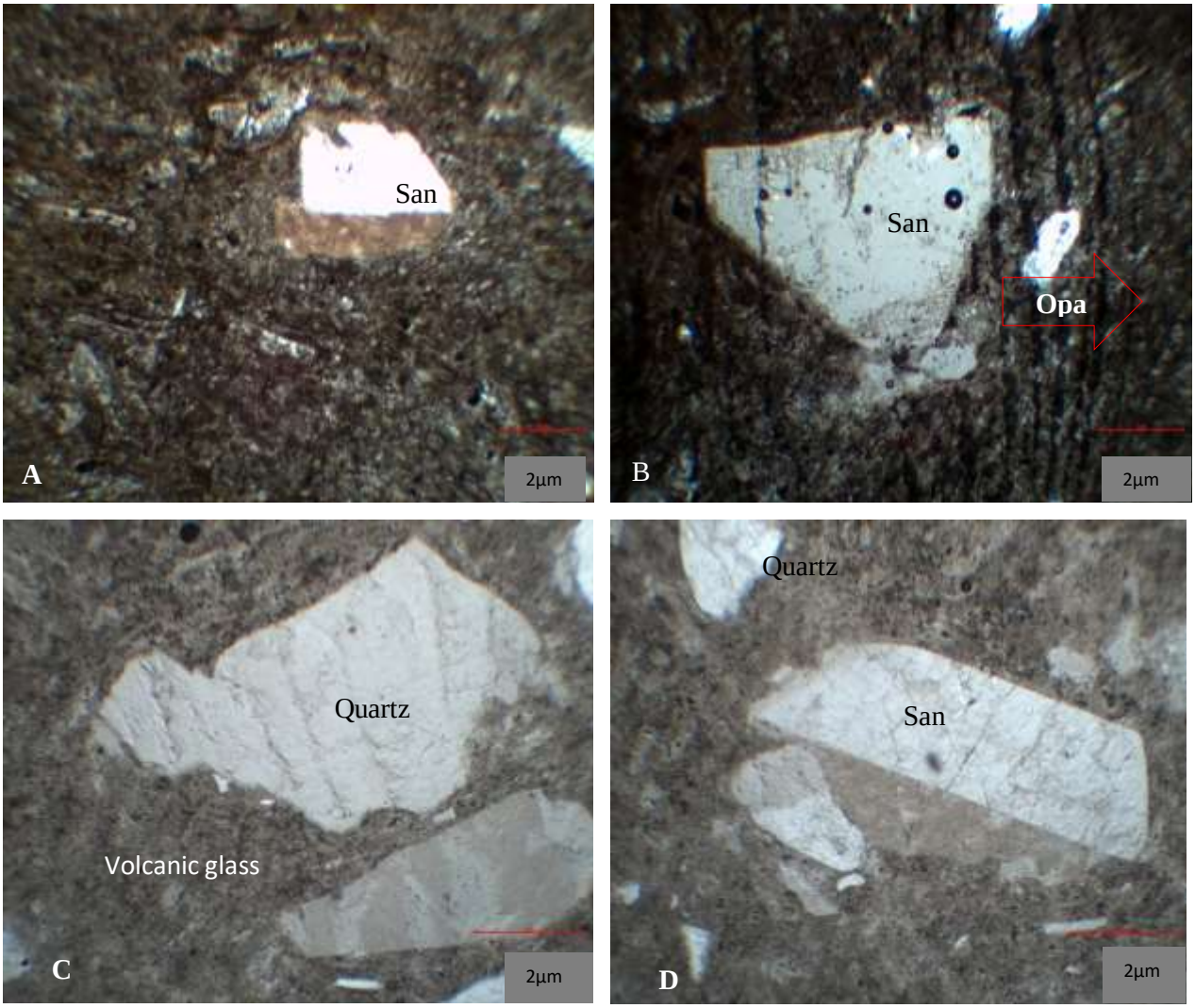

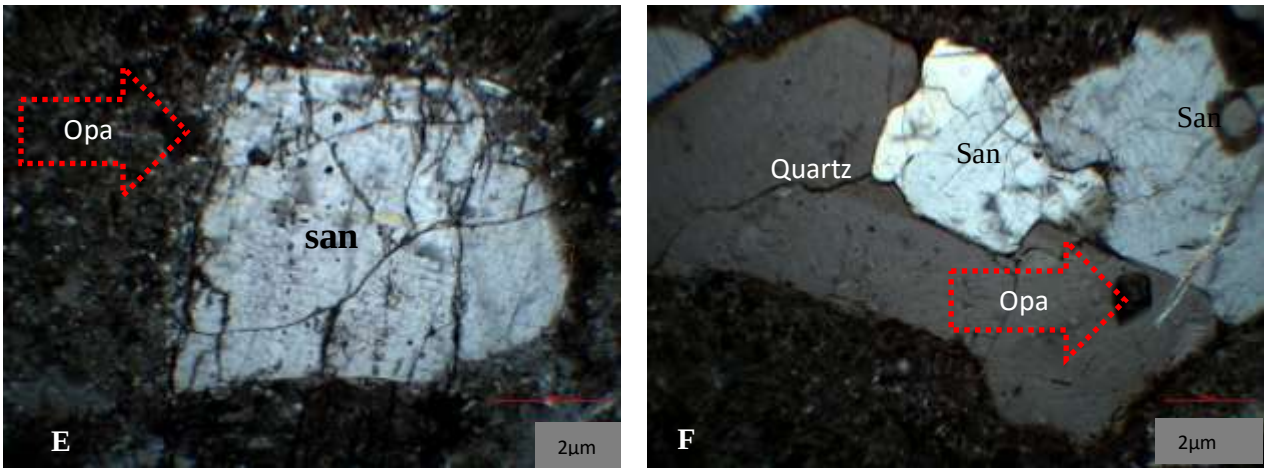

Fig 4. 4 photograph of rhyolite under petrographic microscope of A and B from sample T1S6,C, and D from T2S5, E from sampleT3S4 and F from sample T4S5 (A), phenocryst of sanidine with a groundmass of microlithic sanidine, and volcanic glass. (B), Megacryst of sanidine phenocryst in the groundmass of quartz and volcanic glass with flow banding texture. (C), subhedral quartz megacryst phenocryst with a groundmass of volcanic glass and opaque minerals and (D), euhedral sanidine and anhedral quartz phenocrysts embedded in volcanic glass and microlithic sanidine and quartz (E), a euhedral phenocryst of alkali feldspar (sanidine) embedded in volcanic glass and microlithic sanidine, and quartz (F), anhedral to subhedral sanidine and quartz embedded in volcanic glass.

4.2.5 Rhyolitic Ignimbrites

One sample T3S1 from the pyroclastic flow deposit is classified as welded tuff/ignimbrite. It has up to 21.25% nepheline, 3.75% clinopyroxene, perlitic crack 16%, 10.24% rock fragments, and 54.4% volcanic glass. Crystals are euhedral sanidine and anhedral clinopyroxene and quartz and also contain skeleton-like glass shards.

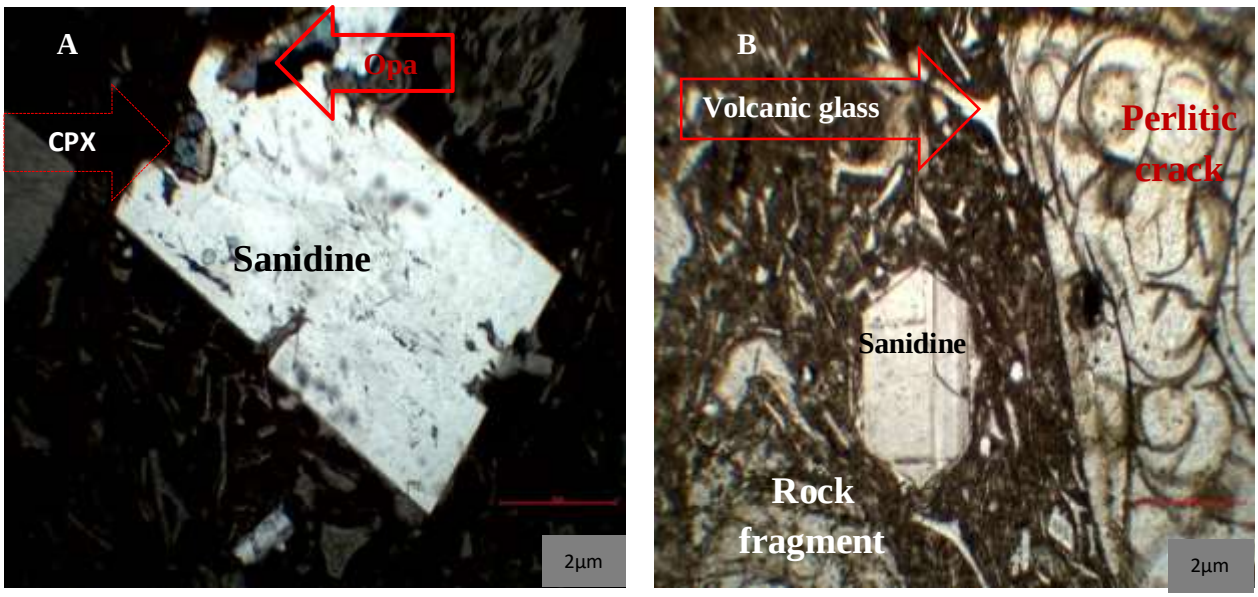

Fig 4. 5 Photograph of ignimbrite under petrographic microscope A and B from sample T3S1 (A), Rectangularlly developed euhedral shape sanidine, clinopyroxene and rock fragment with groundmass volcanic glass (B), phenocrysts of Perlitic crack (there is alteration following the cracks), hexagonal sanidine, rock fragments and embedded in the groundmass of volcanic glass. Both A and B are from ignimbrite/welded tuff samples at an elevation of 2027 masl and are under XPL, 4X.

CHAPTER FIVE

5. WHOLE ROCK GEOCHEMISTRY

5.1 INTRODUCTION

A total of 10 fresh samples were selected and analyzed for whole-rock geochemistry from flood basalts and rhyolite rock based on their stratigraphic position, types of rock/lithological variation from the study area, field description, and also by their petrographic examination. The analytical results for both major and trace elements are presented in table 5.1 below. Accordingly, most of the analyzed samples have a low loss on ignition (LOI) value ranging from 0.44-1.57wt% but there is one sample of LOI 3.07wt% and this indicates the samples are fresh and unaltered. Diagrams with their descriptions and interpretation of major elements are based on the recalculated volatile free basis results presented in appendix II. Major elements include SiO_2, Al_2O_3, Fe_2O_3, CaO, MgO, Na_2O, K_2O, TiO_2, and P_2O_5 account for more than 1% by weight in volcanic rock. Trace element abundances are used to determine whether minerals were present during melting or fractional crystallization using the Harker variation diagram and for Total Alkali-Silica (TAS) classification. The trace elements Ni, Cr, Sc, V, Ba, Sr, Zr, Y, Nb, Rb, and the rare earth elements (REEs) are the most common trace elements used to explain the petrogenesis of igneous rocks based spider diagram (normalized-chondrite and normalized-primitive mantle).

Table 5. 1: Geochemical data of Whole-rock of Lake Hayk volcanic rocks

	Oligocene Basalt			Basaltic andesite	Trachydasite		Oligocene Rhyolite			
Sample	T1S1	T2S3	T7S5	T7S1	T3S2	T3S6	T1S3	T3S4	T5S2	T2S1EA
Major elements in wt%										
SiO_2	45.5	48.4	48.5	55.9	63.7	66.7	69.7	71.3	72.3	77
TiO_2	3.04	2.08	2.37	1.96	1.04	1.08	0.41	0.54	0.71	0.47
Al_2O_3	11.9	15.25	14.25	15.15	15.55	13	14.65	11.95	13.65	10.5
Fe_2O_3	13.1	11.9	12.25	11.15	5.29	5.36	2.99	3.49	2.72	2.17
FeO	11.79	10.71	11.03	10	4.76	4.83	2.691	3.2	2.25	1.95
MnO	0.21	0.18	0.18	0.17	0.18	0.24	0.06	0.08	0.07	0.07
MgO	9.16	6.16	7.56	3.94	1.35	0.92	0.16	0.25	0.25	0.08
CaO	11.85	11.75	9.93	7.61	3.1	1	0.22	0.28	1.04	0.1
Na_2O	2.31	2.66	2.62	3.34	5.22	4.69	3.76	4.4	4.57	2.66
K_2O	0.88	0.45	0.81	1.88	2.58	4.48	4.09	5.02	4.21	5.53
P_2O_5	0.53	0.28	0.32	0.29	0.26	0.26	0.03	0.09	0.1	0.01
LOI	1.49	1.07	1.5	0.44	1.57	1.55	3.07	1.04	0.68	1.01
Total	100.13	100.27	100.42	101.94	99.98	99.39	99.19	98.48	100.39	99.61
#Mg	58.31	50.87	55.24	41.41	33.8	25.56	9.6	12.53	6.87	6.08
Trace element in ppm										
Sc	33	32	29	25	8	8	4	5	6	6
V	337	301	287	268	23	41	10	18	11	14
Cr	490	110	410	30	<10	10	<10	<10	<10	<10

Co	53	44	46	34	3	4	1	1	2	1
Ni	135	51	97	15	<1	13	4	2	3	1
Cu	159	96	40	31	1	6	1	1	1	<1
Zn	113	103	108	109	117	161	122	163	108	176
Ga	20.5	20.6	19.7	20.2	24.5	31	29.9	34.4	25.1	28.8
As	<5	<5	<5	<5	<5	<5	<5	5	<5	<5
Rb	20.6	8.5	10.9	40.2	67.8	102	111.5	123	124.5	136
Sr	546	471	405	342	455	222	26.5	30.1	151	7.6
Y	25.6	23.7	25.3	29.9	39.2	56.8	95.7	90.6	57.2	18.8
Zr	247	146	161	215	452	849	893	1010	623	1190
Yb	1.89	2.26	2.42	2.91	3.76	5.01	10.2	8.1	5.99	3.33
Nb	35.4	17	19.7	14.9	51.6	100.5	114.5	120	73.7	117
Mo	1	1	<1	1	3	2	2	1	2	<1
Ag	<0.5	<0.5	<0.5	<0.5	<0.5	<0.5	<0.5	<0.5	<0.5	<0.5
Cd	<0.5	0.5	0.6	0.5	<0.5	<0.5	<0.5	<0.5	<0.5	<0.5
Sn	2	1	1	2	3	5	5	7	3	8
Cs	0.33	0.11	0.07	0.22	1.26	0.66	0.81	0.76	1.01	0.61
Ba	256	176.5	260	501	738	774	430	343	698	105
La	31.1	18.1	19.5	27	52.7	88.2	106	104	79.6	59.8
Ce	66.4	39.3	42.1	54.9	110.5	190.5	103.5	219	149.5	92
Pr	9	5.5	5.61	6.98	13.8	24.3	28.4	28.7	19.25	10.1
Nd	37.8	24.4	24.6	30.5	57.4	99.5	110	116.5	74.3	39.9
Sm	8.1	5.8	5.63	6.56	11.15	20.5	21.8	24.9	14.25	7.57

Eu	2.33	1.88	1.9	1.88	3.09	5.28	3.12	4.82	2.66	1.44
Gd	6.82	5.81	5.81	6.48	10	16.45	18.7	21.1	12	5.46
Tb	0.94	0.88	0.88	0.97	1.42	2.31	2.99	3.27	1.9	0.76
Dy	5.45	5.13	4.98	5.52	7.51	12.1	17.8	17.9	10.6	3.89
Ho	0.91	0.92	0.93	1.09	1.39	2.19	3.36	3.28	2.02	0.77
Er	2.36	2.6	2.6	3.11	3.97	5.85	10.15	9.1	5.93	2.28
Tm	0.31	0.35	0.35	0.43	0.58	0.81	1.52	1.29	0.85	0.42
Yb	1.89	2.26	2.42	2.91	3.76	5.01	10.2	8.1	5.99	3.33
Lu	0.3	0.29	0.34	0.42	0.56	0.69	1.45	1.16	0.86	0.57
Hf	5.8	4	4	5.7	11.2	20.7	22.1	24.7	15.7	28.1
Ta	2.1	0.8	0.9	0.9	3.3	6.1	6.8	7.4	4.4	8.1
W	<1	<1	1	<1	1	1	2	1	1	1
Tl	<10	10	10	<10	<10	<10	10	<10	<10	<10
Pb	<2	<2	2	7	10	5	15	14	13	15
Th	2.9	1.5	2.1	2.93	7.2	11.65	17	16.05	14.3	16.9
U	0.86	0.43	0.43	0.48	2.39	4.04	3.4	5.23	3.38	1.18
Eu/Eu*	0.98	1.00	1.01	0.89	0.90	0.88	0.48	0.65	0.63	0.62

#Mg = {(MgO/40)/ (MgO/40+ Fe_2O_3/80)}*100 (Wager and Deer, 1939)

Eu* = EuN/(SmN + GdN)$^{1/2}$; Miller and Harris, 2007)

FeOt = Fe_2O_3* 0.9 (Rollinson, 1993)

5.2. Classification variation diagram

Igneous rocks classified using silica content (SiO_2%), into acidic > 66 wt%, intermediate 52-66 wt%, basic 45 to 52 wt%, and ultra-basic <45 wt; whereas the volcanic rock in lake Hake are basic (45.5 – 48.5), intermediate(55.9 - 63.7) and acidic (66.7 - 77) SiO_2%. In addition major element variation diagram of SiO_2 versus $Na_2O + K_2O$ (wt %) used to classify rock suites based on chemical composition. Lake Hayk volcanic rocks are classed as basalt, basaltic andesite, trachydacite, and rhyolite using Total Alkali-Silica (TAS) classification diagrams (following Le Bas et al, 1986). The samples are T1S1 (46.2 wt % of SiO_2), T2S3 (48.84 wt% of SiO_2) and T7S5 (49.1 wt% of SiO_2) which is basaltic rock, sample T7S1 (55.13 wt% of SiO_2) which is basaltic andesite rock and T3S2, T3S6, T1S3, T3S4, T5S2 and T2S1 with 64.82, 68.25, 72.55, 73.3, 72.76 and 78.1 wt% of SiO_2 respectively and the first two samples are trachydacite and the second consecutive four samples are rhyolite (fig.5.1). One of trachydacite (T3S6) fall in the alkaline field and T1S1and T3S4 are on the boundary line of alkaline and sub alkaline/tholeiitic field but the other basaltic to rhyolitic rock are sub alkaline/tholeiitic which indicating mostly transitional to sub-alkaline/tholeiitic affinity. However, samples T1S1 and T3S4 have a transitional affinity relative to other rock sample. These classifications show a bimodal composition with scars intermediate (andesite and trachy-andesite) composition.

The CIPW normative minerals value is important to characterize basalts, basaltic andesite, trachydacite, and rhyolite rocks. The normative data of the analyzed rock units are presented in appendix II, show that all basaltic to rhyolitic rock unit contain Hypersthene (7.56 – 13.46 wt %) and quartz normative (3.37 – 11.17 wt %) which suggest that these rocks are classified as silica oversaturated; exceptionally T1S1 which has lower silica (45.5wt %) and higher #Mg (58.31) concentration is olivine (2.62) and hypersthene (9.68) normative which is classified as silica undersaturated. Only one rhyolite (T3S4) rock which have Acmite normative = 3.273 wt% classified as peralkaline rock; whereas the other are peraluminous.

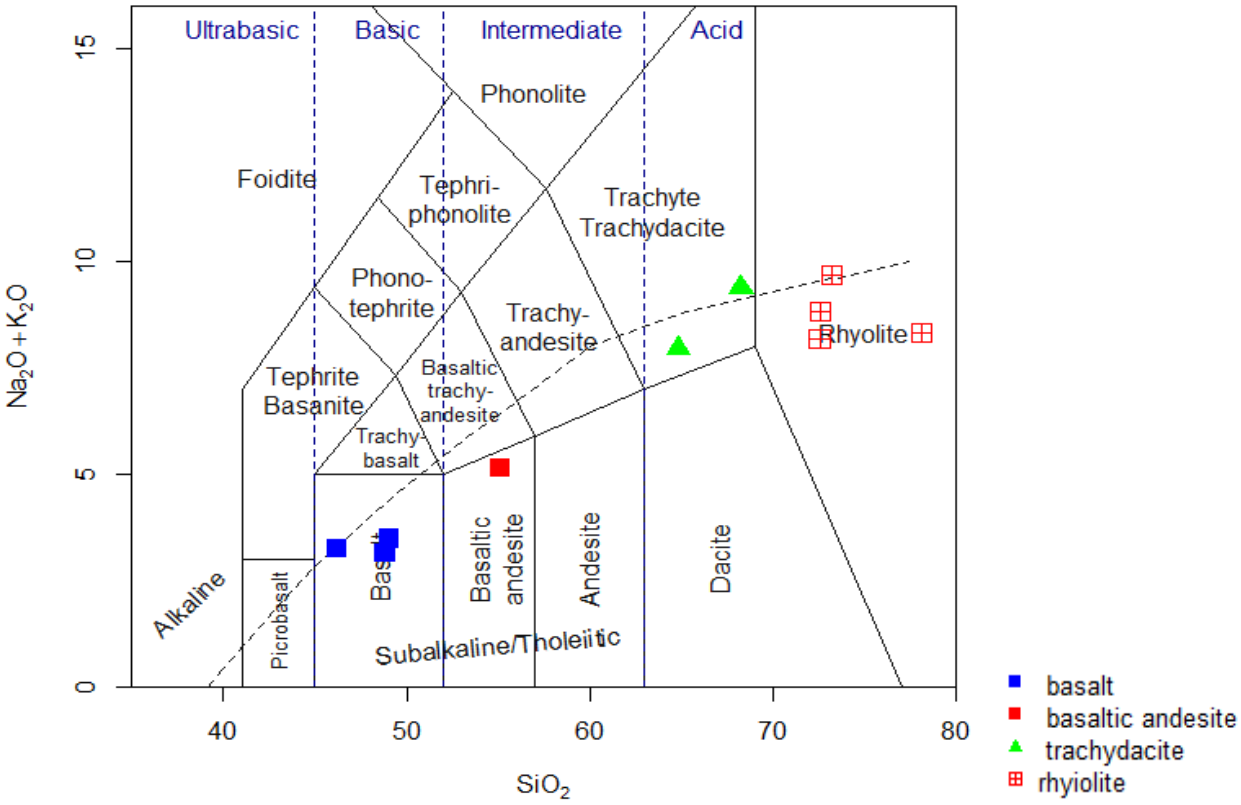

Fig 5. 1: TAS classification diagrams of Lake Hayk flood basalts to rhyolite.

5.3. Major element variation diagrams

Major elements against silica SiO_2 are illustrated below in Harker variation diagram (Fig.5.2). The SiO_2 (which show large variation) is taken as the x-axis and used as a differentiation index in variation diagrams constructed for major element which are at the y-axis; because SiO_2 shows a wide range of variation (45.5 to 77 wt%). Major element concentration is variable for the analyzed rock sample. Flood basalts, relative to rhyolite of the study area, have a very higher concentration of TiO_2, FeOt, MnO, CaO, P_2O_5, Al_2O_3, but a lower concentration of, SiO_2, K_2O, and Na_2O.The examined samples loss of ignition (LOI) ranges from 0.44 to 1.57 %, showing that the sample is fresh; whereas one sample (T1S3) has a LoI of 3.07 %, showing that it has minimal alteration compared to the other samples. The major element against SiO_2 plots shows both positive and negative correlations. MgO, FeOt, TiO_2, and CaO have negative correlations as a function of SiO_2, but K_2O against SiO_2 variation diagrams have a well-defined positive correlation, whereas Na_2O against SiO_2 show a positive correlation for basalt to trachydacite and becoming negative correlation after (~70 wt.%) inflection points and declined in rhyolite. Further

Al_2O_3 shows a positive trend at low SiO_2 and inflicted when silica concentration increased and Al_2O_3 declined and P_2O_5 show a negative trend of continuous decreasing but not sharply as the other negatively correlated major oxides as SiO_2 continuously increasing.

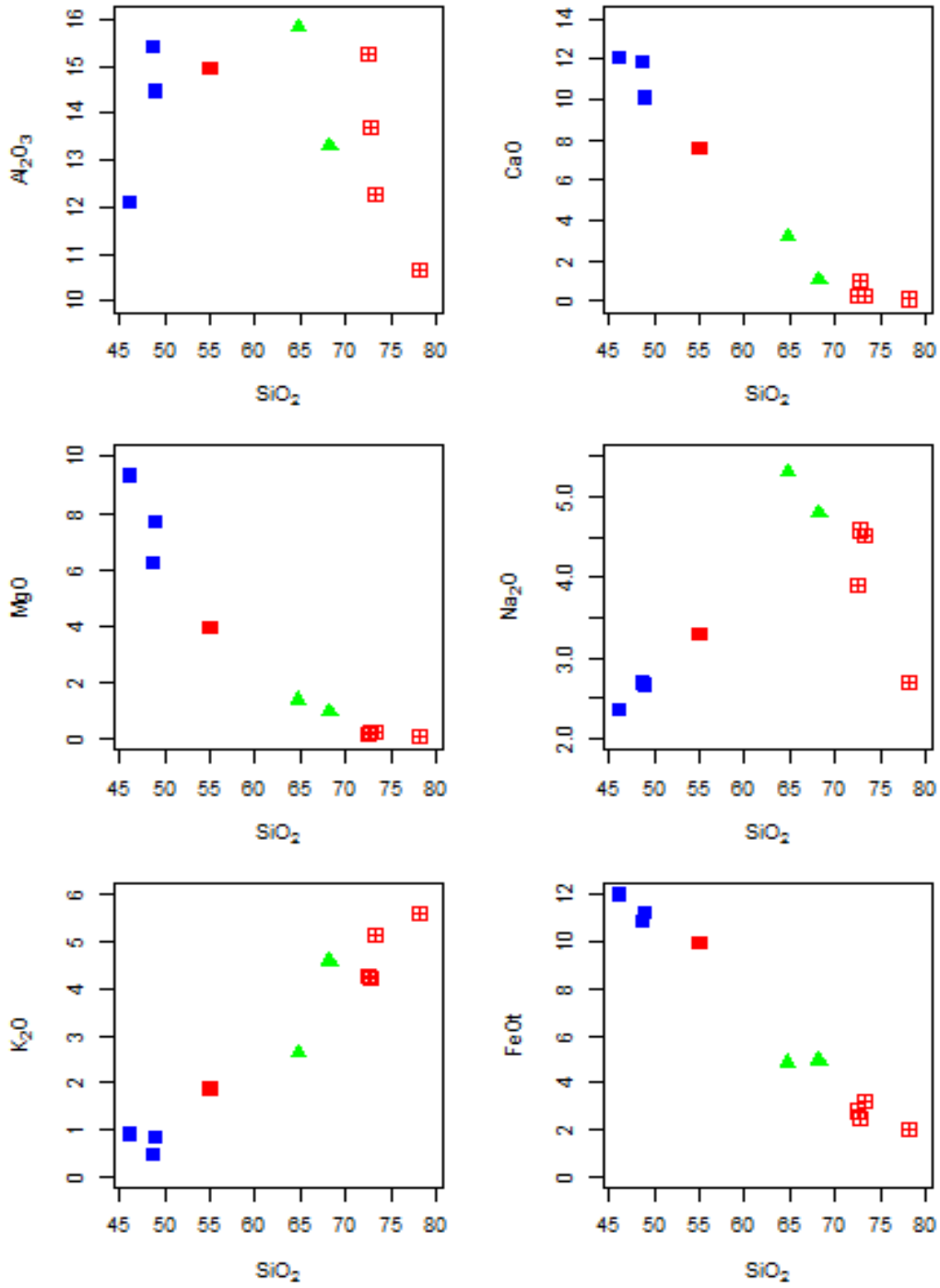

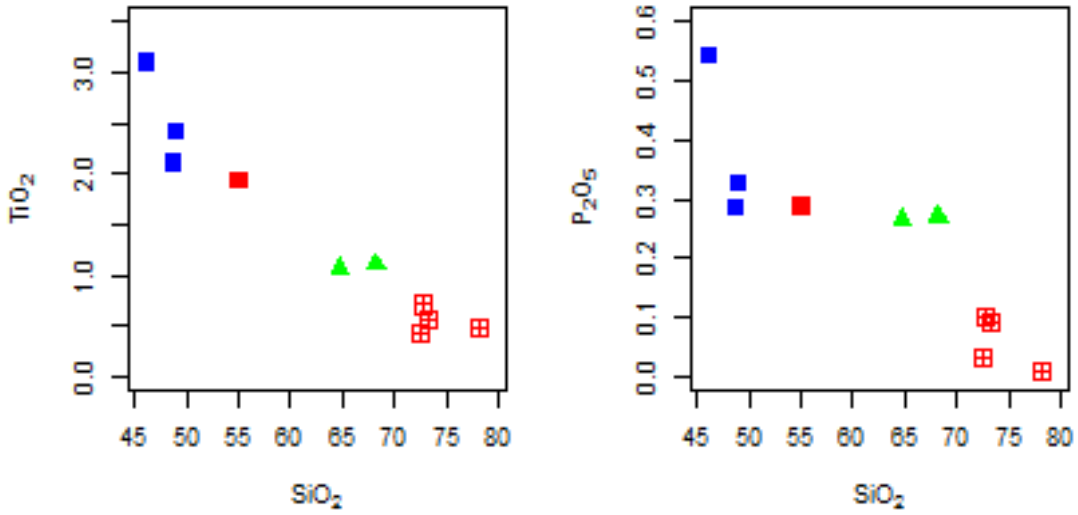

Fig 5. 2 Harker variation diagrams of major element against SiO_2 for Lake Hayk volcanic rock.

5.4. Trace element variation diagrams

Trace elements constitute small fractions in the phase with concentrations of < 0.1 expressed in ppm and the geochemical data analyzed, synthesized, and presented. Trace elements are mandatory for providing geochemical and geological (petrogenesis and source rock) information regardless of their abundance in the system of interest. The most common incompatible elements are large ion Lithophile (LIL)/low field strength elements (Cs, K(not shown figure), Rb, Eu, Ba, and Sr) and high field strength (HFS) elements (e.g. Zr, Hf, Ti, Nb, Th, U, Ce, Ta, and Pb). In Fig.5.3, diagrams of incompatible trace element (ppm) variation as a function of SiO_2 demonstrate a clear trend of magma generation and evolution. K and Rb have a significant positive correlation/trend as a function of SiO_2, but Sr has a strong negative correlation/trend. Eu as a function of SiO_2 decrease at low SiO_2 then increase as SiO_2 and sharply decreased after SiO_2 > 65 wt % and Ba positively correlated but after the concentration of SiO_2 > 68wt% then continuously decreasing in rhyolite. Positively steep slope increasing in incompatible elements of Rb and K is from basalt towards rhyolite. Variation diagrams of HFSE (U, Hf, Y(which is not shown in the diagram below) Th, La, Zr, Nb,) against SiO_2 plotted in below (Fig.5.3) show positive correlations variably with well-defined evolution trend. Plots of Th, U, La, Zr, Hf, and Nb as a function of SiO_2 show negative correlation up to ~50 wt% then gradually increase and positive correlation with SiO_2, but narrow variation for those incompatible elements as silica

increase spatially in La and U negatively correlated after ~70 wt%; whereas, Pb against SiO_2 show positive correlation and Y gradually increase up to ~65 wt% and in between ~65 wt% - ~70 wt% sharply increase and positively correlated; whereas after > 70 wt% inflected and negatively correlated.

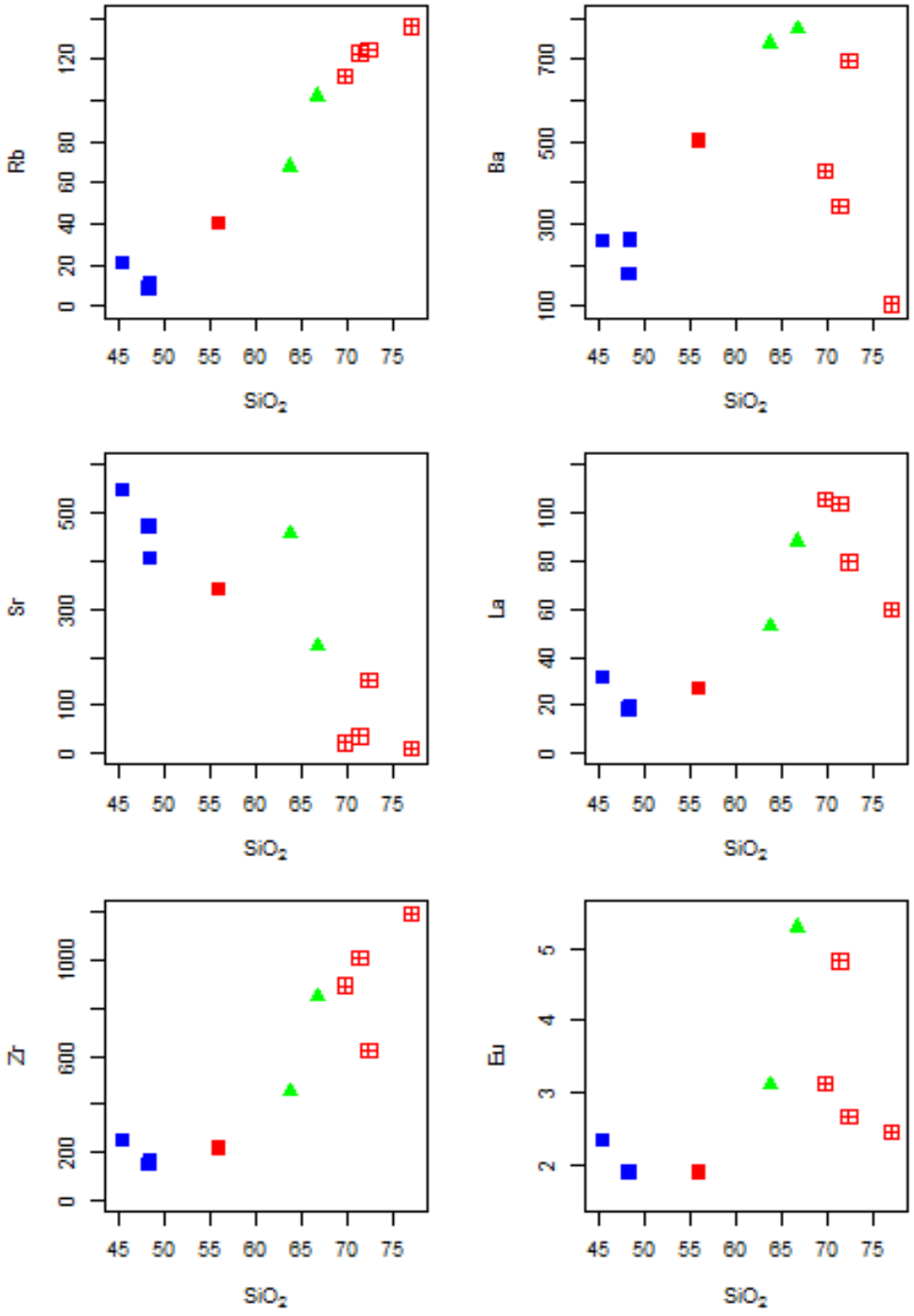

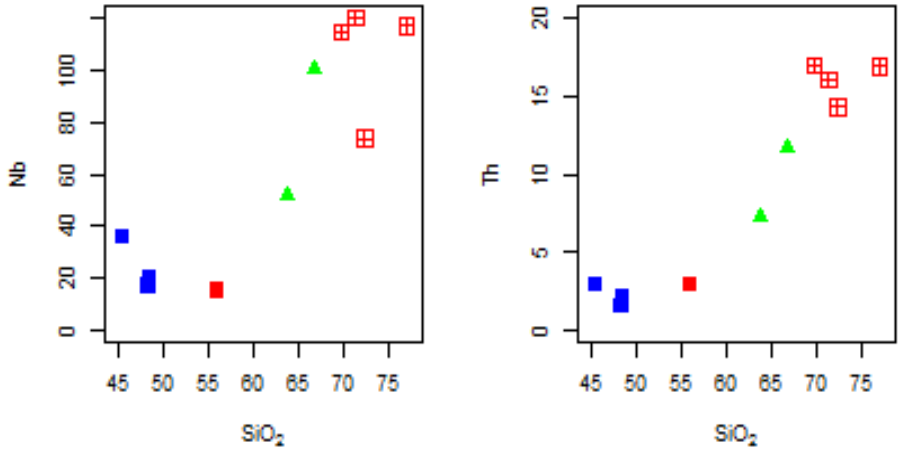

Fig 5. 3 Harker variation diagrams of Trace element against SiO_2. Symbols are the same as in Fig.5.1.

The magma evolutions of the volcanic products can be additionally determined from highly compatible trace elements such as Ni and V shown in (fig 5.4) and Cr and Co not shown in the figure. The samples concentrations of V vary from 287- 337 ppm, 268 ppm, 23-41 ppm, 10-18ppm, Ni ranges in 51-135 ppm,15 ppm, <1-13 ppm,1-3 ppm, Co ranges in 44-53 ppm,34 ppm, 3-4 ppm 1-2 ppm, Cr ranges in 110-490 ppm,30 ppm, <10-10 ppm and <10 ppm of basalt, basaltic andesite, Trachydasite, and rhyolite based on TAS classification respectively for each compatible elements. All compatible elements in the variation diagrams show negative correlation plotted as a function of SiO_2 wt % but Ni and Cr sharply decrease relative to V and Co. Generally, these elements are enriched in basalts, progressively depleted in intermediate and rhyolite. This shows almost similar characteristics to corresponding major elements having negative correlation e.g. Fe_2O_3, MgO, CaO, and TiO_2. Magma differentiation also traced from the concentrations of these highly compatible trace elements and #Mg (50.37-58.31% for basalts, 41.41% for basaltic andesite, 25.56-33.8% for trachydacite, and 6.08-12.53% for rhyolite) values. Basalts have higher #Mg values than intermediate to felsic units has lower concentration through differentiation processes of magma.

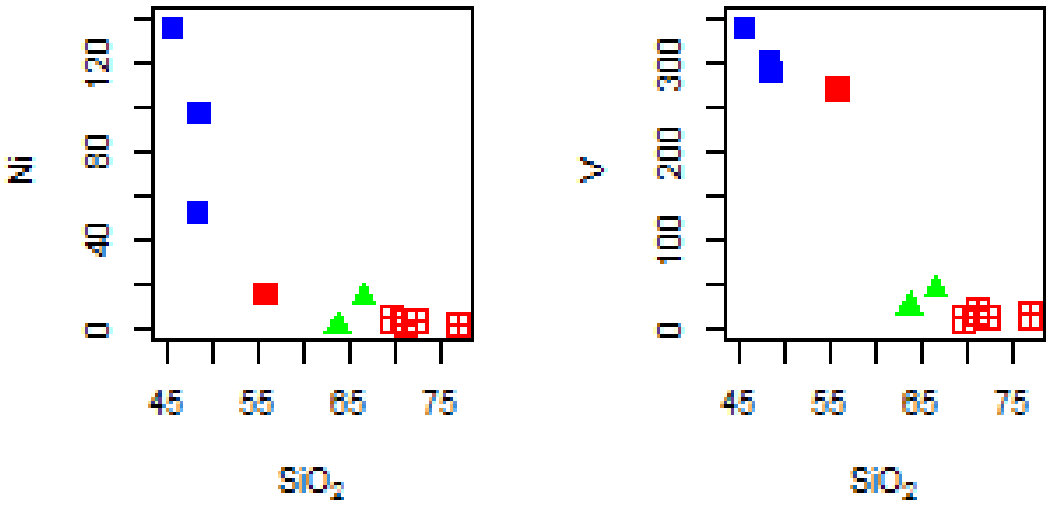

Fig 5. 4 Harker Variation diagrams for compatible trace elements (ppm) as a function of SiO_2 (wt %) symbols are the same as in (fig.5.1)

5.5. Spider Diagrams for Trace Element

The spider diagram of mafic to felsic rocks is plotted in (fig.5.5) below. All the basaltic and rhyolitic samples are parallel and trachydacite to rhyolitic samples show sub-parallel patterns. The chondrite normalized REEs diagram of mafic, intermediate, and rhyolitic rocks are enriched in LREEs elements, but felsic rocks are much more enriched in REE than intermediate and mafic rocks as illustrated in (Fig.5.5). Further T1S1 sample of basaltic rock has higher LREE and lower HREE than other basalt and basaltic andesite (which has a higher concentration of REE than basalt except for T1S1 and lower REE than trachydacite and rhyolitic rock). The sequence of REE enrichment in volcanic rocks for the Lake Hayk area is higher in LREE, intermediate in MREEs, and lower in HREE. The REE chondrite normalized diagram for samples shows a likely pattern of OIB basalt which is enriched in LREE and depleted in HREE. The break-in pattern is due to the concentration of Pm being below the detection limit during analysis and REE chondrite scattering shows a Pattern of the nearly steep sloping trend from La to Sm (LREE – MREE) and which tend to flatten from MREEs towards HREEs (Gd – Lu). The normalized value of Eu/Eu* is 0.98 -1.01 for mafic/ basalt, 0.88-0.89 for basaltic andesite to trachydacite, and 0.48 -0.65 for acidic/rhyolitic samples. Basaltic rock show slight negative anomaly of Ce

and also, There is one rhyolite sample (T1S3) showing highly depleted Ce than the other and also which has higher LOI 3.07.

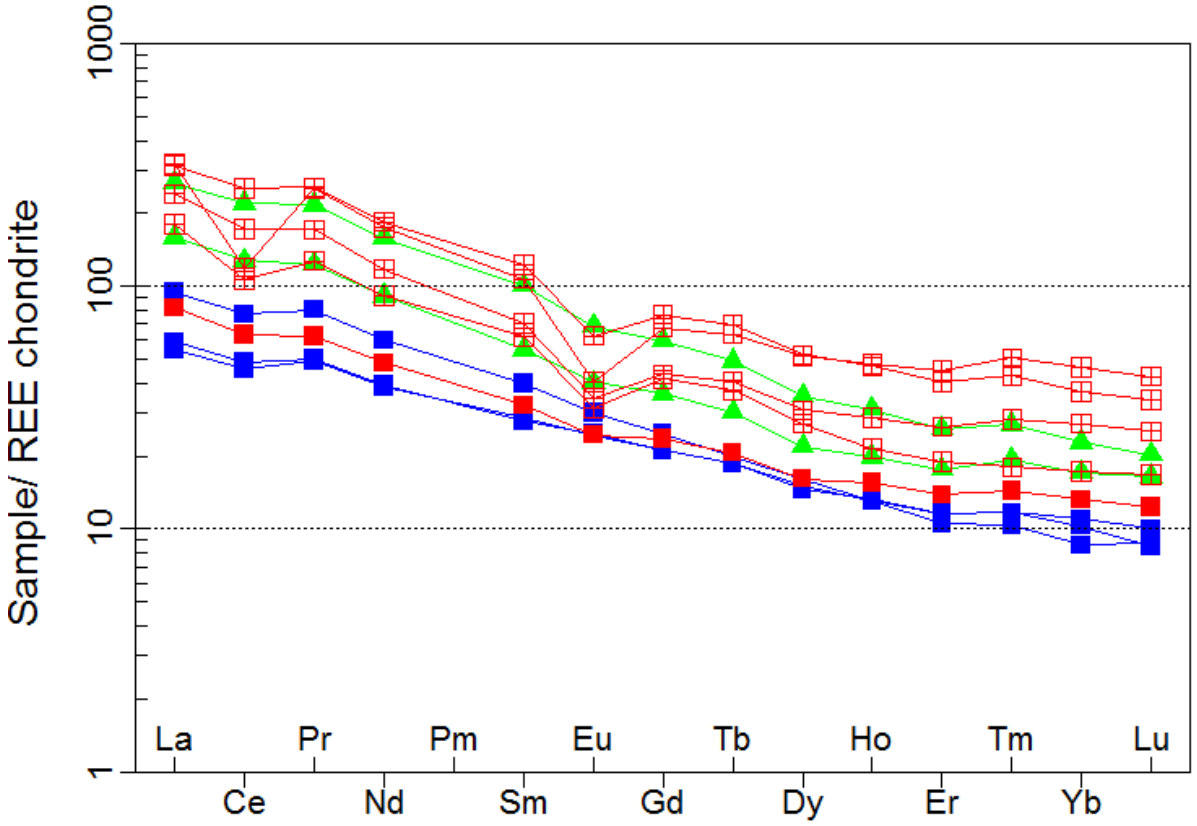

Fig 5. 5 Chondrite normalized REE pattern for Lake Hayk basalt to rhyolite. The normalization values are from Nakamura,(1974). Symbols are the same as in Fig. 5. 1.

The multi-element variation diagram is used to better understand and clarify the magmatic evolution of volcanic rocks in the Lake Hayk area (Fig 5.6). Spider diagrams made with primitive mantle can also be used to understand the evolution of Lake Hayk volcanic products (McDonough , 1989). Mafic to rhyolitic samples are enriched in highly incompatible elements and depleted in less incompatible elements, as illustrated in (fig. 5.6). The basalt rocks show Rb, Th, P, and Sm troughs and positive spikes at Ba, La, Pr, Nb, Sr, Nd, and Ta with slight steep and parallel from Zr-Lu and basaltic rock show variation in K by showing positive spike at sample

T7S5 and trough at T1S1 and T2S3, and U show a positive anomaly in T1S1 and T2S3 and slight trough in T7S5. Basaltic andesite has the same trend with basalt from Zr to Lu but has a positive anomaly at K, Nd, and Pb ;whereas negativ anomaly at Ba (slightly),Th, U, Nb, Ta, P, and Ce. Trachydacite (T3S2 and T3S6) has the same trend to but lower concentration of trace elementes than rhyolite but less depleted in Sr, Ba, Pb and Ti. Rhyolites as compared to the primitive mantle (Fig.5.6) they are enriched in the incompatible trace elements such as Rb,Th, Pb, Hf, K , LREE, Ta, U and Zr but they present marked troughs at Sr, Ti, P, Ba, Ce, Sm and Eu slight troughs in Nb and these samples are slight flatten from Nb–Ce and from Y-Lu and steep slope pattern from Pb-Sr and Zr-Ti.

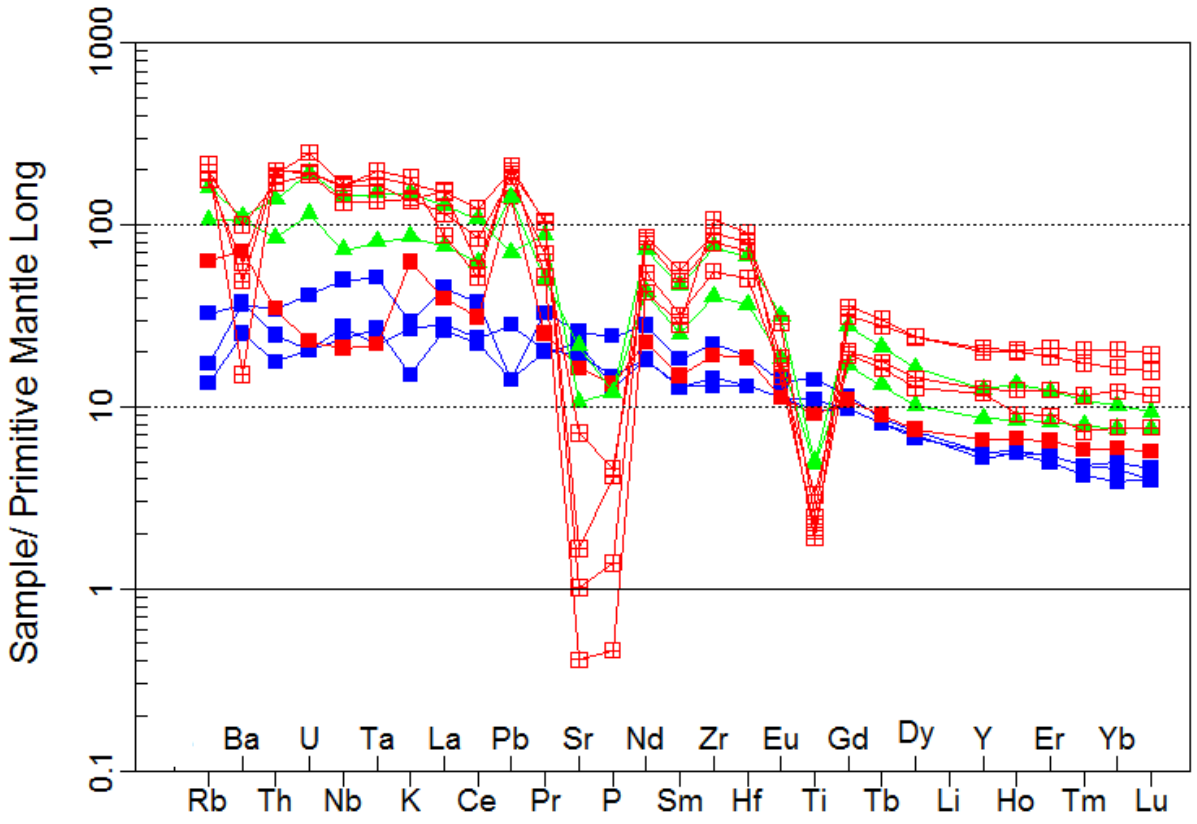

Fig 5. 6. Primitive mantle normalized multi-element variation diagram (Sun and McDonough, 1989) for Lake Hayk basalt to rhyolite rock unit. Symbols are the same as in (Fig5.1).

CHAPTER SIX

DISCUSSION

6. Introduction

Geochemically associated Oligocene basaltic erupted at 31 Ma and rhyolitic volcanic rocks ranges in age from 28.5 – 30.8 Ma around Lake Hayk are belonging to a bimodal suite. Geochemical data, such as major and trace elements, are used to study the petrogenetic evolution of Lake Hayk flood basalt (31 Ma) and differentiation of rhyolite volcanic rocks. In this section discusses the petrogenetic progression of basalt to rhyolite volcanic rocks in detail.

6.1. Petrography

The mineralogical modal composition of analyzed samples shows a wide range of textural and mineralogical compositions as presented in chapter Four. Porphyritic basalt, aphyric basalt, rhyolite, and ignimbrite are the volcanic rocks that are petrographically examined which are stratigraphically from bottom to top. Different mineral phases of phenocrysts, microphenocrysts, and groundmass levels with different modal percentages are presented in the rock units. The phenocrysts of porphyritic basalt are olivine and clinopyroxene with a groundmass of microcrystals of plagioclase and opaque mineral (Fe-Ti oxide) which is the bottom part of the study area overlain by aphyric basalt which is composed of plagioclase, some pyroxene with a groundmass of opaque mineral and this aphyric basalt which is overlain by strongly welded rhyolite rocks unit which constitutes of alkali feldspar (sanidine), quartz with a groundmass of volcanic glass and very less opaque mineral it intercalated with less welded rhyolite, ignimbrite(composed of nepheline, rock fragments, and volcanic glass) and with aphyric basalt in some part of the study area(mostly western part).

The textural arrangements, the zoning in plagioclase, alteration effects in olivine, clinopyroxene and plagioclase, the euhedral-Subhedral-anhedral shape of phenocryst phase with variations in size, are very common in petrographic analyzed flood basalt rocks and euhedral sanidine, and subhedral to anhedral quartz in silicic rocks. Furthermore, the analyzed volcanic rock show differences in crystal shape which implying the order of magma crystallization as euhedral-Subhedral which is the first crystallized minerals, and anhedral crystals crystallized at the last.

As presented in chapter four Plagioclase is normally zoned with a compositional change from the high-temperature mineral phase at the core (Ca-plagioclase) and to low-temperature composition mineral at its rim (Na-plagioclase) and it shows complex zoning, polysynthetic twin, the inclusion of clinopyroxene, overgrowth in olivine, and sieved texture in plagioclase which is the effect of alteration. This sequence can be explained as the enclosed mineral grain olivine is assumed to be the first to crystalize followed by clinopyroxene, plagioclase, K-feldspar (sanidine), and quartz which support/complementary with fractional crystallization trend in geochemical variation plots as discussed below (6.2).

Generally the trend which show decrease in mafic mineral and increasing of felsic mineral from flood basalt to shield volcano show the decrease of magma influx (Krans et al., 2018).

6.2. Fractional Crystallization

The examined basaltic rock samples from Lake Hayk are characterized by compatible trace element content of such as Ni ranges from (51-135 ppm), Cr ranges in (110-490 ppm, MgO ranges in (6.16 - 9.16) wt%. However, Primary magma in equilibrium with a typical upper mantle mineral assemblage is characterized by their higher compatible trace element contents such as Ni (>400–500 ppm), Cr (>1000 ppm), and MgO content (10–15 wt. %) (Frey et al., 1978; Hess, 1992 as cited in Dereje Ayalew et al.,2016). Hence, the values of compatible element and MgO lower than primary magma this suggest that the examined basalt do not represent primary magmas but it testify the fractionation of olivine and clinopyroxene. In addition to this the concentrations of basalt, basaltic andesite, trachydacite, and rhyolitic volcanic rocks are Sr (405-546 ppm), (345ppm), (222 - 455ppm), and (8.6-151 ppm) and for V (287-337 ppm), (268 ppm) (23-41) and (10-18 ppm) respectively for each rock unit based on TAS classification. These reflect/implicate there is less fractionation of plagioclase and Fe–Ti oxides in basalt than basaltic andesite to rhyolite (Dereje Ayalew and Gibson, 2009). Further, basaltic rock fractional crystallization can be accessed through the plot of SiO_2 versus major oxides (Winter, 2001; Cox, 1979). With increasing SiO_2 content MgO, Fe_2O_3, CaO, TiO_2 and P_2O_5 display negative correlation implying fractionation of Mg- Fe- Ca- Ti and P-bearing minerals such as olivine and/or clinopyroxene, plagioclase, Fe-Ti oxides, and apatite respectively. Al_2O_3 positively correlated from basalt to trachydacite, which suggest the accumulation of plagioclase,

and in rhyolite, suite shows a negative correlation with SiO_2 which implicates the fractionation of Al-bearing mineral of plagioclase. K_2O is a positive trend with increasing SiO_2, indicating the accumulation of alkali feldspar (sanidine is common phenocryst in rhyolite).Na_2O which show a positive correlation ~70% of SiO_2 and negative correlation after trachydacite which suggest the fractionation of Na-feldspar fractionation.

In order to test fractional crystallization hypothesis major elements mass balance calculated (Appendix III). Major element modeled based on the calculation of mass balance by following steps from the most mafic to felsic rocks (Stormer and Nicholls, 1978). The mineral chemistry of basaltic rock is taken from northwestern flood basalt (Pik et al.,1998) and basaltic andesite to rhyolite rock is from Boseti volcanic complex of main Ethiopian rift(Ronga), this choice is due to minerals of rift margin mineral chemistry is not available. However, this model obviously considered as semi-quantitative.

The calculated mass balance indicates that the evolution modeled from basalt (T2S3) to basaltic andesite (T7S1) by 60.51% solid fractional crystallization with sum of the calculated residual (R^2) 0f 0.5.The evolutions from basaltic andesite (T2S3) to trachydacite (T3S6) by 43.41% of solid fractional crystallization with sum of the calculated residual (R^2) of 1.3 and trachydacite (T3S6) to rhyolite (T5S2) by 29.47% of solid fractional crystallization with sum of the calculated residual (R^2) of 0.8721. The variation diagram of major element against silica of the calculated composition and the analyzed/parent composition fit linear to curvilinear line which suggest the fractional crystallization is the major process.

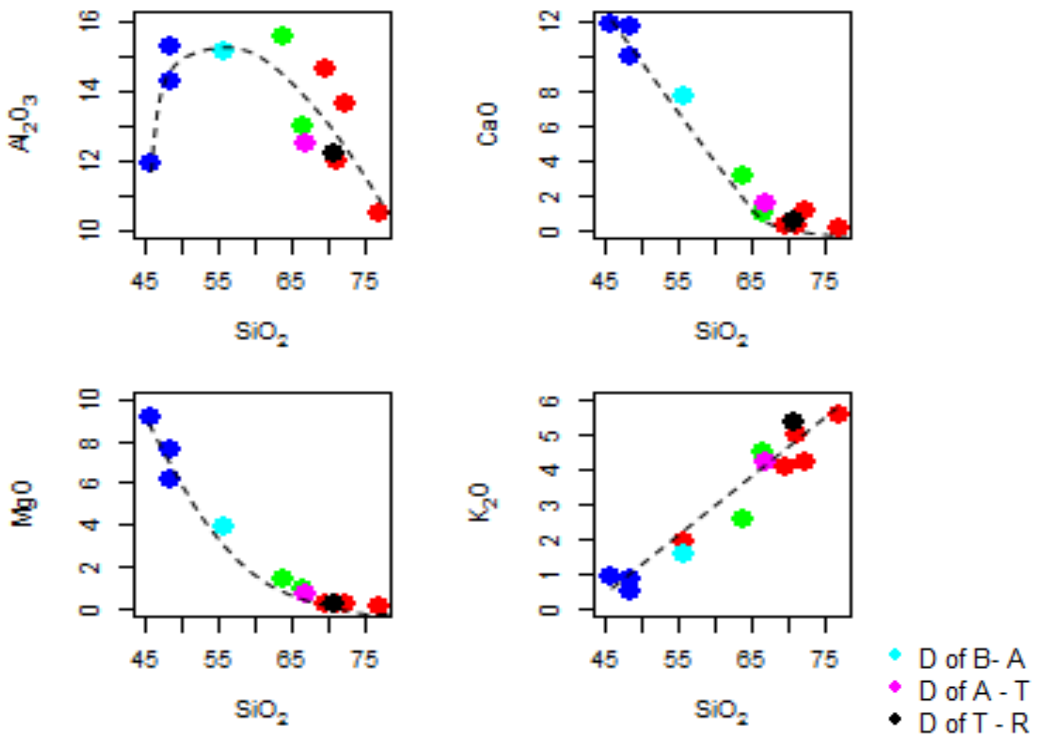

Fig 6.1 variation diagram of major element vs. silica of calculated composition and the parent. D of B –A is daughter of calculated composition between basalt and basaltic andesite, D of A-T is daughter of calculated composition between basaltic andesite and trachydacite, D of T –R is daughter of calculated composition between trachydacite and rhyolite. The other symbols are the same as the color from fig 5.1

As illustrated in (Fig.5.3), the plots of incompatible trace elements (Rb, Zr, Sr, Eu, Nb, Th, Ba, and La) against SiO_2, suggest that fractional crystallization is a major role in the petrogenetic evolution of these volcanic rocks (Dereje Ayalew et al., 2006).There is a strong negative Eu anomaly of the REEs of all trachydacite to felsic/rhyolitic rocks and positive anomaly Eu of basalt than basaltic andesite to rhyolite. Eu anomalies (Eu/Eu*) from positive to negative are as follows; basalt, basaltic andesite to trachydacite, and rhyolite (0.99-1.01),(0.88,0.90), and (0.48-0.68) respectively. This suggests there is high fractionation of plagioclase of rhyolite and basalt lack to minimal fractionation on the early fractionating phases (Dereje Ayalew and Gezahegne Yirgu, 2014) positive Eu anomaly in the REE pattern of basalt suggest incorporation of Eu^{2+} in feldspar. There is highly negative anomalies of Ce for rhyolite (T1S3) which has highest LOI =

3.07 than other sample this may suggest a result of alteration and slight negative anomaly of Ce for basaltic rock generated by REE differential diffusion at the contact between basaltic and rhyolitic magmas (Peccerillo et al., 2003).

Primitive-mantle-normalized trace element plots of rhyolites are enriched in incompatible trace elements (LREE) such as Rb, Th, Pb, Hf, Gd, U, and Zr as compared to the primitive mantle (Fig.5.6).The pronounced positive anomaly of Pb could be linked to mobility because this element is highly mobile (Rollison, 1993). However, rhyolite present marked troughs at Eu, Sr, P, Ti, and Ba which implicate that fractionation of plagioclase (Eu, Sr), apatite, ilmenite, and alkali feldspar respectively during the chemical evolution of rhyolite (Halder et al., 2020). The (La/Yb)N ratio values of basalt and basaltic andesite to rhyolite (5.34-10.97) and (6.19-11.74) respectively. Moderately fractionated volcanic rock have 6 < (La/Yb)N<14(Dereje Ayalew et al.,2002). Hence it is concluded that Lake Hayk basalt seems to be less to moderately fractionate than moderately fractionated basaltic andesite to rhyolite.

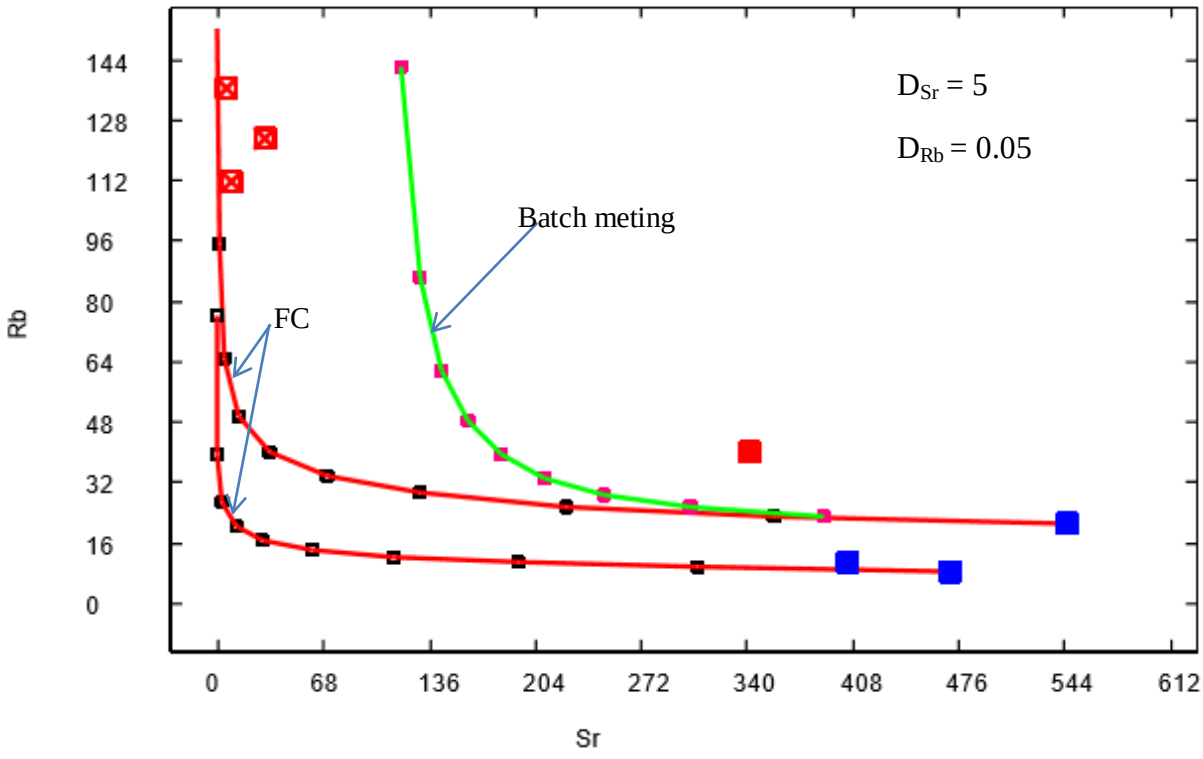

Fig 6 1 Variation diagram of fractional crystallization (FC) and batch melting model of compatible (Sr) vs. incompatible (Rb) trace element for lake Hayk volcanic rocks. Basalt T1S1which is less evolved rock (SiO_2 = 45.5) has been assumed as the starting composition for both fractional crystallization and batch melting. The partition coefficient for the model is 5 = Sr and 0.05= Rb (after Ewart and Griffin, 1994). Symbols the same as in (Fig.5.1).

The model of fractional crystallization for some compatible (Ni and Cr) and incompatible elements (Fig 6.2) of calculated trends show a sharply decreasing in Ni and Cr is slight as compared with Ni; whereas incompatible elements and slightly increasing up to %F = 0.4 and sharply increase up to %F = 0.

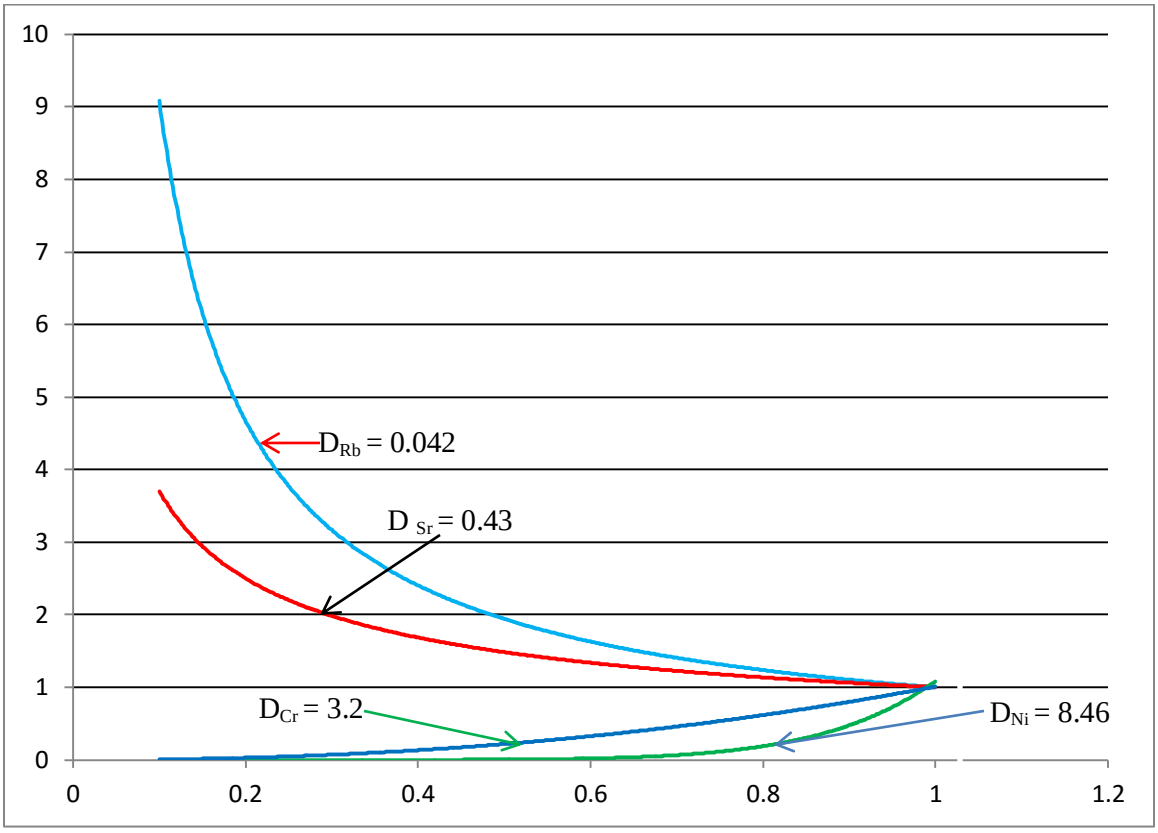

Fig 6.2 Fractional crystallization model for the most primitive basaltic (T1S1) rock of Lake Hayk. Weight fraction of residual liquid F% .See the calculated bulk partition coefficient and crystal fractionation (CL/Co)(Appendix III .3).

6.3. Crustal Contamination

The studied samples of lake Hayk basalts, have a positive anomaly of Nb and Ta (with exception of a slight trough in a sample (T7S5 slight trough at Ta)) and trachydacite to rhyolite show slight trough at Nb and positive spike at Ta on the primitive mantle normalized multi-element variation diagrams (McDonough and Sun, 1989) as illustrated in the previous section (fig.5.6), and this testifies there is minimal crustal contamination in basalt (with exception of T7S5) than trachydacite to rhyolite (Rollinson., 1993; Cox., 1980). Basaltic andesite (T7S1) show a negative anomaly of Nb and Ta with high Rb and Th which suggest that the involvement of upper crust or contaminated by upper curst (Dereje Ayalew et al., 2019). Basalt have low Rb/Nb = 0.5 - 0.58, La/Nb = 0.88 - 1.06 and higher TiO_2 = 2.08 - 3.04, basaltic andecite have higher Rb/Nb =2.7, La/Nb = 1.81 and low TiO_2 1.96 and rhyolite Rb/Nb = 0.97-1.69, La/Nb = 0.51 - 1.08 and lower TiO_2 = 0.41 - 0.71this suggest that there is more crustal involvement in basaltic andecite as compared to basalt and rhyolite; whereas lower in basalt as relative to rhyolite(Rollinson, 1993;Dereje Ayalew and Gezahegne Yirgu, 2003). Additionally, the basalt, basaltic andesite to rhyolite samples have ratios of Ce/Pb >19.65-33.2 and 6.13-15.6 (with exception T3S6 has 38.1) respectively and the basalt sample has ratios of Nb/U = 39.55-45.81 and basaltic andesite to rhyolite have Nb/U= 21.59-33.68(exceptionally T1S2EA sample Nb/U=99.15) (fig 6.2 B) and basalt sample has ratios of Nb/Th=9.7-12.3 and for basaltic andesite to rhyolite Nb/Th=5.08-8.63.However, the trace elements ratios values of basalt sample are very similar to OIB and MORB which have Ce/Pb ratio=25 ± 5 and Nb/U=47±10 (Hofmann et al., 1986 as cited in Dereje Ayalew et al., 2016) and Hofmann, (2003), (Nb/Th =10-20). As a result, Lake Hayk basalt appears to have less crustal contamination than basaltic andesite to rhyolite rock units, which have lower Ce/Pb, Nb/U, and Nb/Th. One rhyolitic Sample (T1S2EA) exhibits elevated Nb/U (99.15) which may testify there is U loss during secondary hydrous alteration (Dereje Ayalew., 2016). Furthermore, MgO against incompatible trace elements such as Th, La, and U have a negative correlation as shown below (Fig.6.3), this testifies that there is insignificant continental crust involvement (Zhang et al., 2009). Furthermore, Ce/Pb has a positive correlation with MgO (Fig.6.2 A), this suggest that crustal contamination is minimal (Dereje Ayalew et al., 2016; Haldera et al., 2020). Thus, rather than crustal contamination, the trace element characteristics of Lake Hayk basaltic lavas can be attributed to an elevated mantle source.

Therefore, it is concluded that in the genesis of the investigated Lake Hayk volcanic rock (basalt to rhyolite) crustal contribution is insignificant or minimum.

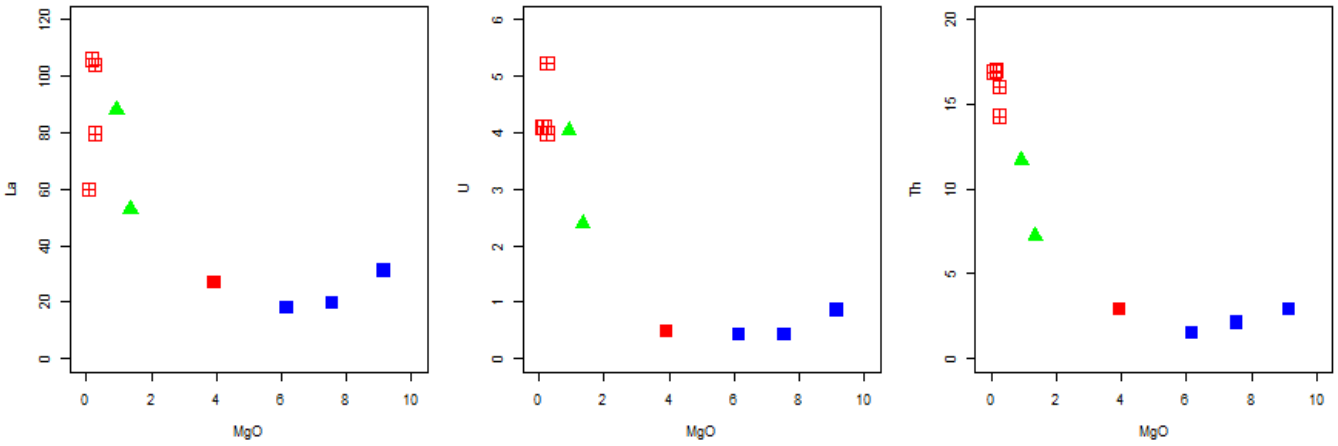

Fig 6.3 MgO against for selected incompatible trace elements (La, U, Th) variation diagrams of the Lake Hayk volcanic rocks. Symbols are the same as in fig.5.1

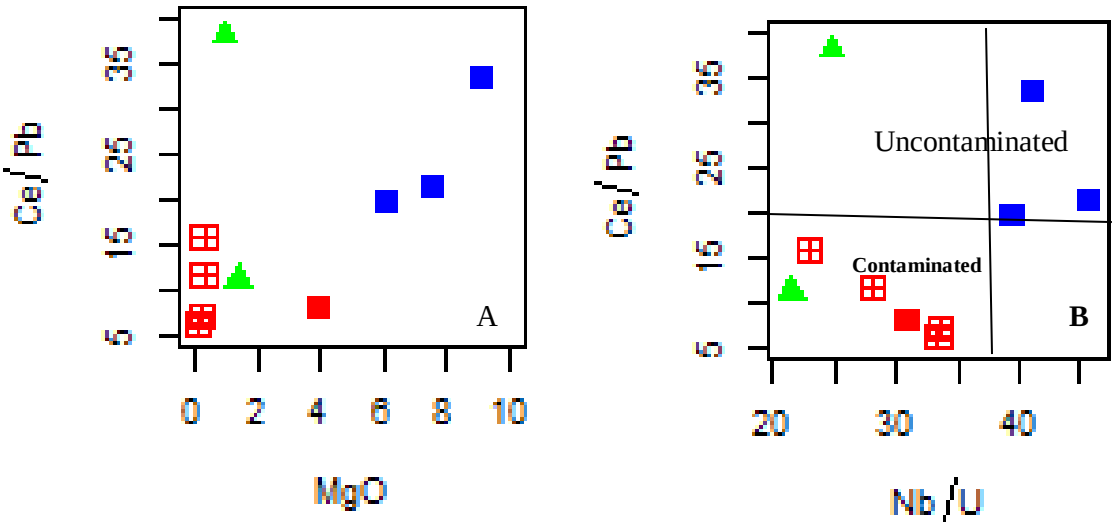

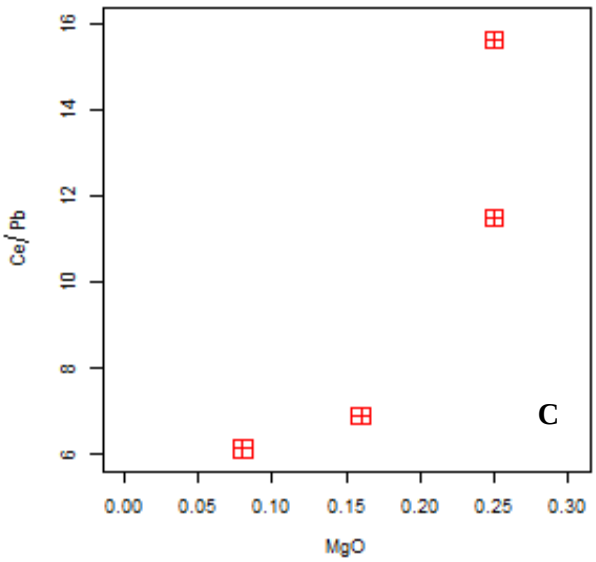

Fig.6.4 variation diagrams (A), Ce/Pb vs. MgO and (B),Ce/Pb vs. Nb/U of volcanic rock of Lake Hayk. (C), Ce/Pb vs. MgO of rhyolite rock only. The symbol has the same as (fig.5.1)

6.4. Magma Generation and Source Rock Characterization

The basalt rock unit from lake Hayk is characterized by low CaO/Al_2O_3 ratios (0.71–0.99) and in primitive mantle normalized multi-element variation diagram (Sun and McDonough, 1989) HREE relatively no fractionation/flat patterns with (TbN/YbN = 1.75-2.33). This value most likely suggests a mantle source containing spinel rather than garnet, and the gentle slope in HREE show the source for mafic rock is garnet-free (Dereje Ayalew et al., 2016). The REE chondrite normalized diagram for samples shows a likely pattern of OIB basalt which is enriched in LREE and depleted in HREE (Nakamura.,1974). Furthermore, the basalt in the studied area has a positive anomaly/enrichment of Ba, and a negative anomaly/depletion of K (positive anomaly at (T7S5)), and Rb in comparison to other primitive mantle normalized multi-element variation diagrams (Sun and McDonough., 1989), as shown in (Fig.5.6). Such positive and negative anomaly of Ba, and K respectively, testify related to amphibole and phlogopite(for K positive sample(T7S5) mantle source (e.g., Jung et al., 2005, 2012; Furman and Graham, 1999; Ayalew et al., 2006; Rooney et al., 2014; Mayer et al., 2013 as cited in Dereje Ayalew et al.,2016). Additionally, basalt samples have $Na_2O > K_2O$, such observation suggests that the source is formed through melting of the amphibole-bearing mantle (Rosenthal et al.,2009 as cited in Dereje Ayalew et al.,2016).

Based on the above observation the lake Hayk basalt was derived from the melting of amphibole-bearing spinel peridotite sources rather than Phlogopite bearing source (Dereje Ayalew., 2016). Amphibole may also occur in the lithospheric mantle, because it is not stable in the sub-lithospheric mantle source of asthenosphere or mantle plume (Class and Goldstein, 1997).

6.5. Petrogenesis of Rhyolite

To explain the petrogenesis of rhyolites and associated silicic volcanic rocks (60-81 wt% SiO_2), two models are required. (Dereje Ayalew et al., 2002;Haldera et al.,2020; Peccerillo et al., 2003; Ayalew and Yirgu, 2003) ; These are via (i) Fractional crystallization of the parent mafic magma with minor crustal contamination. And (ii) with a considerable crustal contribution, continental crust melting or mafic magma assimilation and fractional crystallization (AFC) occurs. Rhyolites produced by significant fractional crystallization have steep negative slopes in bivariate major oxides plots and a moderate to no Nb-Ta anomaly, (Haldera et al.(2020), while Rhyolites formed by large crustal contribution exhibit significant Nb-Ta negative anomalies. Hence, the rhyolite of Lake Hayk has a steep negative correlation in bivariate major oxides such as MgO, Fe_2O_3, TiO, and CaO against SiO_2, as well as a positive anomaly of Ta with a slight Nb trough, implying that Rhyolites formed by fractional crystallization with insignificant crustal contribution. Rb/Nb ratio of lake Hayk rhyolite varies between 0.97-1.69 (Table 5.1). Furthermore, rhyolites formed by crustal melting had an Rb/Nb ratio >10; whereas, the analyzed rhyolitic sample Rb/Nb < 1.69 (fig 6.7b) this indicates that partial melting of the continental crust did not contribute to the formation of rhyolite rock unit (Gezahegne Yirgu ,1997).

Volcanic rock of lake Hayk plot of TiO_2 vs. SiO_2 (Fig 5.2) shows negative correlations and a positive correlation of HFSE such as Zr vs. Rb, Zr vs. Hf, Zr vs. Nb, and Zr vs. Ta forming a single trend that show the genetic relationship or co-magmatic nature of the basaltic and rhyolitic rocks around Lake Hayk area (Haldera et al., 2020). Hence this suggests that rhyolite is related with basalt by Fractional crystallization as illustrated in (fig 6.1).

Furthermore, The bivariate plots of incompatible trace element pairs Nb, Hf, Ta, and Rb against Zr (fig.6.5), will not vary both in the course of fractional crystallization, suggest the samples of the suite are linked to a common source by the same petrogenetic process or not (Dereje Ayalew et al. ,2019). The Most sample from Lake Hayk define a strong linear trend without any

dispersion. This supports the view that the lake Hayk basalt to rhyolite was derived from a common source. The Zr/Nb ratio of basalt to rhyolite vary between 7.01-8.76 and basaltic andesite (T7S1) and one rhyolite (T1S2 EA) sample Zr/Nb = 14.43 and 10.17 respectively. The little variation of Zr/Nb ratios in basalt to rhyolites indicates that fractional crystallization has been the major process in their history of petrogenesis (Barberi et al., 1975). The only exceptions are basaltic andesite and one rhyolite sample, which have a different array (high Zr/Nb of T2S1 EA = 10.17 and T7S1 - 14.43), suggesting derivation from a depleted plume head source (Ferguson et al.,2010, 2013 as cited in Dereje Ayalew et al.,2019).

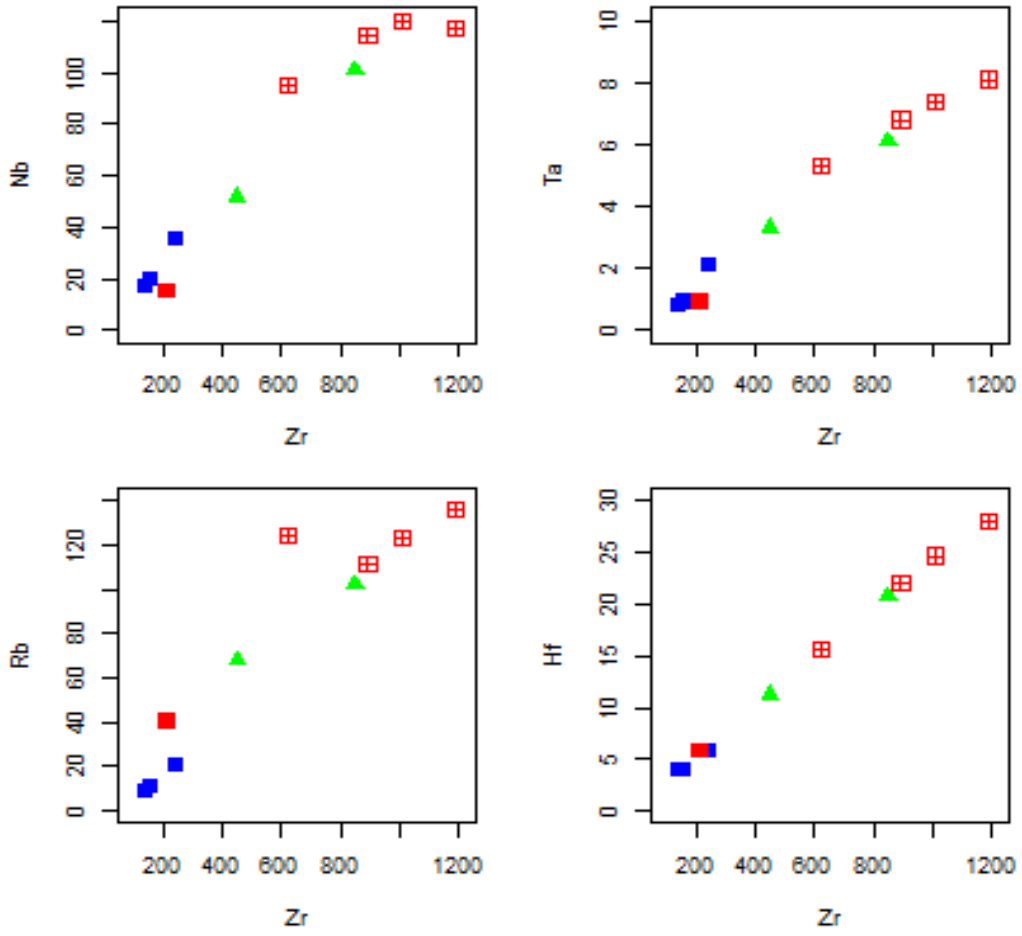

Fig 6.5 Incompatible against incompatible trace elements variation diagrams (ppm)of Lake Hayk, analyzed samples. Symbols the same as in (Fig.5.1).

The crust is depleted in Nb, because of this La/Nb ratio of magma is expected to show a positive correlation with La with progressive assimilation of crustal material and A plot of La vs. La/Nb steep positive slopes suggest that assimilation fractional crystallization (AFC) is the major process, whereas less steep slopes indicate the dominant process for the formation of rhyolite is fractional crystallization of mafic parental magma (Haldera et al.,2020). Hence the rhyolitic rock unites plot of La vs. La/Nb in the Lake Hayk area show a less steep slope as illustrated in (fig.6.6) below. Therefore, the rhyolitic rock units are formed by dominantly fractional crystallization of mafic parental magma rather than assimilation of continental crust. Most of the rhyolite at lake Hayk Nb value range from 114.5 – 120 ppm (exceptionally one sample (T5 S2) has (Nb=73.7ppm)) and Nb/La ratio of 0.93-1.97. Several authors have divided the rhyolites into two groups based on the Nb (1) Rhyolite having low Nb-Ta and Nb <30 ppm and Nb/La ratio of 0.48 - 0.62 and (2) Rhyolite having high Nb-Ta and Nb >80 ppm and Nb/La ratio of 0.82-1.16, (Tian et al., 2010, as cite Haldera et al.,2020). Hence the examined rhyolite sample is more related with the second class having high Nb-Ta and Nb >80 ppm and Nb/La = 0.93-1.97 but there is a slight trough at Nb.

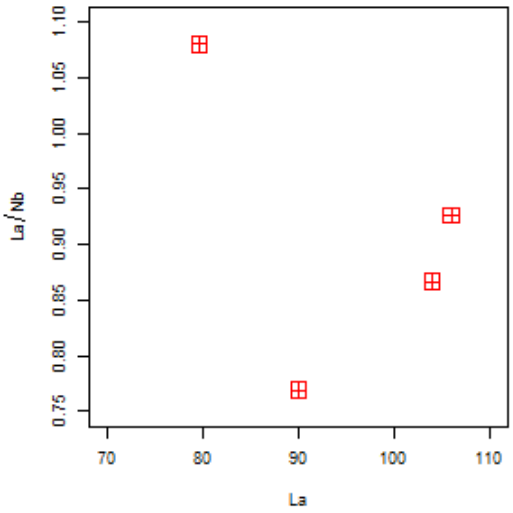

Fig 6.6 Diagrams illustrating La vs. La/Nb variation in volcanic rocks from the Lake Hayk area. Symbol the same as (fig 5.1)

Rhyolites that have (Gd/Lu)N ratio (>2.2), suggest that the parental melts may have been generated at higher depths in the garnet stability field (Haldera et al.,2020).The ratio of (Gd/Lu)N of rhyolite in the study area varies between 1.59 - 2.48. Hence the rhyolite sample

(T3S4 GdN/LuN = 2.24 and T1S1 EA GdN/LuN = 2.48) from Lake Hayk which has (Gd/Lu)N ratio (>2.2) implicate that parental melts may have been generated at higher depths in the garnet stability field and the other two sample(T5S2 Gd/Lu)N = 1.72 and T1S3 GdN/LuN =1.59) which have (Gd/Lu)N ratio (<2.2) are from spinel stability field.

In addition, that bivariate plot of highly incompatible trace element Rb against highly compatible trace element Sr in silicic melts is significant to identify the likely physical processes (Halliday et al.,1991). The Rb against Sr bivariate plot of rhyolite (Fig .6.7 A), which shows a large variation in Sr (8.6 – 151ppm) with limited variation in Rb (111.5 – 136ppm) abundances. Accordingly, Such highly incompatible against highly compatible trace element trend suggests that the rhyolite of the Lake Hayk area related to erupted basaltic magmas by the fractional crystallization process than partial melting (Ayalew et al.,2019; Haldera et al.,2020).

Eventually, the fieldwork and petrography which supports the above interpretation because stratigraphically basaltic rock units are overlain by rhyolitic rock unit in the same volcanic bodies, and petrographically from bottom to top are as follow; olivine, clinopyroxene, plagioclase, k-feldspar (sanidine) and quartz which show they originated within the same magma chamber and that the rhyolitic volcanic rocks were derived from by fractional crystallization of the mafic/basaltic magma.

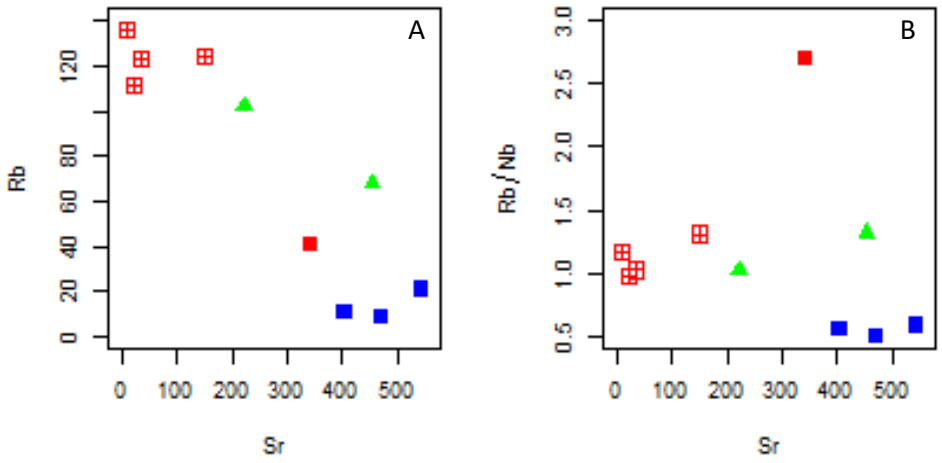

Fig 6.7 Variation diagrams of (A), Sr vs. Rb and (B),Sr vs. Rb/Nb of Lake Hayk area volcanic rocks. Symbol the same as (fig 5.1)

Daly Gap Problem

As discussed in above section Basalt and rhyolite have been genetically related and rhyolite produced through Crystal fractionation of mafic magma. However, rhyolite rocks are formed by the process of fractional crystallization there is lack of intermediate composition rocks (Daly Gap) such as trachyandesite and andesite. This is beyond the scope of this study to explain Daly Gap problem. Nevertheless, researchers explained Daly Gap through models of Classical models of magma chambers suggest that at the wall of the magma chamber crystal fractionation produce light silica rich liquids, which moves toward the top of the chamber and mafic magma accumulated at the bottom of the magma chamber which subjected to continuous mixing and stirring with injected newly mafic melts, which hindering the evolution toward silicic compositions. The mafic magma which is overlain by lighter silicic layer acts as a density barrier which is protects the upward migration of mafic magma to reach the surface; whereas silicic magmas with variable degrees of evolution are preferentially erupted. Further, several processes have been apply to explain this Daly Gap. These include control of heat and water content of magma systems, silicate liquid immiscibility, and rapid crystallization over a short temperature range (Haldera et al., 2020).

6.6. Comparison of Lake Hayk Primary data with previous works

The Lake Hayk area has a bimodal composition whith scarce intermidate rock unit. As a comparison, four samples (two basalt, one rhyiolite, and one trachyite) from the Guguftu shield volcanics (Kiffer et al.,24) and eleven samples from Wegel Tena, Kobo, and Hara (Ayalew et al.,2019). The outcomes of the samples are generally consistent with the primary data studied in the current study approach. Ten samples from Lake Hayk and fifteen samples from previous samples were combined for comparison in various diagrams. Both major and trace Variation Elements diagrams of the investigated primary basalts of Lake Hayk plotted against previous basalts and primary felsic sample plotted against previous felsic sample demonstrate that the signatures are most likely the same. When compared to previously reported Gugugguftu shield and marginal Hara,kobo and Wegel Tena volcanic suites of geochemical data obtained by previous investigations, the current study does not demonstrate a significant difference in composition. With the exception one basalt from Guguftu, almost all samples from Lake Hayk fall near the transition between alkaline and sub alkaline fields. As shown in (Fig.6.8) below, the

other basalt, trachyte, and rhyolite samples are alkaline, as well as one trachydacite, basaltic trachyte, and rhyolite sample from Lake Hayk, Hara, and Kobo.

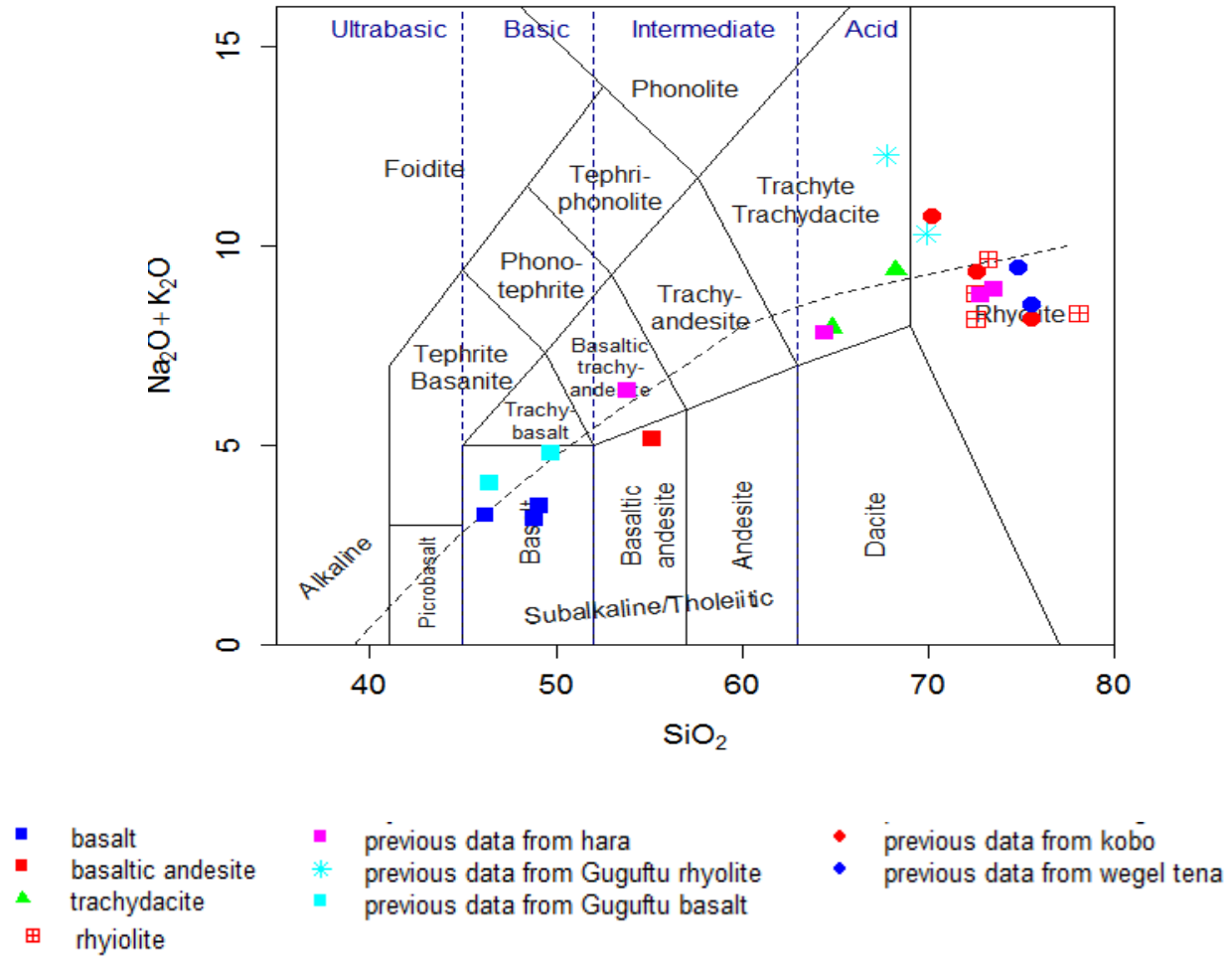

Fig 6 8: TAS classification diagrams of Lake Hayk flood basalts and rhyolite for composition of Lake Hayk basalt to rhyolite from the previous works.

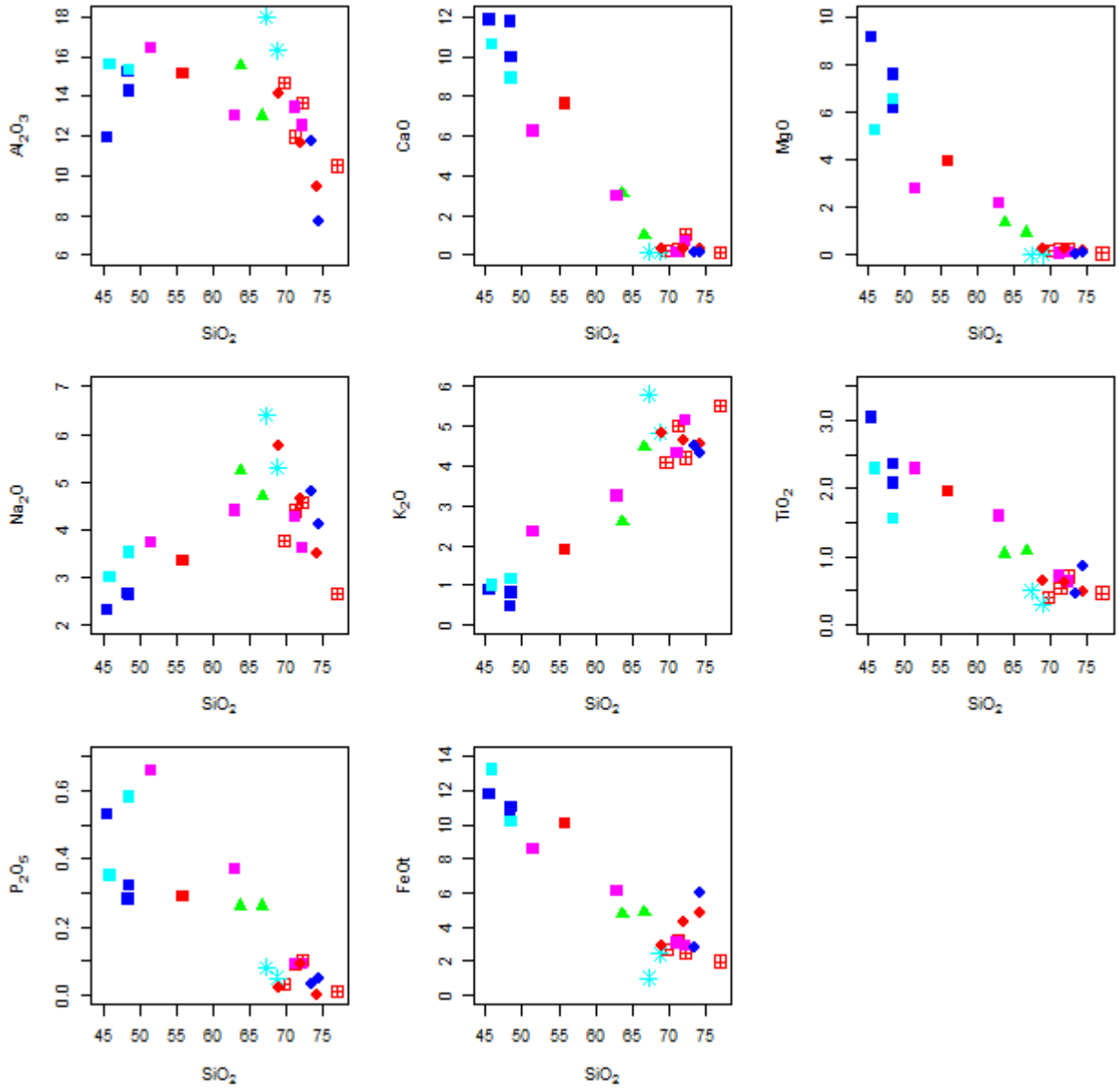

Fig 6.9. Variation diagrams of major element contents as a function of SiO_2 for comparison of Lake Hayk volcanic rock with previous work. Symbol the same as fig .6.8

The variation diagram of major element against SiO_2 (fig. 6.9) for both primary and previous data show the same trend (primary basalt with previous basalt, primary basaltic andesite with previous basaltic andecite and primary felsic with previous felsic) as described in the previous section (Chapter Five). Both primary and previous samples show steep negative trend of these compatible trace elements and the accommodating major elements (Fe, Mg, Ca); show

pronounced evolution trend starting from basalt-intermediate –rhyolite suites. The available primary data show Lake Hayk rhyolites show similar signature of major and trace element abundance with Hara, kobo, and Wegel Tena silicics analyzed in previous works.

Basaltic systems show Sr depletion in response to the fractionation of plagioclase and or crustal assimilation (Haliday et al, 1991); and Rb increases corresponding to the more or less vertical trend (see Fig. 6.10). Incompatible trace elements like Sr drops to very low concentrations both in Hara, Guguftu and Lake Hayk felsic rocks; whereas strongly incompatible trace elements like Rb, Nb, and La showing very high concentration. Previous work results have presented that, the felsic rocks of Hara formation display similar patterns with Lake Hayk felsic rock.

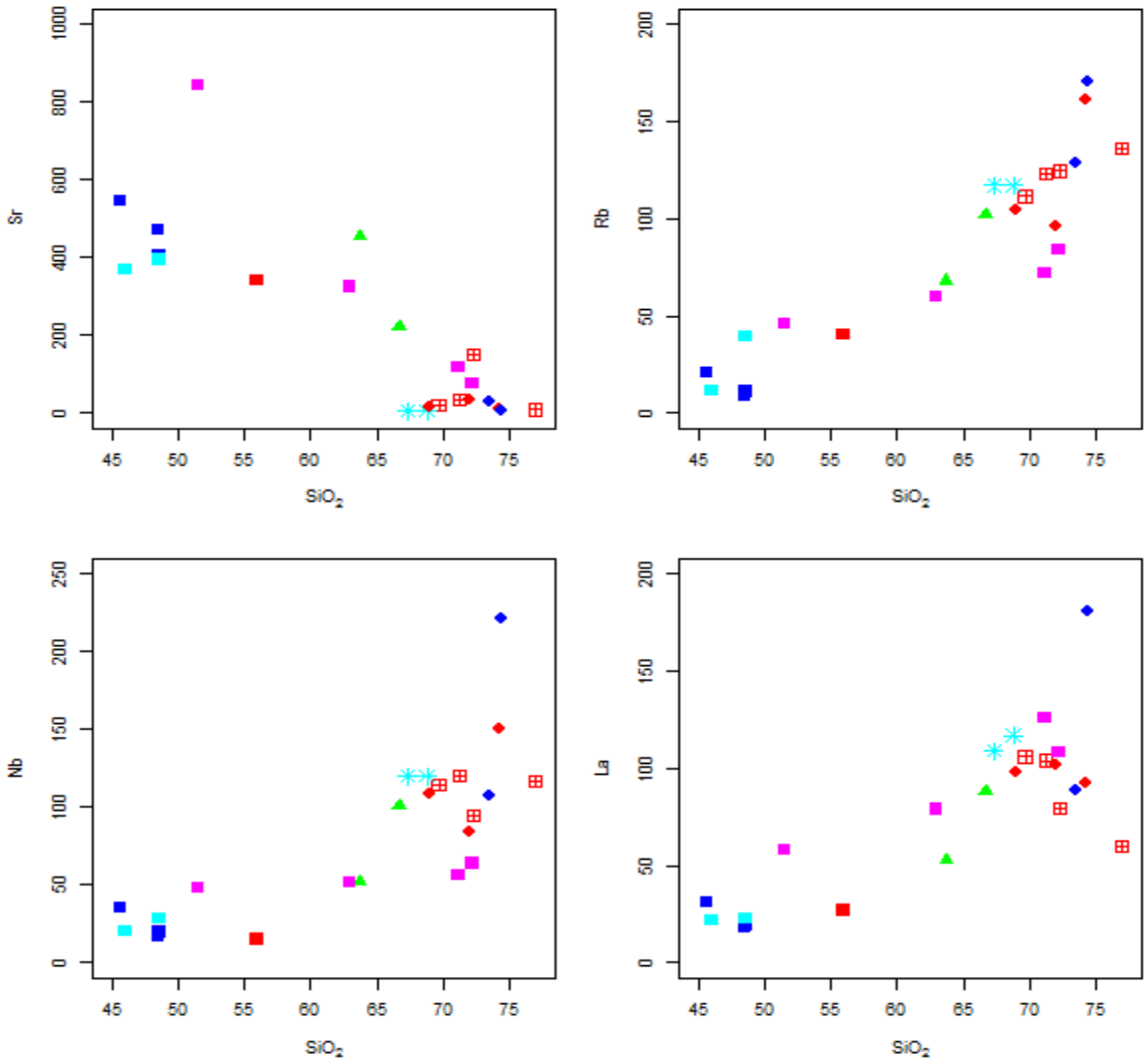

Fig 6.10.Trace element variation diagrams show the variation of incompatible trace elements against SiO_2 for composition of Lake Hayk basalt to rhyolite to the previous work. Symbols are the same as in Fig.6.8.

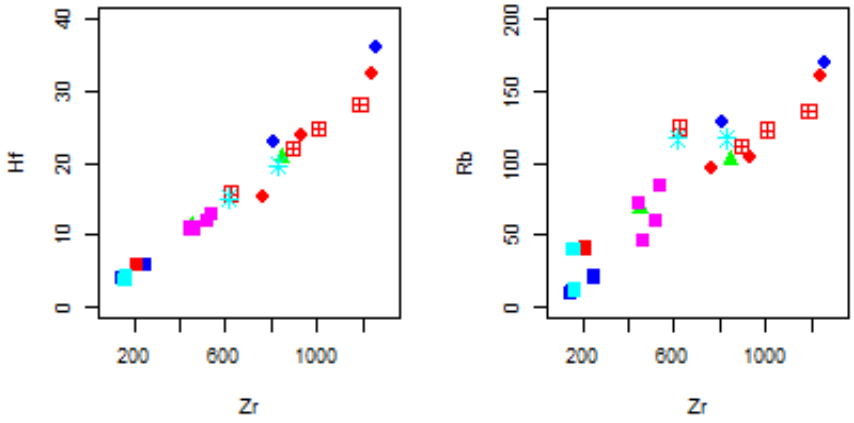

Fig 6.11 plots of Rb against Zr variation diagram which shows comparison of Lake Hayk volcanic rock with previous work. Symbol the same as fig .6.8

Volcanic rock of lake Hayk, Wegel Tena, Guguftu and Hara plots of TiO_2 vs. SiO_2 (Fig 5.2) shows negative correlations and a positive correlation of HFSE such as Zr vs. Rb, Zr vs. Hf, Zr vs. Nb, and Zr vs. Ta forming a single trend that show the genetic relationship or co-magmatic nature of the basaltic and rhyolitic rocks those area.

The spider diagram of mafic to silicic rocks of primary and previous data is plotted in (fig.6.10). All the samples show parallel to sub-parallel patterns. The chondrite normalized REEs diagram of mafic, intermediate, and rhyolitic rocks are enriched in LREEs elements, but felsic rocks are much more enriched in REE than intermediate and mafic rocks as illustrated in (Fig.6.10). The sequence of REE enrichment in volcanic rocks from the primary and previous rock unit is higher in LREE, intermediate in MREEs, and lower in HREE. The REE chondrite normalized diagram for samples shows a likely pattern of OIB basalt which is enriched in LREE and depleted in HREE. Wegel Tena rhyolite is more enriched in REE and less depleted in Eu than other and Guguftu rhyolite is more depleted in Eu than other.

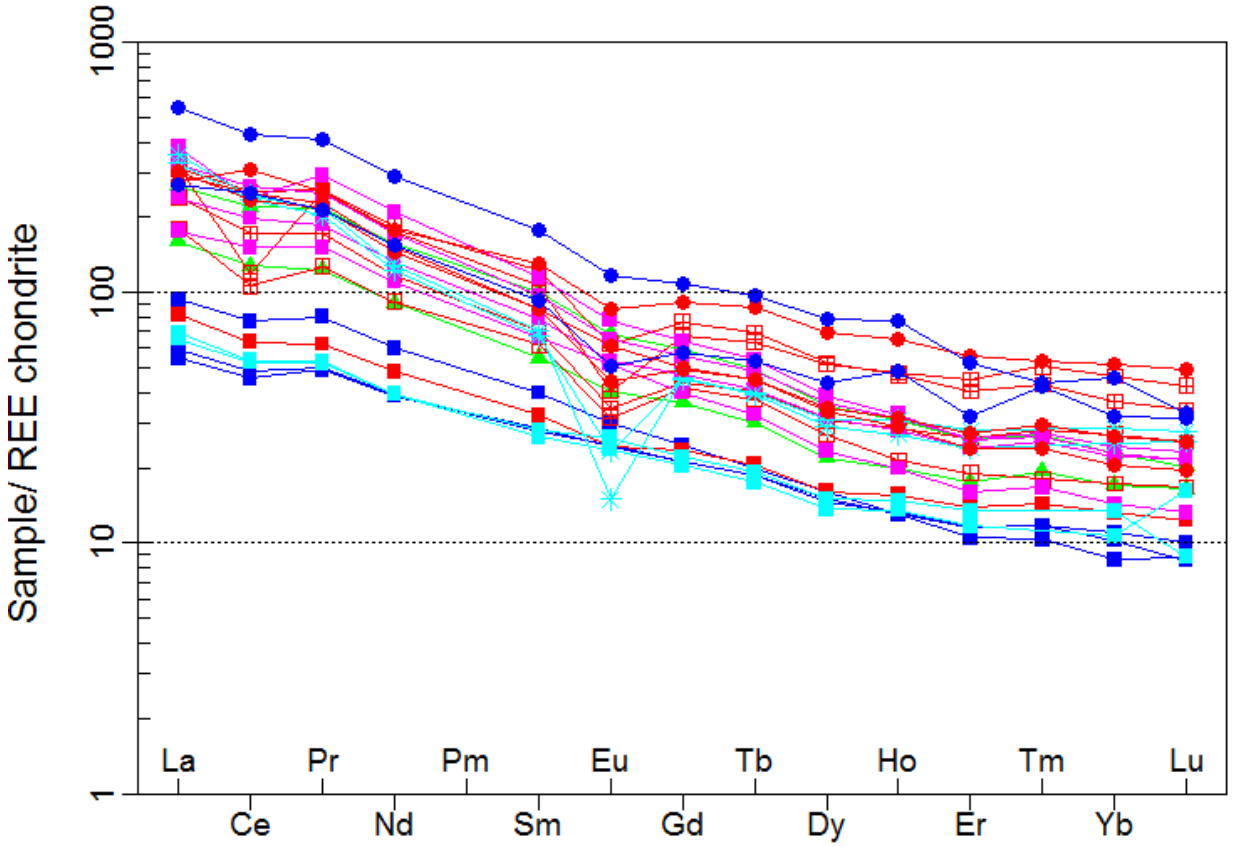

Fig 6.12 Chondrite normalized REE pattern for composition of Lake Hayk basalt to rhyolite to the previous work. The normalization values are from Nakamura,(1974). Symbols are the same as Fig. 6.6.

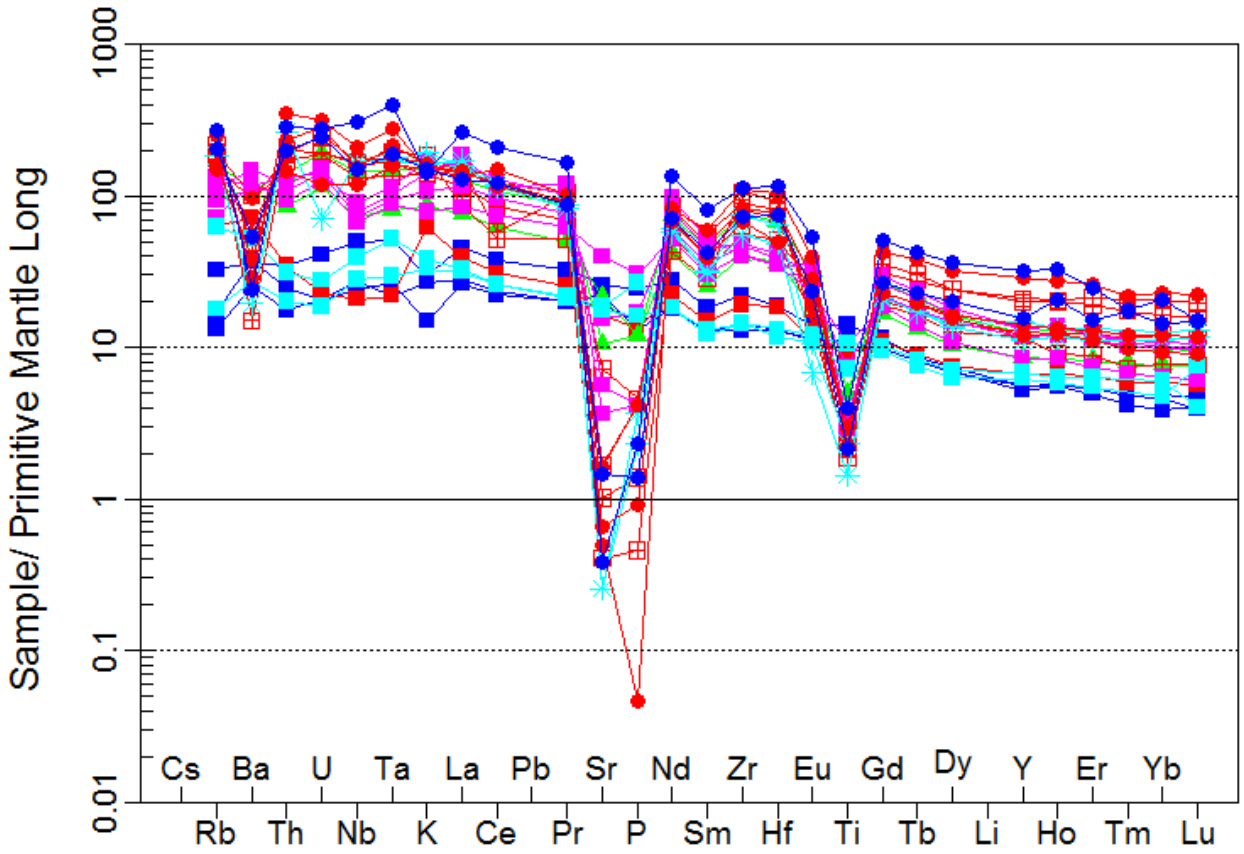

Fig 6 13: Primitive mantle-normalized multi-element variation diagram for composition of Lake Hayk basalt to rhyolite to the previous work. Symbols are identical to those in (Fig.6.8)

Spider diagrams for Primitive mantle-normalized multi-element comparing the analyzed primary data with previous work data of Wegel Tena, kobo, Hara, and Guguftu felsic rocks (see Fig. 6.13) show similar signatures in all cases. From all Primary and secondary data of felsic rocks show similar incompatible trace element patterns having strong negative anomaly of Ba, Sr, Ti and positive anomaly of Th, Ta, Zr and slight negative at Nb (see Fig. 6.13) with exceptionally one Hara rhyolite sample have positive anomaly of Ba and negative Rb and Th. These negative anomalies have an implication to fractional crystallization and positive spikes of various incompatible elements suggest the accumulation of rock forming minerals. With the same idea discussed in previous sections (section 5.2); strong negative anomaly displayed in Ba, Sr, and Ti are indicatives of roles of alkali feldspars, plagioclase, and accessory minerals (magnetite), respectively during the evolution/ or genesis of analyzed rocks. This similar characteristic

features suggest the direct genetic relationship of acid rocks with basalts through the process of differentiation controlled by fractional crystallization.

Table 6. 1: Trace element and TiO_2 of the Lake Hayk area volcanic rocks compared with other marginal rhyolites and Guguftu shield volcano.

	Rock type based on TSA classification	Rb/Nb	La/Nb	TiO_2	Source of data
Hara	Basaltic trachyte	0.96	1.21	2.29	Dereje Ayalew et al.,(2019)
	Trachydacite	1.16	1.52	1.60	
	Rhyolite	1.13-1.19	1.49-2.25	0.57 – 071	
Guguftu	Basalt	0.57-1.41	0.81-1.07	1.56 – 2.29	Kieffer et al.,(2004)
	Trachydacite	0.98	0.91	0.51	
	Rhyolite	0.98	0.98	0.53	
Kobo	Rhyolite	0.95 – 1.14	0.91-1.21	0.63 -0.65	Dereje Ayalew et al.,(2019)
Wegel Tena	Rhyolite	0.77-1.21	0.81- 0.83	0.46 – 0.86	Dereje Ayalew and Gezahegne Yirgu,(2003)
Lake Hayk	Basalt	0.5-0.58	0.88-1.06	2.08-3.04	present study of this work
	Basaltic andesite	2.70	1.18	1.96	
	Trachydacite	1.01-1.32	0.88-1.02	1.04-1.08	
	Rhyolite	0.97-1.69	0.51-1.08	0.41-0.71	

Furthermore, Lake Hayk rhyolites unit have the same Rb/Nb (0.51-1.08) and La/Nb (0.41-0.71) ratios to that of Kobo, Wegel Tena, and Guguftu rhyolite rock units; whereas relatively lower than Hara rhyolite rock unit, which implicate that in Kobo, Guguftu, and Lake Hayk rhyolites unit there is only limited crustal material was involved in their genesis or minimal amount of crustal contamination than Hara rhyolite. Generally this work is support the previous work.

CHAPTER SEVEN
CONCLUSION AND RECOMMENDATION

7.1. Conclusion

The following conclusions have been drawn based on the petrographic, field observations, and geochemical data obtained in this study:

- Petrographically, the basaltic lavas have generally aphyric to porphyritic texture with phenocrysts of olivine, clinopyroxene, and groundmass of microcrystalline plagioclase and Fe-Ti oxides and rhyolite rock unit constitute phenocrysts of sanidine, quartz, volcanic glass, and opaque with vitrophyric, Porphyritic, and glassy texture. Generally the trend which show decrease in mafic mineral and increasing of felsic mineral from flood basalt to shield volcano show the decrease of magma influx.
- Geochemistry studies testify that volcanic rocks of Lake Hayk are a bimodal suite, with scarce intermediate composition. The Oligocene basalts and rhyolite rocks are transitional to tholeiitic/sub alkaline affinity and rhyolite rocks are peraluminous (exceptionally one rhyolite rock sample (T3S4) is peralkaline).
- Basalts have a positive anomaly of Nb and Ta (with exception of a slight trough in a sample (T7S5 slight trough at Ta) and trachydacite to rhyolite show slight trough at Nd and positive spike at Ta this testifies there is minimal to no crustal contamination in basalt (with exception of T7S5) than trachydacite to rhyolite.
- Basaltic andesite show a negative anomaly of Nb and Ta with high Rb and Th which suggest that the involvement of upper crust or contaminated by upper crust. Basalt have low Rb/Nb = 0.5-0.58, La/Nb = 0.88-1.06 and high TiO_2 = 2.08-3.04, basaltic andecite have higher Rb/Nb =2.7, La/Nb = 1.81 and low TiO_2 1.96 and rhyolite Rb/Nb = 0.97-1.69, La/Nb = 0.51-1.08 and lower TiO_2 = 0.41- 0.71.
- Volcanic rock from lake Hayk area have negative anomaly of K, this suggest related to amphibole (exceptionally for K positive sample (T7S5) phlogopite mantle source) mantle source and basalt samples have $Na_2O > K_2O$, such observation suggests that the source is formed through melting of the amphibole-bearing mantle. Rhyolite sample (T3S4 GdN/LuN = 2.24 and T1S1 EA GdN/LuN = 2.48) from Lake Hayk which has (Gd/Lu) N ratio (>2.2) implicate that parental melts may have been generated at higher depths in the garnet stability field and the other two sample (T5S2 Gd/Lu)N = 1.72 and T1S3 GdN/LuN =1.59) which have (Gd/Lu)N ratio (<2.2) are from spinel stability field.
- The parallel pattern of basalt and rhyolite in chondrite normalized REE pattern, Nb, Hf, Ta, and Rb against Zr, and flood basalt and rhyolitic flow range in age from 28.5 to 31 Ma do to these evidences basaltic to rhyolitic rocks generated from the same magma source/ co-magmatic nature.

- The rhyolitic rock units of Lake Hayk area are formed by fractional crystallization of mafic parental magma rather than assimilation of continental crust. Stratigraphic position, petrographic descriptions also support this investigation.

7.2. Recommendation

Isotope geochemistry and mineral chemistry studies are much recommended to adequately understand the magma source characteristics, and geochemical processes involved to produce the rock suites of the Lake Hayk area.

Reference

Abbate , E., Sagri, M. (1980).Volcanites of Ethiopian and Somali Plateaus and major tectonic lines. Atti Convegni Acc Lincei Roma 47:219– 227

Abbate ,E., Bruni ,P., Ferretti,M,P., Delmer, C., Laurenzi,M, A., Hagos, M., Bedri,O., Rook,L., Sagri, M., Libsekal,Y.(2014). The Oligocene intertrappean beds: regional distribution, depositional environments and Afro/Arabian mammal dispersal corridors. J Afr Earth Sci 99:463–489

Arndt, N., Chauvel, C., Czamanske, G. and Fedorenko, V. (1998). Two mantle sources, two plumbing systems: tholeiitic and alkaline magmatism of the Maymecha River basin,Siberian flood volcanic province. Contributions to Mineralogy and Petrology, 133(3), pp.297–313.

Baker, J., Snee, L and Menzies, M. (1996). A brief Oligocene period of flood volcanism in Yemen: implications for the duration and rate of continental flood volcanism at the Afro- Arabian triple junction. Earth and Planetary Science Letters, 138, 39-55.

Baker J. A., Macpherson C. G., Menzies M. A., Thirlwall M. F., Al-Kadasi M., and Mattey D. P. (2000). Resolving crustal and mantle contributions to continental flood volcanism, Yemen: Constraints from mineral oxygen isotope data. J. Petrol. 41, 1805–1820.

Barberi F., Ferrara G., Santacroce R., Treuil M., and Varet J. (1975). A transitional basalt-pantellerite sequence of fractional crystallization, the Boina Centre (Afar Rift, Ethiopia). J. Petrol. 16, 22–56.

Blanford, W.T. (1870). Observations on the geology and zoology of Abyssinia. Made during the progress of the British Expedition to that country in1867-8. Macmillan. 487p.

Bohrson, W. A. & Reid, M. R. (1997). Genesis of peralkaline volcanic rocks in an ocean island setting by crustal melting and open-system processes: Socorro Island, Mexico. Journal of Petrology 38, 1137---1166.

Chazot, G. & Bertrand, H.(1995). Genesis of silicic magmas during Tertiary continental rifting in Yemen. Lithos, 36, 69–83.

Class, C., Goldstein, S. (1997). Plume lithosphere interaction in the ocean basins: constraints from source mineralogy. Earth and Planetary Science Letters 150, 245–260.

Cleverly R. W., Betton P. J., and Bristow J. W. (1984) Geochemistry and petrogenesis of the volcanic rocks of the Lebombo rhyolites. In Petrogenesis of the Volcanic Rocks of the Karoo Province. Geol. Soc. S. Afr. Spec. Publ. 13, 171–195.

Courtillot, V., Jaupart, C., Manighetti, I., Tapponnier, P. and Besse, J. (1999).On causal links between flood basalts and continental breakup. Earth and Planetary Science Letters, 166: 177-195.

Coulie, E. (2001).Chronologie Ar/Ar et K/Ar de la dislocation du plateou ethiopien et de la dechirure continetale dans la Corne de I"Afrique depuis 30 Ma. Ph.D. thesis, University de paris Sud. Orsay.

Coulié, E., Quidelleur, X., Gillot ,P., Courtillot ,V., Lefèvre ,J., and Chiesa, S. (2003). Comparative K-Ar and Ar/Ar dating of Ethiopian and Yemenite Oligocene volcanism: Implications for timing and duration of the Ethiopian Traps. Earth and planetary Science Letters 206, 477–492.

Cox, K.G., J.D. Bell and R.J. Pankhurst . (1979). The Interpretation of Igneous Rocks. Allen and Unwin.

Davidson, A. and Rex, D.C. (1980).Age of volcanism and rifting in south-western Ethiopia. Nature, 283: 654–658.

Dereje Ayalew., Gezahegne Yirgu., &Pik, R. (1999). Geochemical and isotopic (Sr, Nd and Pb) characteristics of volcanic rocks from southwestern Ethiopia. Journal of African Earth Sciences, 29(2), 381–391.

Dereje Ayalew, Barbery, P., Marty, B., Reisberg, L., Gezahegn Yirgu, and Pik, R. (2002). Source, genesis and timing of giant ignimbrite deposits associated with Ethiopian continental flood basalts. Geochemica et Cosmochimica Acta 66(8): 1429-1448.

Dereje Ayalew and Gezahegn Yirgu. (2003).Crustal contribution to the genesis of Ethiopian Plateau rhyolitic ignimbrites, basalt and rhyolite geochemical provinciality. Journal of the Geological society 160(1): 47-56.

Dereje Ayalew & Gibson, I.S. (2009). Head-to-tail transition of the Afar mantle plume: geochemical evidence from a Miocene bimodal basalt–rhyolite succession in the Ethiopian large igneous province. Lithos,112: 461–476.

Dereje Ayalew, Marty, B., Barbey, P., Gezahegn Yirgu and Endale Ketefo .(2006).Sublithospheric source for quaternary alkaline Tepi shield, southwest Ethiopia. Geochemical Journal40: 47–56.

Dereje Ayalew, Jung, S., Romer, R.L., Kerstend, F., Pfänder, J.A., Garbe-Schönberg, D. (2016). Petrogenesis and origin of modern Ethiopian rift basalts: Constraints from isotope and trace element geochemistry. Lithos 258–259: 1–14

Dereje Ayalew1 , Pik,R., Bellahsen,N.,France,L., and Gezahegn Yirgu.(2019). Differential Fractionation of Rhyolites During the Course of Crustal Extension, Western Afar (Ethiopian Rift). Geochemistry, Geophysics, Geosystems, 20. https://doi. org/10.1029/2018GC007446

Dercq, M., Arndt,N.,Lapierre, H. and Yirgu, G. (2001). Les pitons trachytiquesd'Ethiopiene sont pas les conduits d'alimentation des trapps.C.R.Acad. Sci. paris332:609-615.

Doe, B.R., Leeman, W.P., Christiansen, R.L., Hedge, C.E.(1982). Lead and strontium isotopes and related trace elements as genetic tracers in the Upper Cenozoic rhyolite basalt association of the Yellowstone Plateau volcanic field. J. Geophys. Res. 87, 4785–4806. https://doi.org/10.1029/JB087iB06p04785

Ebinger, C., Tesfaye Yemane, Gidey Woldegabriel, Aronson, J., and Walter, R. (1993). Late Eocene– Recent volcanism and faulting in the southern main Ethiopian rift. Journal of the Geological Society 150(1): 99-108

Ellam, R.M. and Cox, K.G.(1991). An interpretation of Karoo picrite basalts in terms of interaction between asthenospheric magmas and the mantle lithosphere. Earth and Planetary Science Letters, 105(1–3), pp.330–342.

Ewart, A. and Griffin, W. (1994). Application of proton-microprobe data to trace-element partitioning in volcanic rocks. Chemical Geology 117(1):251-284.

Ferguson, D. J., Barnie, T. D., Pyle, D. M., Oppenheimer, C., Yirgu, G., Lewi, E., Kidane, T. (2010). Recent rift-related volcanism in Afar, Ethiopia. Earth and Planetary Science Letters, 292, 409–418.

Ferguson, D.J., Calvert, A. T., Pyle, D. M., Blundy, J.D., Yirgu, G., & Wright, T. J. (2013). Constraining timescales of focused magmatic accretion and extension in the Afar crust using lava geochronology. Nature Communications, 4, 14 –16

Feyissa Dejen hayilemaryam., Shinjo, R., Kitagawa, H., Meshesha, D. and Nakamura, E. (2017). Petrologic and geochemical characterization of rift-related magmatism at the northern most Main Ethiopian Rift. Lithos, 282, pp.240–261.

Fodor, R.V.(1987). Low-and high-TiO2 flood basalts of southern Brazil: origin from picritic parentage and a common mantle source. Earth and Planetary Science Letters, 84(4), pp.423–430.

Frey, F., Green, D., Roy, S. (1978). Integrated models of basalt petrogenesis: a study of quartz tholeiites to olivine melilites from South Eastern Australia utilizing geochemical and experimental petrological data. Journal of Petrology 19, 463–513.

Furman, T. (2007). Geochemistry of East African Rift basalts: an overview. Journal of African Earth Sciences, 48(2–3), pp.147–160.

George, R., Rogers , N., and Kelly, S. (1998). Earliest magmatism in Ethiopia: evidence for two mantle plumes in one flood basalt province. Geology 26, 923–926.

Gezahegn Yirgu. (1997). Magma – crust interaction during emplacement of Cenozoic volcanism in Ethiopia: geochemical evidence from Sheno-Megezez area, central Ethiopia. SINET: Ethiopia J. Sc. 20(1): 49-72.

Ghinassi, M., D'oriano, F., Benvenuti, M., Awramik, S., Bartolini, C., Fedi, M., Ferrari, G., Papini, M., Sagri, M., And Talbot, M. (2012). Shoreline fluctuations of Lake Hayk (northern Ethiopia) during the last 3500 years; 365(3): 209–226.

Gidey Woldegebriel, Aronson, J. L., and Walter, R. C. (1990). Geology, geochronology, and rift basin development in the central sector of the Main Ethiopia Rift. Geological Society of America Bulletin 102(4): 439-458.

Halder,M.,Paul,D.,Sensarma,S.(2020). Rhyolites in continental mafic Large Igneous Provinces: Petrology, geochemistry and petrogenesis.Geoscience Frontiers 12 (2021)53–80. https://doi.org/10.1016/j.gsf.2020.06.011

Halliday, A.N., Davidson, J.P., Wildreth, W., and Holden, P. (1991). Modeling the petrogenesis of high Rb/Sr silicic magmas. Chemical Geology 92: 107-114.

Hess, P. (1992). Phase equilibria constraints on the origin of ocean floor basalts. Geophysical Monograph, 71: 67–102.

Hawkesworth, C., Kelley, S., Turner, S., Le Roex, A. and Storey, B. (1999). Mantle processes during Gondwana break-up and dispersal. Journal of African Earth Sciences, 28: 239-261.

Hofmann, A.W., Jochum, K.P., Seufert, M. and White, W.M. (1986). Nb and Pb in oceanic basalts: new constraints on mantle evolution. Earth and Planetary Science Letters, 79: 33–45.

Hofmann, C., Courtillot, V., Féraud, G., Rochette, P., Gezahegn Yirgu, Endale Ketefo, and Pik, R. (1997). Timing of the Ethiopian flood basalt event and implications for plume birth and global change: Nature, 389: 838–841.

Juch ,D. (1975). Geology of the south eastern escarpment of Ethiopia between 39° and 42° long, East. In: Pilger A, Roesler EA (eds) Afar depression of Ethiopia. Schweizerbart, Stuttgart, pp 310–316

Kazmin, V. (1973). Geological map of Ethiopia, scale 1:2,000,000. Geological Survey of Ethiopia, Addis Ababa

Kieffer, B., Arndt ,N., Lapierre, H., Bastien ,F., Bosh. D., Pecher, A., Yirgu,G., Ayalew, D., Weis, D., Jerram, DA., Keller ,F., Meugniot, C. (2004). Flood and shield basalts from Ethiopia: magmas from the African superswell. J Petrol 45:793–834.

Kurkura Kabeto .(2010). Geological and geochemical variations in Mid-Tertiary Ethiopian Flood Basalt Province, Maychew, Tigray Region, and Ethiopia.MEJS, 2 (1): 4-25.

Kunz ,K., Kreuzer, H, Muller, P. (1975). Potassium-argon age determinations of the Trap Basalts of the SE part of the Afar rift. In: Pilger A, Roesler EA (eds) Afar depression of Ethiopia. Schweizerbart, Stuttgart, pp 370–374

Lamb, H.F., Leng, M.J., Telford, R.J., Ayenew, T., And Umer, M. (2007). Oxygen and carbon isotope composition of authigenic carbonate from an Ethiopian lake: a climate record of the last 2000 years: The Holocene, v. 17, p. 515–524.

Le Bas, M. J., Le Maitre, R., Streckeisen, A. and Zanettin, B. (1986). A chemical classification of volcanic rocks based on the total alkali-silica diagram. Journal of Petrology 27(3):745750.

Lightfoot, P.C., Hawkesworth, C.J. & Sethna, S.F. (1987). Petrogenesis of rhyolites and trachytes from the Deccan trap: Sr, Nd and Pb isotope and trace element evidence. Contributions to Mineralogy and Petrology, 95, 44–54.

Mengesha Tefera, Tadiwos Chernet and Workineh Haro .(1996).Exploration of the geological map of Ethiopia (1:20,000,000). Ethiopian institutes of geological surveys. Unpublished technical report, Addis Ababa, Ethiopia, 83pp.

Merla, G., Abbate, E., Azzaroli, A., Bruni, P., Fazzuoli, M., Sargi, M.,Tacconi, P. (1979). A geological map of Ethiopian and Somalia: Comment. Petgamon, 95p.

Miller,J.A.,&Harris,C.(2007). Petrogenesis of the Swaziland and northern Natalrhyolites of the Lebombo marginal graben, southeast Africa. Journal of Petrology, 48, 185–218.

Mohr, P. and C.A. Wood. (1976).Volcano spacings and lithospheric attenuation in the Eastern Rift of Africa. Earth planet sci. Lett. 33: 126-144.

Mohr P. (1983). Ethiopian flood basalt province. Nature 303, 577–584.

Mohr, P. and Zanettin, B. (1988). The Ethiopian flood basalt province. In: Macdougall, J.D.(ed), continental flood basalts. Klwuer Academic Publishers, Dordrecht, PP 63-110.

Morbidelli,L., Nicoletti ,C., Petrucciani, C., Piccirillo ,E. (1975). Ethiopian south-eastern plateau and related escarpment: K/Ar ages of the main volcanic events (Main Ethiopian Rift from 8° 10’ to 9° 00’ lat. N). In: Pilger A, Roesler EA (eds) Afar depression of Ethiopia. Schweizerbart, Stuttgart, pp 362–369

Nakamura, N. (1974). Determination of REE, Ba, Fe, Mg, Na and K in carbonaceous and ordinary chondrite. Geochimica Cosmochimica Acta, 38: 757-775.

Peccerillo, A., Barberio, M.R., Yirgu, G., Ayalew, D., Barbieri, M., Wu,T.W. (2003). Relationships between mafic and peralkaline acid magmatism in continental rift settings: a petrological, geochemical and isotopic study of the Gedemsa volcano, central Ethiopian rift.Journal of Petrology 44, 2003–2032.

Pik, R., Deniel, C., Coulon, C., Yirgu, G., Hoffmann, C. & Ayalew, D. (1998). The northwestern Ethiopian Plateau flood basalts: classification and spatial distribution of magma types. Journal of Volcanology and Geothermal Research 81, 91-111.

Pik, R., Deniel, C., Coulon, C., Yirgu, G. & Marty, B. (1999). Isotopic and trace element signatures of Ethiopian basalts: evidence for plume lithospheric interactions. Geochimica et Cosmochimica Acta 63,2263-2279.

Pik, R., Marty, B., Carignan,J. and Lave,J.(2003). Stability of the Upper Nile drainage network (Ethiopia) deduced from (U-Th)/He thermochronometry: implications for uplift and erosion of the Afar plume dome.

Richards, M.A., Duncan, R.A., Courtillot, V.E.(1989). Flood basalts and hot-spot tracks: plume heads and tails. Science 246, 103–107.

Rogers N.W. (2006). Basaltic magmatism and the geodynamics of the East African Rift System. In:Yirgu G., Ebinger C.J., and Maguire P.K.H. (Eds.), The Afar Volcanic Province within the EasAfrican Rift System. Geological Society, London, Special Publication 259, 77–93.

Rollinson, H.R. (1993). Using Geochemical Data: Evaluation, Presentation and Interpretation. Longman Group, London, 352p.

Ronga,F.,Lustrino,M., Marzoli,A.,Melluso,L.(2009). Petrogenesis of a basalt-comendite-pantellerite rock suite: the Boseti Volcanic Complex (Main Ethiopian Rift). Mineral. Petrol. 160, 407–425. https://doi.org/10.1007/s00410-009-0485-3.

Rooney, T., Furman, T., Bastow, I., Dereje Ayalew, and Gezahegn Yirgu. (2017). Lithospheric modification during crustal extension in the Main Ethiopian Rift. Journal of Geophysical Research: Solid Earth 1978–2012.

Rosenthal, A., Foley, S.F., Pearson, D.G., Nowell, B.M., Tappe, S.(2009). Petrogenesis of strongly alkaline primitive volcanic rocks at the propagating tip of the western branch of the East African Rift. Earth and Planetary Science Letters 284, 236–248.

SeifeMichael Berhe, Belay Desta, Nicoletti, and Mengesha Teferra. (1987). Geology, Geochronology and Geodynamic Implications of the Cenozoic magmatic province in W and SE Ethiopia. Journal of the Geological Society, London 144: 213-226.

Tian, W., Campbell, I.H., Allen, C.M., Guan, P., Pan, W., Chen, M., Yu, H., Zhu, W. (2010). The Tarim picrite-basalt-rhyolite suite, a Permian flood basalt from Northwest China with contrasting rhyolites produced by fractional crystallization and anatexis.Contrib. Mineral. Petrol. 160, 407–425. https://doi.org/10.1007/s00410-009-0485-3.

Ukstins, I.A., Renne, P.R., Wolfeden, E., Baker, J., Dereje Ayalew and Menzies, M. (2002).Matching conjugate volcanic rifted margins: 40Ar/39Ar chronostratigraphy of pre- and syn-rift bimodal flood volcanism in Ethiopia and Yemen. Earth and Planetary Science Letters, 198:289–306.

Violle, P. Y. (1999). Relations entre la g e eomorphologie et la lithologie des trapps d'Ethiopie. Dipl^ o ome d' E Etudes Approfondies de l'Universit e e Joseph Fourier, Grenoble II, 31 pp.

Winter, J.D.(2001). An introduction to Igneous and Metamorphic petrology, Prince Hall Inc., Upper Saddle River, New Jersey.

Zanettin ,B., Justin-Visentin, E., (1974) . The volcanic succession in central Ethiopia. 2-The volcanics of western Afar and Ethiopian rift margins. Mem Ist Min Univ Padova 31:1–19

Zanettin, B. (1992). Evolution of the Ethiopian Volcanic Province. Memorie Lincee Scienze Fisiche e Naturali 1:155---181

Zanettin ,B., Justin-Visentin,E., (1973). Serie di vulcaniti etiopiche: 1-La serie dell'altopiano etiopico centro-orientale. Boll Soc Geol It 92:313–327

Zhang J.J., Zheng, Y.F. and, Zi-Fu Zhao, Z.F. (2009). Geochemical evidence for interaction between oceanic crust and lithospheric mantle in the origin of Cenozoic continental basalts in east-central China. Lithos.110, 305–326

Appendix I

1. Petrographic Descriptions

Thin section code	Rock name	Location(UTM) and elevation	Description
T8S5	Olivine-clinopyroxene phyric basalt	0575284E-1235046N 2468m	Subhedral to Euhedral shaped mega phenocrysts of olivine and clinopyroxene embedded in groundmass of very fine grain of plagioclase and opaque mineral. Modal proportions of phenocryst are Olivine 41.5% and clinopyroxene 35.3% and the groundmass of plagioclase 10.5% and opaque mineral 6.7%.
T9S4	Plagioclase phyric basalt	05754582E-1234895N 2493m	The phenocrysts of plagioclase are mostly subhedral to anhedral in shape and also the groundmass of plagioclase phyric basalt is clinopyroxene and opaque minerals. Plagioclase 74.63%, clinopyroxene 14.19%,opaque mineral 11.25%
T7S8	Plagioclase phyric basalt	0575029E-1241105N 2202m	It is Porphyritic texture with phenocrysts of plagioclase, clinopyroxene and few opaque minerals. The megacrysts of plagioclase crystals are generally subhedral to euhedral and show zoning. phenocryst of Plagioclase 75% with groundmass of clinopyroxene 5% and opaque mineral 20%
T5S2	Plagioclase phyric basalt	0573919E-1243227N	It is Porphyritic texture with phenocrysts of plagioclase, clinopyroxene and few opaque minerals. The megacrysts of

		2248m	plagioclase crystals are generally subhedral to euhedral and show zoning. phenocryst of Plagioclase 71.6% with groundmass of clinopyroxene 18.7% and opaque mineral 9.7%
T1S5	Plagioclase phyric basalt	0575206E-1245420N 2193m	It is Porphyritic texture with phenocrysts of plagioclase, clinopyroxene and few opaque minerals. The megacrysts of plagioclase crystals are generally subhedral to euhedral and show zoning. phenocryst of Plagioclase 81.3% with groundmass of clinopyroxene 5.5% and opaque mineral 13.2%
T8S4	Olivine-clinopyroxene phyric basalt	0575206E-1245420N 2556m	It is Porphyritic texture with Subhedral to Euhedral shaped mega-phenocrysts of olivine and clinopyroxene embedded in groundmass of very fine grain of plagioclase and opaque mineral. Modal proportion of phenocryst are Olivine 36.88% and clinopyroxene 33.625% and phenocryst of plagioclase 8.6%,opaque mineral 14.7%
T6S4	Plagioclase aphyric basalt	0575579E-1242766N 2339m	It is Porphyritic texture with phenocrysts of plagioclase, clinopyroxene and few opaque minerals. The megacrysts of plagioclase crystals are generally subhedral to euhedral and show zoning. phenocryst of Plagioclase 71.6% with groundmass of clinopyroxene 7.4% and opaque mineral 22%
T3S4	Rhyolite	0575319E-1245349N	Euhedral shaped mega phenocrysts of sanidine and anhedral fine grain of quartz embedded in groundmass of volcanic glass

		2126m	and opaque mineral. Modal proportion of phenocryst are Sanidine 21.4% and quartz 11.3% and groundmass of opaque mineral 5% and volcanic glass 62.3%
T2S5	Rhyolite	05777858E-1246206N 2161m	Subhedral shaped mega phenocrysts of quartz and fine grain of sanidine embedded in groundmass of volcanic glass and opaque mineral. Modal proportion of phenocryst are quartz 44.5% , Sanidine 18.5% biotite 1%, and groundmass of opaque mineral 4.2,86 %,volcanic glass 30.8%,
T1S6	Rhyolite	0573362E-1248648N 2036m	Phenocryst composed of sanidine and quartz embedded groundmass is composed of opaque and volcanic glass. Mineralogical modal composition phenocryst Sanidine 27.5% and quartz 2% with opaque mineral 8.9% and volcanic glass 61.7%.
T3S1	Ignimbrite	0573415E-1248470N 2027m	Crystals are euhedral to subhedral sanidine and anhedral pyroxene with groundmass of volcanic glass and rock fragments. sanidine 21.25%, pyroxene 2% ,opaque mineral 5.63%,rock fragment 26.74% ,volcanic glass 48.75%
T3S2	Rhyolite	0572830E-1248262N 2168m	Phenocryst composed of sanidine and quartz embedded groundmass is composed of opaque and volcanic glass. Mineralogical modal composition phenocryst Sanidine 24.5%

			and quartz 7% with opaque mineral 8.9% and volcanic glass 59.7%.
T5S2	Plagioclase aphyric basalt	0573919E-1243227N 2248m	It is an aphyric texture with of very fine grain of plagioclase, clinopyroxene and opaque mineral. The mineralogical modal proportion are Plagioclase78.75%,clinopyroxene 13.75% and opaque mineral 7.5%
T4S5	Rhyolite	0573183E-1249769N 1990m	Subhedral shaped mega phenocrysts of sanidine and fine grain of quartz embedded in groundmass of volcanic glass and opaque mineral. Modal proportion of phenocryst are Sanidine 40% , quartz 15%, and groundmass of opaque mineral 5%,volcanic glass 50%,

Appendix II

1. Recalculated (volatile free basis) major element data

Sample	SiO_2	Al_2O_3	Fe_2O_3	CaO	MgO	Na_2O	K_2O	TiO_2	MnO	P_2O_5	SUM
T7 S1	55.13	14.94	11	7.57	3.89	3.29	1.85	1.93	0.168	0.286	101.39
T3 S2	64.82	15.82	5.38	3.15	1.37	5.31	2.63	1.058	0.18	0.265	98.27
T1 S1	46.2	12.08	13.3	12.03	9.3	2.35	0.89	3.09	0.21	0.54	98.48
T2 S3	48.84	15.39	12	11.86	6.22	2.684	0.454	2.1	0.182	0.283	99.11
T7 S5	49.1	14.45	12.42	10.07	7.67	2.66	0.82	2.4	0.183	0.325	98.61
T3 S6	68.25	13.3	5.48	1.02	0.94	4.8	4.58	1.11	0.25	0.27	97.4

T5 S2	72.76	13.7	2.73	1.04	0.25	4.59	4.23	0.71	0.07	0.1	98.59
T1 S3	72.55	15.25	3.11	0.23	0.17	3.91	4.26	0.43	0.063	0.03	96.07
T2 S1EA	78.1	10.65	2.2	0.1	0.08	2.7	5.61	0.48	0.07	0.01	99.62
T3 S4	73.2	12.27	3.58	0.287	0.257	4.52	5.15	0.554	0.55	0.092	97.73

2. Trace element ratio

Sample	T1S1	T2S3	T7S5	T7S1	T3S2	T3S6	T1S3	T3S4	T5S2	T2S1EA
CaO/Al_2O_3	0.99	0.77	0.71	0.50	0.20	0.08	0.02	0.025	0.076	0.01
(La/Yb)N	10.97	5.34	5.37	6.19	9.34	11.74	6.93	8.56	8.86	10.49
(La/Sm)N	2.36	1.96	2.13	2.53	2.91	2.65	2.99	2.57	3.44	2.93
(Gd/Lu)N	2.8	2.47	2.11	1.9	2.2	2.94	1.59	2.24	1.72	2.48
(Ce/Yb)N	8.94	4.42	4.42	4.80	7.47	9.67	2.58	6.88	6.35	6.16
(Ce/Sm)N	1.92	1.59	1.75	1.96	2.33	2.18	1.11	2.06	2.46	1.72
(Eu/Yb)N	3.52	2.38	2.24	1.85	2.35	3.01	0.87	1.70	1.27	1.83
(Tb/Yb)N	2.33	1.82	1.75	1.56	1.77	2.16	1.37	1.89	1.48	2.17
(Gd/Yb)N	2.88	2.05	1.91	1.77	2.12	2.62	1.46	2.08	2.60	2.40
Sum_REE	173.71	113.22	117.65	148.75	277.8	473.69	438.99	563.12	379.71	272.29
Th/Ta	1.38	1.86	2.33	3.26	2.18	1.91	2.5	2.17	3.25	2.09
La/Nb	0.88	1.08	0.99	1.81	1.02	0.88	0.93	0.87	1.01	0.51
Nb/La	1.13	0.94	1.01	0.55	0.98	1.14	1.08	1.15	0.93	1.97
Rb/Nb	0.58	0.5	0.55	2.7	1.31	1.01	0.97	1.03	1.69	1.16
Hf/La	0.19	0.22	0.21	0.21	0.21	0.23	0.21	0.24	0.20	0.47
Ce/Pb	>33.2	>19.65	21.05	7.84	11.05	38.1	6.9	15.6	11.5	6.13

Nb/Y	1.38	0.72	0.78	0.49	1.32	1.76	1.20	1.32	1.2	6.22
Nb/Ta	16.86	21.25	21.89	16.55	15.64	16.47	16.84	16.22	16.75	14.44
Zr/Nb	7.01	8.59	8.17	14.43	8.76	8.45	8.0	8.41	8.45	10.17
Zr/Ce	3.72	3.72	3.82	3.92	4.09	4.46	8.63	4.61	4.17	12.93
Nb/U	41.16	39.55	45.81	31.04	21.59	24.88	33.68	22.94	21.8	99.15
Th/Nb	0.08	0.09	0.11	0.20	0.14	0.12	0.15	0.13	0.19	0.14
Ba/Nb	7.23	10.38	13.20	33.62	14.30	7.70	3.76	2.86	9.47	0.90
Ba/La	8.23	9.75	13.30	18.56	14.00	8.78	4.06	3.30	8.79	1.76
La/Yb	16.45	8.01	8.06	9.28	14.02	17.60	10.39	12.8	13.29	15.73
Dy/Yb	2.88	2.27	2.058	1.90	2.01	2.41	1.74	2.21	1.77	1.17
La/Tb	33.09	20.57	22.16	27.84	37.11	38.18	35.45	31.8	41.9	75.70
La/Ta	14.81	22.63	21.67	30	16	14.46	15.59	14.05	18.09	7.38
Nb/Th	12.21	11.33	9.38	5.08	7.17	8.63	6.73	7.47	5.15	6.92

N is denotes that the concentration is normalized by REE chondrite (Anders & Grevesse 1989).

3. CIPW (wt %) norm for the Lake Hayk Volcanic rocks

	T3 S2	T3 S6	T5 S2	T1 S3	T2 S1EA	T3S4	T1 S1	T2 S3	T7 S5	T7 S1
Quartz	16.045	19.949	27.339	31.559	40.078	26.808	0.000	3.711	3.365	11.174
Carbon	0.000	0.000	0.000	3.709	0.000	0.000	0.000	0.000	0.000	0.000
Orthoclase	15.247	26.476	24.880	24.171	32.681	29.667	5.201	2.659	4.787	11.110
Albite	44.170	39.685	38.670	31.816	22.508	33.516	19.547	22.508	22.170	28.262
Anorthite	11.378	1.187	4.297	0.895	0.377	0.000	19.502	28.342	24.729	20.793
Acmite	0.000	0.000	0.000	0.000	0.000	3.273	0.000	0.000	0.000	0.000

Diopside	0.000	0.000	0.000	0.000	0.000	0.000	20.284	16.800	11.594	6.932
Hypersthene	3.363	2.292	0.623	0.399	0.199	0.623	9.681	7.557	13.458	6.601
Olivine	0.000	0.000	0.000	0.000	0.000	0.000	2.617	0.000	0.000	0.000
Ilmenite	0.385	0.513	0.150	0.128	0.150	0.171	0.449	0.385	0.385	0.364
Hematite	5.290	5.360	2.720	2.990	2.170	2.359	13.101	11.901	12.251	11.151
Titanite	1.623	1.462	0.147	0.000	0.038	0.565	6.882	4.609	5.321	4.342
Rutile	0.176	0.214	0.571	0.343	0.376	0.220	0.000	0.000	0.000	0.000
Apatite	0.616	0.616	0.237	0.071	0.024	0.213	1.255	0.663	0.758	0.687
Sum	98.29	97.75	99.63	96.08	98.60	97.41	98.52	99.13	98.82	101.42

Appendix III

1. Major element calculated mass balance

Step 1 from T2S3 to T7S1 solid fraction % = 60.51				
	T2S3	T7S1	Calc.comp	R
SiO2	48.4	55.9	55.897	0.003
TiO2	2.08	1.96	1.563	0.397
Al2O3	15.25	15.15	15.11	0.037
FeOtot	10.71	10	10.156	-0.156
MnO	0.18	0.17	0.197	-0.027
MgO	6.16	3.94	3.87	0.069
CaO	11.75	7.61	7.692	-0.082
Na2O	2.66	3.34	3.752	-0.412
K2O	0.45	1.88	1.54	0.34
P2O5	0.28	0.29	0.46	-0.169
			$\sum R^2 = 0.51$	
	Olivine	CPX	Plagioclase	Opaque
SiO2	40.66	47.15	50.71	0
TiO2	0	3.38	0	24.91
Al2O3	0	4.78	30.67	1.46
FeOtot	23.44	10.99	0.54	71.73
MnO	0.35	0.19	0	0.64
MgO	34.88	11.86	0.18	1.24
CaO	0.76	21.09	14.72	0
Na2O	0	0.54	3.05	0
K2O	0	0	0.14	0.01
P2O5	---	---	---	---
Fract.Solidwt.%	-42.53	-32.25	-21.74	-3.48

Step 2 from T7S1to T3S6 solid fraction % = 43.41				
	T7S1	T3S6	Calc.comp	R
SiO_2	55.9	66.7	67.093	-0.093
TiO_2	1.96	1.08	1.391	-0.311
Al_2O_3	15.15	13	12.453	0.547
FeOtot	10	4.83	4.805	0.025
MnO	0.17	0.24	0.254	-0.014
MgO	3.94	0.92	0.649	0.271
CaO	7.61	1	1.583	-0.583
Na_2O	3.34	4.69	4.11	0.58
K_2O	1.88	4.48	4.21	0.27
P_2O_5	0.29	0.26	0.43	-0.169
			$\sum R^2 = 1.3$	
Chemical compositions	Olivine	CPX	Alkali Feldspar	Opaque
SiO_2	39.87	49.06	51.92	0.51
TiO_2	0.03	0	0.77	50.02
Al_2O_3	0	32.14	1.85	0
FeOtot	14.06	0.27	32.19	46.37

MnO	0.22	0	0	1.44
MgO	45.38	0.2	0	0.46
CaO	0.25	15.38	0	0.71
Na_2O	0.04	2.57	12.86	0
K_2O	0.01	0.17	0.19	0
P_2O_5	---	---	---	---
Fract. Solid wt.%	-14.61	-57.99	-19.67	-7.72
Step 3 from T3S6 to T3S4 solid fraction % = 29.47				
	T3S6	T3S4	Calc.comp	R
SiO_2	66.7	71.3	71.04	0.26
TiO_2	1.08	0.54	0.69	-0.15
Al_2O_3	13	11.95	12.19	-0.24
FeOtot	4.83	3.1	2.79	0.312
MnO	0.24	0.08	0.195	-0.115
MgO	0.92	0.25	0.233	0.017
CaO	1	0.28	0.483	-0.203
Na_2O	4.69	4.4	3.749	0.651
K_2O	4.48	5.02	5.345	-0.325
P_2O_5	0.26	0.09	0.297	-0.207
			$\sum R^2$ = 0.8721	
Chemical compositions	Olivine	CPX	Sanidine	Opaque
SiO_2	29.84	48.46	68.31	0
TiO_2	0	0.46	0	22.57
Al_2O_3	0	0.2	18.74	0.28
FeOtot	64.69	28.6	0.38	74.56
MnO	4.73	1.7	0	2.44
MgO	0.43	1.77	0	0.12
CaO	0.31	18.4	0.07	0
Na_2O	0	1.42	9.17	0
K_2O	0	0	3.33	0.01
P_2O_5	---	---	---	---
Fract. Solid wt.%	-5.89	-9.6	-77.74	-6.77

2. Calculated weight percent (Wt%) of minerals and partition coefficients

Mineral	Mode	Density	Wt. Proportion	Wt%
Olivine	44.5	3.6	160.2	47.66
Cpx	37.3	3.4	126.82	37.73
Plag	18.2	2.7	49.14	14.62
Sum	100	------	336.16	100

Partation coefficients of incompateble and compatible element			
Element	Olivine	Clinopyroxine	Plagioclase
Rb	0.04	0.05	0.05
Sr	0.02	0.09	2.53
Zr	0.01	0.17	0.02
Ni	16	2.2	0.01
Cr	5.3	1.8	0.01

3. Calculated bulk partition coefficient and crystal fractionation (CL/Co)

D_{Rb} = 0.042D_{Sr} = 0.43 D_{Rb} = 0.042 D_{Ni} = 8.46 D_{Cr} = 3.2			
CL/Co at D_{Rb}	CL/Co at D_{Sr}	CL/Co at D_{Ni}	CL/Co at D_{Cr}
9.08	3.7	3.47E-08	0.0063
4.67	2.5	0.000061	0.029
3.17	1.99	0.00013	0.071
2.41	1.69	0.0011	0.133
1.94	1.48	0.0057	0.22
1.63	1.34	0.022	0.33
1.41	1.23	0.07	0.46
1.23	1.14	0.19	0.62
1.11	1.06	0.46	0.8
1	1	1	1